Molecular Biology of Octocoral Mitochondria:

mtDNA Repair, Expression, and Evolutionary Implications

Dissertation zur Erlangung des Doktorgrades
der Fakultät für Geowissenschaften
der Ludwig-Maximilians-Universität München

vorgelegt von
Gaurav Gokul Shimpi
München, November 16, 2015

Betreuer: Prof. Dr. Gert Wörheide

Zweitgutachter: PD. Dr. Dirk Erpenbeck

Datum der mündlichen Prüfung: 21.12.2015

Acknowledgements

First of all, I am greatly indebted to the DAAD (Deutscher Akademischer Austauschdienst) for the scholarship and for providing me the opportunity to carry out research and earn a Doctorate in Germany.

I am particularly grateful to my advisor Prof. Dr. Gert Wörheide for trusting and supporting me from the first email-contact onwards. I am also thankful to you for allowing me the freedom to explore the areas of science that interested me, and for being there with your scientific expertise and vast experience ready to help. I feel lucky to have been a part of your team and submitting this dissertation under your mentoring, and I sincerely hope I fulfilled your expectation as a PhD student.

I can't thank Dr. Sergio Vargas enough for his involvement in my project and for revising manuscripts. I learnt a lot from him on scientific as well as philosophical front. Thank you for showing interest in my ideas, for encouraging discussions, and for scientific insights whenever I needed the most. Thank you for being there through all the good and the bad times in the lab and outside. I would also like to thank Dr. Dirk Erpenbeck for making sure that I was comfortable in a new environment from the first day itself. Thank you for encouragement and expert advices. I am highly obliged to you for caring and supporting throughout. I am also thankful to Dr. Oliver Voigt for his constructive discussions, for answering my questions from time to time patiently, and for support.

I am thankful to Astrid Schuster, Angelo Poliseno and Edwin Setiawan who are not only best colleagues in the lab but also best friends. Special thanks to Astrid for always accompanying me during the afternoon coffee breaks, for helping me understand German documents, for arranging birthday cards for everyone, discussions; and to Angelo for always being generous in providing help in the lab and for accompanying me for sightseeing.

I want to thank Gabriele Büttner, Simone Schätzle and Peter Naumann for their technical assistance in the lab and aquarium. Thank you Gabi for interesting discussions outside of science about India, Yoga, Bavaria, Oktoberfest, etc. It was a pleasure sharing office with you. I am much obliged to all MolPal lab fellows for accepting me wholeheartedly in the lab.

Many people provided basic resources that helped me get my work done and get through my time at the Department of Earth and Environmental Sciences Paleontology & Geobiology more easily, including Frau Bommhardt, Frau Roeske, Frau Brinkrolf, and Frau Schönhofer for taking care of the administrative part, to René Neumaier for the assistance with all computer-related issues all colleagues of the department. Thank you all for your support.

On a personal note, I am grateful to my family, my grandparents, especially Shri. Baburao Shimpi for being a source of wisdom, and Late Shri. Madhav Shimpi, who was instrumental in sparking my interest in science since childhood by providing me inspirational reading material. I want to thank my mother Sau. Kalpana Shimpi and my father Shri. Gokul Shimpi for never compromising on my educational needs and for letting me pursue my own interests. Thanks to my best friend Dr. C.P. Antony supporting and inspiring me always. I am grateful to Prof. S.D. Biju, and Dr. Ashish Thomas, Dr. Nitesh Khonde for supporting me during crucial times. I express my sincere gratitude towards Prof. V.L. Maheshwari, Prof. B.L. Chaudhari, Prof. P.M. Vyavahare, Dr. Shouche and all my teachers for inspiring me during school/college years. I want to thank all my friends back in India for always believing in me and encouraging me. This has been a long journey and all those who accompanied me on the ways, I am thankful to them for walking along, and I apologize for not being able to mention them all.

The most special thanks goes to the most special person in my life, my better-half Deepti Birhade-Shimpi, for her unconditional love, unending support and encouragement. Thank you for your patience throughout these years. I can't express in words how much your love and support means to me besides mentioning that I wouldn't be here, had you not been with me throughout this journey. I also want to thank Deepti's mother Saroj Ahire and her entire family for their trust and encouragement.

Thank you!

Summary

The mitochondria of non-bilaterian metazoans display a staggering diversity of genome organizations and also a slow rate of mtDNA evolution, unlike bilaterians, which may hold a key to understand the early evolution of the animal mitochondrion. Octocorals are unique members of Phylum Cnidaria, harboring several atypical mitochondrial genomic features, including a paucity of tRNA genes, various genome arrangements and the presence of novel putative mismatch repair gene (*mtMutS*) with various potential biological roles. Thus octocorals represents an interesting model for the study of mitochondrial biology and evolution. However, besides its utility in molecular phylogenetics, the mtDNA of octocorals is not studied from the perspective of DNA repair, oxidative stress response or gene expression; and there is a general lack of knowledge on the DNA repair capabilities and role of the *mtMutS* gene, response to climate-change, and mtDNA transcription in absence of interspersed tRNA genes of octocoral mitochondrial genome. In order to put the observed novelties in the octocoral mitochondria in an evolutionary and an environmental context, and to understand their potential functions and the consequences of their presence in conferring fitness during climate change induced stress, this study was undertaken. This dissertation aims to explore the uniqueness and diversity of octocoral mtDNA from an environmental as well as an evolutionary perspective.

The thesis comprises five chapters exploring various facets of octocoral biology. The introductory section provides basic information and elaborates on the importance of studying non-bilaterian mitochondria. The first chapter sets the base for subsequent gene expression studies. Octocorals are extensively studied from a taxonomic and phylogenetic point of view. However, gene expression studies on these organisms have only recently started to appear. To successfully employ the most commonly used gene expression profiling technique i.e., the quantitation real-time PCR (qPCR), it is necessary to have an experimentally validated, treatment-specific set of stably expressed reference genes that will support for the accurate quantification of changes in expression of genes of interest. Hence, seven housekeeping genes, known to exhibit constitutive expression, were investigated for expression stability during simulated climate-changed (i.e. thermal and low-pH) induced stress. These genes were validated

and subsequently used in gene expression studies on *Sinularia* cf. *cruciata*, our model octocoral.

The occurrence of a mismatch repair gene, and the slow rates of mtDNA evolution in octocoral mitogenome calls for further investigations on the potential robustness of octocoral mitochondria to the increased oxidative stress. The second chapter presents a mitochondrion-centric view of climate-change stress response by investigating mtDNA damage, repair, and copy number dynamics during stress. The changes in gene expression of a set of stress-related nuclear, and mitochondrial genes in octocorals were also monitored. A robust response of octocoral mitochondria to oxidative mtDNA damage was observed, exhibiting a rapid recovery of the damaged mtDNA. The stress-specific regulation of the *mtMutS* gene was detected, indicating its potential involvement in stress response. The results highlight the resilience potential of octocoral mitochondria, and its adaptive benefits in changing oceans.

The tRNA genes in animal mitochondria play a pivotal role in mt-mRNA processing and maturation. The influence of paucity of tRNA genes on transcription of the mitogenome in octocorals has not been investigated. The third chapter steps in the direction to understand the mitogenome transcription by investigating the nature of mature mRNAs. Several novel features not present in a "typical" animal mt-mRNAs were detected. The majority of the mitochondrial transcripts were observed as polycistronic units (i.e. the mRNA carrying information for the synthesis of more than one protein). 5' and 3' untranslated regions were delineated for most protein-coding genes. Alternative polyadenylation (APA) of *mtMutS* gene and long non-coding RNA (lncRNA) for ATP6 were detected and are reported for the first time in non-bilaterian metazoans providing a glimpse into the complexity and uniqueness of mtDNA transcription in octocorals.

The mismatch repair (MMR) mechanism plays a crucial role in mutation avoidance and maintenance of genomic integrity. Its occurrence in animal mitochondria remains equivocal. Octocorals are the only known animals to posses an mtDNA-encoded MMR gene, the *mtMutS*, speculated to have self-contained DNA repair capability. In order to gain knowledge of the MMR activity in the octocoral mitochondria MMR assays using the octocoral mitochondrial fraction is necessary. A prerequisite for this assay is the availability of an MMR-substrate, which is a DNA fragment, usually a plasmid,

containing the desired mismatch lesion (i.e. a heteroduplex) and a nicked strand. However, the methods to prepare such a substrate are time consuming and technically demanding. Chapter four describes two convenient and flexible strategies that can be used in parallel to prepare heteroduplex MMR substrate using a common plasmid and routine molecular biology techniques. This method should aid in MMR investigations in general, helping to advance this field of research.

The *mtMutS* gene mentioned above is a bacterial homolog, predicted to have been horizontally transferred to the octocoral mitogenome. However, unlike the bacterial mutS, which is extensively studied, protein expression studies of the octocoral *mtMutS* gene are lacking. To investigate the biological role of the mtMutS protein, in vitro, and to gain knowledge on its structure and function, the expression of the gene in a bacterial host is necessary. The fifth chapter discusses the characteristics of the mtMutS protein, the efforts to express it in E. coli and some necessary precautions to be taken while working with the expression of such mtDNA-encoded proteins for the research in future.

This dissertation elucidates and contributes to the understanding of the unexplored complexity of non-bilaterian mitochondria. It deals for the first time with DNA repair, gene expression and gene function, encompassing an integrative analysis of DNA, RNA and proteins to achieve its goals. This study forms the basis for many future investigations on the molecular mitochondrial biology of octocorals as well as other non-bilaterians, augmenting the understanding of the evolution of animal mitochondria, and also its role in cellular and organismal homeostasis in the context of environmental change.

Table of Contents

Introduction

Octocorals, the softer members of reefs

The great diversity of extant metazoans emerged from the simplest members of the animal kingdom such as sponges and corals (Lipps and Signor, 2013). These early branching animals occupy the base of animal tress of life; hold a key and provide us with an opportunity to understand the evolution of the vast animals diversity seen today.

Among non-bilaterian metazoans, the cnidarian sub-class Octocorallia consists of extraordinarily diverse organisms found in all marine environments, encompassing more than 3400 species (Williams and Cairns, 2005; Daly et al., 2007), inhabiting all the world's oceans in shallow waters, deep seamounts and submarine canyons. Octocorals are crucial in providing structure to reefs as well as supporting a variety of marine life including invertebrates and fishes (Stocks, 2004; Baillon et al., 2012; Figueroa and Baco, 2015). They exhibit an 8-fold radial symmetry and hence are commonly called, octocorals by virtue of their polyps bearing eight pinnate tentacles and eight internal mesenteries (Bayer, 1955). However, they are also known by several other names such as sea fans, sea pens, and sea whips based on their growth forms. They are most commonly referred to as soft corals due to a general lack of "stony" skeleton like that of the scleractinian or hard corals (Fabricius and Alderslade, 2001).

Geological past

Despite holding a key position at the base of the animal tree of life, preceding the evolution of most other metazoans except sponges, the fossil record for the members of Subclass Octocorallia is rather sparse, making it difficult to understand their emergence in the geological past. Earliest fossil remains in the form of fossilized spicules resembling living octocorals dating back to Cambrian period suggest their presence (Bengtson, 1981). Subsequent fossil records indicate the presence of sea fans and sea pens during the Paleozoic (Glinski, 1956; Bengtson, 1981). Octocoral fossils are, however, predominantly Cretaceous or Cenozoic (Deflandre-Rigaud, 1956; Kocurko and Kocurko, 1992).

In the absence of abundant evidence in the form of fossils, the understanding of the past and present of octocorals and its descendants relies largely on the history recorded in the genomes of extant members. And current molecular biological techniques could help us read this history providing a glimpse of important evolutionary transitions in the early evolution of Metazoa.

The Mitochondrion, the tiny subcellular pocket of essential information

Among the transitions that lead to the metazoan evolution so far, the key events that occurred early in animal history were the origin or multicellularity, and subsequently, the emergence of bilateral symmetry. Non-bilaterians, including octocoral, lie within these major transitions as connecting links. Undoubtedly, these transitions also correlate with multiple changes in mitochondrial genome architecture and organization (Lavrov, 2007). Mitochondria are the remnants of an α-proteobacterial ancestor acquired during an ancient endosymbiosis event that gave rise to the eukaryotic life (Dyall et al., 2004). This small event that took place more than a billion years ago, shaped the vast diversity of eukaryotic, aerobic life on planet Earth. Since then, mitochondria have gone through a series of evolutionary transitions (Boore, 1999; Lavrov, 2007).

The Mitochondrion possesses a double membrane just like its bacterial-ancestor and harbors its own circular genome, the mitogenome. During the course of evolution, the mitogenome has gone through several transitions, which predominantly include its compaction by transferring the content to the nuclear genome, loss of tRNA and ribosomal protein genes, changes in the genetic code and appearance of genetic novelties (Wolstenholme, 1992; Adams and Palmer, 2003). Most bilaterian animals possess broadly uniform mitogenome content, with 13 protein-coding genes essential for oxidative phosphorylation and energy production, 2 ribosomal RNA genes and 22 transfer RNA genes while majority of protein complement require for normal functioning is encoded and provided by nuclear genome (Boore, 1999). These tiny organelles are extremely essential for aerobic life. In general, due to its fast evolutionary pace, the mitochondrial DNA (mtDNA) extensively used in phylogenetic and DNA barcoding studies and considered as one of the most suitable marker for species discrimination and to infer evolutionary relationships within or between different animal groups (Bernt et al., 2013), including non-bilaterians (McFadden et al., 2006;

Kitahara et al., 2010; Vargas et al., 2012). However, mitogenomes of non-bilaterians exhibit diverse properties as compared to the bilaterian ones, discussed below in details.

Octocoral mitochondria, the atypical

The general universality of the bilaterian metazoan's quintessential mitogenome changes drastically towards the base of metazoan tree. Phylum Cnidaria is a hotspot of changes in genome architecture and organization. These changes are diverse as well as staggering, and include, loss of tRNA genes (Beagley et al., 1998), presence of group I introns (van Oppen et al., 2002; Fukami et al., 2007), additional protein coding genes and/or unknown ORFs and gene duplications in anthozoans (Pont-Kingdon et al., 1995; Flot and Tillier, 2007; Park et al., 2011; Lin et al., 2014), and linear mitogenomes in medusozoans (Voigt et al., 2008; Kayal et al., 2012).

Octocorals also have undergone extraordinary modifications of its mitogenome content and organization marked by the presence of a single tRNA gene, an additional protein coding gene, and five different genome arrangements (Brockman and McFadden, 2012; Figueroa and Baco, 2015). The most peculiar feature of their mitogenome is the presence of putative mismatch repair gene, the *mtMutS* (Pont-Kingdon et al., 1995), which is present exclusively in octocorals; and is not reported for any other metazoan mitochondria so far. The exact function of this gene is still unknown, however, studies suggest that its unusual presence in octocoral mitochondria is a result of horizontal gene transfer from either a bacteria or a DNA virus, and that the *mtMutS* gene possess all the components to be able to perform a self-contained DNA repair function (Bilewitch and Degnan, 2011).

Another feature of octocoral mitogenomes is the presence of different mitochondrial gene orders. Recent mitochondrial genome sequencing projects have revealed that there are at least five different mitogenomic arrangements present for the member of Subclass Octocorallia (Brugler and France, 2008; Uda et al., 2011; Brockman and McFadden, 2012; Figueroa and Baco, 2014). The peculiarity of these genome rearrangements is that there are conserved blocks having a set of genes, which inverted or translocated together (Figure A). Recombination is suggested as the most likely driving force behind the observed changes in non-bilaterian mitogenome organization, however this remains speculative (Mao et al., 2014).

Figure A: Schematic representation of different mitochondrial genome arrangements in Octocorallia from A to E. Each color represents a conserved block of genes. The inversion and translocation are depicted with arrows and dotted lines whereas, the bold line below genes represent the light strand. Letters a, b represent positions of the inverted repeats. Figure adopted from Brockman and McFadden (2012)

Moreover, octocoral mitogenome encode only a single tRNA gene ($tRNA^{Met}$), contrary to the typical bilaterian mitogenome, which contains 22 tRNA genes. This paucity of tRNA genes in mitogenomes is puzzling, as the tRNA punctuation model is the only know model available for the processing and maturation of animal mitochondrial mRNA transcripts (Ojala et al., 1981; Temperley et al., 2010). How the mitochondrial mRNA are liberated from the precursor polycistronic transcription units in absence of these punctuation marks in non-bilaterians lacking tRNA is unexplored.

DNA repair, the curator

The genomic integrity of the cell is under the constant threat from exogenous as well as endogenous agents capable of damaging the DNA. To cope with the damaging insults and to maintain DNA without any changes that may affect cellular homeostasis and perpetuation, the cells posses several different DNA repair mechanisms. However, the activity and efficacy of DNA repair for nuclear and organellar DNA appears to be different. Nuclei have multiple DNA repair mechanisms whereas ability of

mitochondria appears limited in this respect (Boesch et al., 2011; Blasiak et al., 2013) (Figure B).

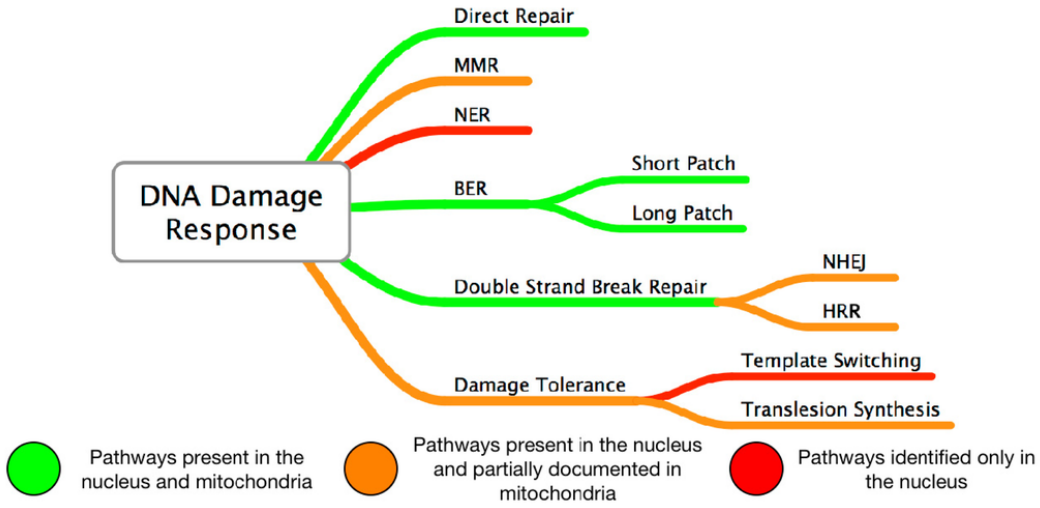

Figure B: DNA repair pathways know for nuclear genome and their occurrence in mitochondria. MMR –mismatch repair; NER–nucleotide excision repair; BER–base excision repair, NHEJ–Non-homologous end joining, HRR–homologous recombination repair. Adopted from Blasiak et al., 2013

In consequence, the rate of substitutions of the mtDNA is found to be several times higher than that of the nuclear DNA (nDNA) for most animals. In mammals, for example, substitutions accumulate up to 10 to 20 times faster in mitogenome than in nDNA (Brown et al., 1982). The ROS (reactive oxygen species) -induced damage is responsible for many more mutations in mtDNA than in nDNA (Shigenaga et al., 1994). Conjointly, the fast mutation rate can be attributed to less efficient DNA repair mechanism for mitochondria (Fernández-Silva et al., 2003; Boesch et al., 2011). Yet, not all animals show high mutation rate in mtDNA. It has been observed that anthozoans and sponges exhibit unusually slow rate of mtDNA sequence evolution, estimated to be 10-100X slower than other metazoans, and up to 5X slower than nuclear genes (Shearer et al., 2002; Hellberg, 2006; Huang et al., 2008; Chen et al., 2009). Interestingly, mtDNA divergence among closely related anthozoans is, in fact, lower than that of nDNA from the same taxa (van Oppen et al., 2001). These observations indicate that the evolutionary forces shaping non-bilaterian mitochondria are likely to be different than those for bilaterians animals. Understanding these forces could provide fundamental insights into mitogenome evolution in general.

The *mtMutS* gene discussed earlier, has also been suggested as potentially responsible for the observed low mutation levels in octocoral mtDNA (Shearer et al., 2002; Hellberg, 2006) by virtue of its predicted DNA mismatch repair (MMR) functionality (Bilewitch and Degnan, 2011). Its role in observed genome rearrangements have also been argued (Brockman and McFadden, 2012). However, the exact function and the evolutionary as well as adaptive benefits of sheltering such a large horizontally transferred gene for mitochondria, cell and organism remains unknown, and calls for investigations.

Changing oceans, oxidative stress and gene expression

The rise in atmospheric CO_2 as a result of increased anthropogenic activities is responsible for exerting a greater abiotic stress on coral ecosystems worldwide, and threatening their existence (Hughes et al., 2003). The consequences of elevated CO_2 levels comprise mainly, the rise in seawater temperatures, and the reduction in ocean pH; both of which result in an increased oxidative stress at cellular level severely affecting the coral health (Lough, 2008) leading to apoptosis, necrosis (Richier et al., 2006; Tchernov et al., 2011); and ultimately causing mass bleaching events (Hughes et al., 2003), due to an additional stress by endosymbiotic dinoflagellates resulting in disrupting the symbiosis (Weis, 2008).

Gene expression profiling has emerged as one of the best ways to understand the cellular response to increased oxidative stress at molecular level, providing deeper understanding of the fundamental questions about coral physiology during abiotic stress imparted on these organisms under such climate change scenarios (Seneca and Palumbi, 2015). Prevalence of oxidative stress and the response of corals antioxidant defenses are crucial to our understanding of coral's future in world's changing oceans and environment (Lesser, 2006; Lesser, 2011).

The energy status of the coral, like every other organism, determines its performance under stressful conditions and is crucial for survival (Lesser, 2013). Mitochondrion is the powerhouse of energy in coral host cells that produces ATP and/or NADPH, fulfilling all energy needs for metabolic pathways of the cell. Hence, mitochondria are vital to multicellular life being central to oxidative metabolism and energy production. However, being a hub of these important cellular events, mitochondria are cell's greatest source of ROS and produces considerable quantities of superoxides and

hydrogen peroxide (H_2O_2) capable of damaging the macromolecules. Therefore, as a principle source of ROS, mitochondria are also the major site of oxidative damage; and the mtDNA is more prone to this damage (Sawyer et al., 2001). The ROS generated by mitochondria not only damages the mtDNA and elicits stress response but also triggers the release of cytochrome c and other pre-apoptotic protein-signaling cascade, ultimately leading to cell death (Gogvadze et al., 2006; Ott et al., 2007). Hence, the mitochondrial integrity is crucial for cellular and organismal homeostasis. However, the impact and response coral mitochondria and their function in abiotic stress tolerance are far from proper appreciation. In light of evidences discussed earlier about the unique slow mtDNA evolution and the unique gene repertoire, clearly more investigations are required on the response of non-bilaterians to oxidative damage in changing oceans from the mitochondrial perspective. This will not only provide insights into the global-change biology of non-bilaterian fauna but also help use understand the potential mitogenomic novelties from an evolutionary point of view.

Studying molecular biology of octocoral mitochondria, mtDNA repair, gene expression and transcription is the first step towards exploring and understanding the causes and consequences of mitochondrial genomic novelties among the members of early branching non-bilaterian, the octocorals, which will provide valuable insights into evolution of mitochondria, and its stress response biology.

Aims of the study

The project explores various facets of octocoral mitochondria by using molecular biology techniques. The aims of the study include,

1. Establishment of experimentally validated, stably expressed reference genes to accurately quantify differential gene expression in octocorals during climate-change scenarios (Chapter 1).

2. Understanding the oxidative stress response of octocoral mitochondria during climate-change related stress by monitoring the mtDNA damage, repair, and copy-number dynamics, along with changes in nuclear stress-marker as well as mitochondrial genes during different climate-change scenarios (Chapter 2).

3. Examining the mitochondrial mRNA processing and maturation in absence of intervening tRNA genes along with characterization of *mtMutS* gene transcript to understand mitogenome and *mtMutS* transcription patterns (Chapter 3).

4. Development of new method for preparation of heteroduplex DNA substrates for *in vitro* mismatch repair (MMR) assay (Chapter 4).

5. Characterization and expression of *mtMutS* protein (Chapter 5).

Authors Contributions

Chapter 1:

Evaluation and validation of reference genes for qPCR analysis to study climate change-induced stresses in *Sinularia* cf. *cruciata* (Alcyonidae: Octocorallia).

Authors: Gaurav G. Shimpi, Sergio Vargas, Gert Wörheide

GGS conceived of the study. GGS and SV designed the experiment. GW participated in the design of the study. GGS performed the experiments, analyzed, interpreted the data and drafted the manuscript. All authors contributed to the discussion.

This chapter will be submitted as a standalone publication to the 'Journal of Marine Experimental Biology and Ecology.

Abstract

Coral reef organisms, including octocorals, are facing the consequences of anthropogenic activities, such as increasing oceanic pH and sea surface temperature, threatening their long-term survival and well-being. Gene expression studies based on quantitative PCR (qPCR) are important tools to provide insight into the molecular basis of octocoral stress responses and their potential resilience mechanisms. However, a lack of experimentally validated, stably expressed reference genes for the normalization of gene expression using quantitative reverse transcriptase PCR (qPCR) methods limits such investigations among octocorals. Here, we assess the expression stability of seven candidate reference genes using a palette of statistical tools for valid qPCR-based gene expression studies on the octocoral *Sinularia* cf. *cruciata* during thermal (34°C) and low pH (pH 7.5) stress and determine the most suitable set of reference genes for such experiments. The reliability of the selected reference genes was confirmed in a qPCR

assay that targeted the heat shock protein 70 (*HSP70*) gene. The *HSP70* gene was found to be significantly upregulated during thermal stress, whereas during low pH stress the expression level of this gene decreased. This study provides experimentally validated stress-specific sets of stably expressed reference genes during climate change-induced stresses, which will benefit future gene expression studies on *Sinularia* cf. *cruciata* as well as other octocorals. Our results also highlight the potentially different acclimation strategies of octocorals to different sources of abiotic stresses, contributing to our understanding of the potential for the adaptation of coral reef organisms to a changing world.

Chapter 2:

Robust mitochondrial response to oxidative DNA damage in octocorals

Authors: Gaurav G. Shimpi, Sergio Vargas, Gert Wörheide

GGS conceived of the study, designed and performed the experiment, analyzed and interpreted the data and drafted the manuscript. GW and SV participated in the design of the study. All authors contributed to the discussion.

This chapter will be submitted as a standalone publication to the journal 'Global Change Biology'.

Abstract

Changing oceans are responsible for exerting excess oxidative stress on coral reef ecosystems, including octocorals, which comprise a large part of cnidarian diversity. Mitochondrial response to oxidative stress is intricately related to cellular homeostasis due to the susceptibility of its genome to oxidative damage. Octocoral mitochondrial genomes possess a unique mismatch repair gene, *mtMutS,* potentially capable of counteracting the effects of oxidative stress induced mitochondrial DNA (mtDNA) damage. Despite this unique feature, the response of octocoral mitochondria to increased oxidative stress has not studied and remains largely unknown. Here we show that the octocoral *Sinularia* cf. *cruciata* subjected to elevated temperature and low pH exhibit a stress-specific response to these changes, and is capable of reversing acute oxidative mtDNA damage caused by exogenous agents like hydrogen peroxide (H_2O_2), suggesting a concomitant recovery of host cell mitochondria necessary for survival. Damage to mtDNA was evident with associated changes in mtDNA copy number during all treatments. Stress-specific transcriptional response was recorded for stress

biomarker as well as mitochondrial genes during climate change-related events, indicating an up-regulation of *mtMutS* gene transcripts despite significant reduction in *COI* expression during pH stress. mtDNA damage, repair and mtDNA copy number variations due to H_2O_2 toxicity were also quantified and subsequent mitochondrial recovery was monitored. Initial mtDNA damage was found reversed within 5 hr. Our results indicate differential stress-specific resilience strategies of octocoral mitochondria to reverse the oxidative stress and its associated damage. These experiments provide the first account on the response of octocoral mitochondria, with its unique gene repertoire among animals, to different stressors and highlight its potential competence in conferring resilience to the host cells during different climate change scenarios.

Chapter 3:

Mitochondrial RNA processing in absence of tRNA punctuations: lessons from octocorals

Authors: Gaurav G. Shimpi, Sergio Vargas, Angelo Poliseno, Gert Wörheide

GGS and SV conceived of the study. GGS designed and performed the experiment, analyzed and interpreted the data. GW and SV participated in the design of the study. AP contributed to briefly at completion phase and analyzed the data. GGS drafted the manuscript. All authors contributed to the discussion.

This chapter will be submitted as a standalone publication to Molecular Biology and Evolution (MBE) Journal.

Abstract

Mitochondria, the energy-generators of eukaryotic cells, are semiautonomous units derived from a prokaryotic ancestor and known to possess a highly reduced though crucial complement of energy production machinery coded in their compact genomes. The diversity of these mitogenomes is staggering among early branching animals with respect to size, gene density and content, genome arrangements, and number of tRNA genes, especially in cnidarians. This last point is of special interest as tRNA cleavage drives the maturation of mitochondrial mRNAs and is a primary mechanism for mt-RNA processing in animals. Information on the expression and processing of mitochondrial gene transcripts from non-bilaterian metazoans, some of which possess a single tRNA gene in their mitogenomes, is essentially lacking. Here we characterized the mature mitochondrial mRNA transcripts in species of the octocoral genus *Sinularia*

(Alcyoniidae:Octocorallia) using different molecular methods. Most mt-mRNAs were polycistronic units containing two or three genes and 5' and/or 3' untranslated regions (UTRs) of varied length. The octocoral specific, mtDNA-encoded mismatch repair gene, *mtMutS*, was found to undergo alternative polyadenylation (APA) suggesting a unique regulatory mechanism for this gene. In addition, a long noncoding RNA (lncRNA) complementary to the *ATP6* gene (lnc*ATP6*), potentially involved in antisense regulation of its gene expression, was detected. Mt-mRNA processing in early-branching animals bearing a reduced mt-tRNA complement appears to be complex. Considering the variety of mitochondrial genome arrangements known in cnidarians our findings provide a first glimpse into mtDNA transcription, mt-mRNA processing and its complexity among the early branching animals and represent a first step towards understanding its evolutionary implications.

Chapter 4:

Alternate strategies for the construction of DNA heteroduplex plasmid substrates for *in vitro* mismatch repair assays

Authors: Gaurav G. Shimpi, Sergio Vargas, Gert Wörheide

GGS and SV conceived of the study, designed and performed the experiment. GW participated in the design of the study. GGS analyzed and interpreted the data, and drafted the manuscript. All authors contributed to the discussion.

This chapter will be submitted as a standalone publication to the 'DNA Repair' journal as a methodological article.

Abstract

Mismatch repair (MMR) is one of the most important DNA repair mechanisms present in the cell, pivotal to maintain genomic integrity. The MMR assay, described in almost two decades ago, is the most basic and commonly used method to detect *in vitro* MMR activity of cellular extracts and/or expressed proteins. However, the ease of using this method is restricted by the lack of simple, reproducible and easy-to-adopt ways of preparing MMR substrates i.e., nicked plasmids containing defined lesions. Here, we demonstrate simple and reproducible strategies of preparing large quantities of pure heteroduplex plasmids containing defined mismatches. The strategies described involve the use of synthetic oligonucleotides, the commercially available plasmid pGEM-T, and

nicking enzymes. Alternatively, bacterial packaging cells lines containing engineered phagemid pGEM-T construct producing ssDNA without the need of helper phage can be utilized, hence providing added flexibility and choice. These integrated approaches help to prepare different mismatch substrates in large quantities, enhancing the usability of MMR assay and extending its range and accessibility to wider research groups.

Chapter 5:

A cautionary tale of the octocoral mitochondrial mismatch repair (mtMutS) protein expression in *E. coli*

Authors: Gaurav G. Shimpi, Sergio Vargas, Gert Wörheide

GGS conceived of the study, designed and performed the experiment, analyzed and interpreted the data, and drafted the manuscript. GW and SV participated in the design of the study. All authors contributed to the discussion.

This chapter will be submitted as a standalone publication.

Abstract

The octocoral mitochondrial mismatch repair gene, the *mtMutS*, is the only known organellar mismatch repair (MMR) gene in animal kingdom encoded entirely by the mitochondrial genome. A self-contained functional role has been proposed for this protein, which shares a common ancestor with the bacterial mutS proteins and appears to have been horizontally transferred to the octocoral mitochondria from an epsilon-proteobacterium or a DNA virus. It is known that the *mtMutS* is transcribed, however, the presence of its protein product in the octocoral mitochondria and its biological activity remains to be experimentally determined. Here, we provide evidence pointing towards the presence of the mtMutS in the mitochondrial fraction. Artificially deleted cDNAs for *mtMutS* gene were detected due to the presence of direct repeats in the coding sequence. Moreover, we amplified, cloned and attempted to express the full mtMutS in *E.coli*. This was however not possible. A partial his_6-tagged protein containing N- and C-terminal mtMutS domains was successfully expressed and purified using Ni^{2+} affinity chromatography from inclusion bodies. Bioinformatic analyses suggested a high local hydrophobicity as a contributing factor associated with difficulties in expressing mtDNA-encoded, potentially matrix-localized, non-membrane proteins inside bacterial hosts.

CHAPTER 1

Evaluation and Validation of Reference Genes for qPCR Analysis to Study Climate Change-Induced Stresses in *Sinularia* cf. *cruciata* (Alcyonidae: Octocorallia)

This chapter will be submitted as a standalone publication to the Journal of Marine Experimental Biology and Ecology

Chapter 1

Evaluation and Validation of Reference Genes for qPCR Analysis to Study Climate Change-Induced Stresses in *Sinularia* cf. *cruciata* (Alcyonidae: Octocorallia)

1.1 Introduction

Coral-reefs consist of hard corals, soft corals, and the other flora and fauna associated with them and are popularly referred to as the rainforests of the oceans by virtue of the vast diversity of organisms they host and the goods and services they provide to mankind (Moberg and Folke, 1999). However, the rise in atmospheric CO_2 due to increasing anthropogenic activities and the consequent rise in the seawater temperature and reduction in oceanic pH has resulted in a collapse of coral-dinoflagellate symbiosis (Weis, 2008) and decreased calcification as well as growth (Marubini et al., 2008). The apparent increase in oxidative stress at the cellular level (Lesser, 2006) leads to apoptosis and necrosis (Richier et al., 2006; Tchernov et al., 2011), and thus, severely affects coral health (Lough, 2008), ultimately causing partial or complete colony mortality and mass bleaching events (Brown, 1997; Hughes et al., 2003). To gain a deeper understanding of the transcriptional response of corals to different sources of abiotic stress and the resulting adverse effects and/or potential resilience, different tools for gene expression profiling have been utilized (Lõhelaid, H et al., 2014; Maor-Landaw et al., 2014; Pratlong et al., 2015). Among them, quantitative real-time reverse transcription polymerase chain reaction (qRT-PCR), or simply qPCR, is a reliable, reproducible and highly sensitive tool for the quantification of selected mRNA transcript levels. qPCR is the method of choice for pinpointing and validating the regulation of specific genes under specific conditions with precision in a cost-effective manner (Higuchi et al., 1993; Gibson et al., 1996; Heid et al., 1996; Fink et al., 1998; Schmittgen et al., 2000).

Despite the power and general applicability, accurate expression profiling using qPCR is influenced by several factors such as RNA quality, stability and purity, reverse transcription efficiency, and amplification efficiency (Vandesompele et al., 2002). These sources of variation make normalization of the samples, which may have been obtained from different sources, time-points and individuals, necessary (Radonić et al., 2004). A commonly used normalization strategy involves assessing changes in the expression of target genes relative to one or more internal control genes also called the reference genes (RGs) (Freeman et al., 1999). However, the usefulness of the qPCR technique heavily relies on these internal/endogenous control genes, which presumably are stably expressed even during specific experimental treatments (Bustin, 2002; Vandesompele et al., 2002). Housekeeping genes (HKGs) are typical RGs due to their constitutive expression in different tissues and under different conditions. However, not all HKGs are free from the influence of the experimental conditions and their expression levels may vary depending on the nature and extent of the treatments, leading to erroneous expression estimates of the gene of interest (Dheda et al., 2005). The use of inappropriate RGs, i.e., genes that may be influenced by the treatment, result in erroneous estimates of target transcript levels and loss or gain of statistical significance (Ferguson et al., 2010), and thus, adversely influence the outcome and conclusion of a study (Dheda et al., 2004; Dheda et al., 2005). Hence, an important consideration for the successful quantification of gene expression using qPCR is the selection of the reference(s) to be used for normalization. Consequently, proper evaluation and validation of a specific set of the most stably expressed RGs is a prerequisite for any gene expression study to avoid biases in determining target gene expression and to obtain an accurate and reliable estimation of the changes induced by the experimental treatments (Vandesompele et al., 2002; Bustin et al., 2009; Guénin et al., 2009; Kozera and Rapacz, 2013).

Only a few published studies on the members of phylum Cnidaria carried out an analysis of gene expression to deal specifically with a systematic validation of internal control genes used (Pagarigan and Takabayashi, 2008; Rodriguez-Lanetty et al., 2008). Most other studies either utilized several different internal control genes or those recommended in the above-mentioned publications (DeSalvo et al., 2008; Meyer et al., 2009; Meyer et al., 2011). Moreover, among cnidarians, a strong emphasis has been placed on scleractinian (stony) coral (Hexacorallia, Scleractinia) gene expression profiling while there is still a lack of information on experimentally validated, stably

expressed internal control genes for other cnidarians, such as those from the subclass Octocorallia.

Octocorals (soft corals), a dominant benthic component of many coral reefs, are important constituents of a healthy reef ecosystem. The genus *Sinularia* is among the most widespread zooxanthellate soft coral belonging to the Octocorallia. These corals occur abundantly in the Indo-Pacific where they are one of the most dominant species of large ecological importance (Benayahu and Loya, 1977). Moreover, the members of this genus are pharmaceutically important because they produce a wide range of bioactive metabolites (Aceret et al., 1998; Ahmed et al., 2006; Lakshmi and Kumar, 2009; Yang et al., 2013; Chen et al., 2015) that exhibit several different biological activities (Aceret et al., 1998; Li et al., 2005; Su et al., 2008). However, the ecological dominance of the *Sinularia* species is challenged by coral-bleaching events, where up to a 90% mortality rate has been recorded (Fabricius, 1995; Loya et al., 2001).

If we aim to better understand the response and potential for the resilience of these organisms to climate change at the transcriptional level, we must determine a properly validated abiotic stress-specific set of RGs that can be used to accurately determine the effect of various abiotic stressors at the expression level using qPCR for the members of the subclass Octocorallia. Hence, in this study we evaluated the expression stability of seven genes using five different statistical methods during thermal and low-pH stress, the two important climate change-induced threats to reef organisms, focusing on the octocoral *Sinularia* cf. *cruciata*. We assessed the suitability of those seven genes as endogenous RGs for the relative gene expression quantification in qPCR assays using the *HSP70* gene as a case in point. By investigating the best normalizing gene combination for each stress-type as well as the stress-specific differential expression of the *HSP70* gene, this study aims to provide a basis for future gene expression studies on the genus *Sinularia* and other octocorals to gain a better mechanistic understanding of octocoral stress responses and their future in the changing oceans.

1.2 Materials and Methods

1.2.1 Coral collection and maintenance

All of the corals used in this study were maintained in a closed circuit seawater aquarium under controlled conditions (Temperature 25 ± 1 °C, pH 8.2 ± 0.1). Every week, half of the seawater was changed with fresh artificial seawater. All of the corals

were maintained on a 12 h light / 12 h dark light-regime provided by LED light (GHL Mitras LX 6200-HV) at a light intensity of 14 ± 2 kLux. A similar light regime was used for both the control and the experimental system mentioned below.

1.2.2 Experimental design

To determine the effect of rising seawater temperature and decreasing pH on the gene expression stability of selected candidate genes, nubbins of *Sinularia cf. cruciata* were exposed to these conditions (see below). All of the experiments were performed in biological and technical triplicates, and the controls and the treated samples were snap frozen in liquid nitrogen and subsequently stored at -80°C until RNA extraction.

1.2.2.1 Thermal stress experiment

Three *Sinularia* nubbins of similar size were placed in an experimental 10 L tank exposed to acute thermal stress. The temperature in the experimental tank was raised gradually from 26 °C to 34 °C over a period of 2 h after which it was maintained at 34 °C for a subsequent 6 h. Three control nubbins were maintained in a similar tank as the experimental tank but the temperature was kept at 26ºC during the entire course of the experiment. Strychar et al. (Strychar et al., 2005) observed a mortality of *Sinularia sp.* within 24 h upon exposure to the 34 °C temperature. Here, *Sinularia* cf. *cruciata* were therefore exposed to 34 °C for only 6 h to understand the short-term acute thermal stress response.

1.2.2.2 Low pH stress

The rise in carbon dioxide emissions is leading to a lowered oceanic pH apparent from a reported decreased pH of 0.1 units since the pre-industrial era and is predicted to further decrease by another 0.4 units by the end of this century (Haugan and Drange, 1996; Orr et al., 2005; Solomon et al., 2007; Kleypas and Langdon, 2013). Based on these report, to understand the effect low-pH, three *Sinularia* nubbins were subjected to lowered seawater pH by pumping carbon dioxide (CO_2) into the experimental tank to maintain a stable low pH value of 7.5 units. The pH was first reduced to a value of 7.5 over a period of 2 h and then maintained at this value for 24 h. The pH value was recorded throughout the experiment and was observed to be constant at 7.5. The corals were sampled after this 24 h period. The control nubbins were maintained under a normal pH of 8.2, and the temperature in both of the tanks was kept constant at 26 °C.

1.2.3 Total RNA extraction and cDNA synthesis

Total RNA was extracted from the control as well as the treated samples using TRIzol reagent (Invitrogen, USA) following the manufacturer's instructions. Contaminating DNA was eliminated from the RNA extracts upon using RQ RNase-free DNase (Promega, USA) according to the manufacturer's protocol. This treated RNA was precipitated using Sodium Acetate-Ethanol precipitation. The purity of the RNA was determined using a Nanodrop ND-1000 spectrophotometer (Thermo Fisher Scientific, USA). The RNA samples with an absorbance at OD260/280 and OD260/230 ratio ~ 2.0 were used for further analysis. The RNA integrity was verified by 1% agarose gel electrophoresis as well as by using Bioanalyzer (Agilent Inc., USA). The RNA extracts with a RIN value ≥ 7.5 were used for cDNA synthesis (data not shown). For each sample, approximately 1 µg of total RNA was reverse transcribed using the ProtoScript® II First Strand cDNA Synthesis Kit (New England Biolabs, Germany) employing an anchored oligo-(dT) primer in a 20 µl reaction according to the manufacturer's instructions.

1.2.4 Candidate reference genes

The candidate genes β-actin (*ACTB)*, α-tubulin (*TUBA)*, β-tubulin (*TUBB)*, elongation factor 1-α (*EF1A)*, glyceraldehyde-3-phosphate dehydrogenase (*GAPDH),* ribosomal protein L12 (*RPL12*) and signal recognition particle 54 (*SRP54*) were amplified from the cDNA using previously described and newly designed degenerate primers (Appendix 1.6.1). In most of the cases a touchdown PCR approach was employed. The PCR conditions were as follows: 95 °C for 2 min followed by 10 cycles at 95°C for 20 s, 55°C for 30 s, and 72°C for 60 s, reducing the annealing temperature by 1°C per cycle, followed by 25 cycles at 95°C for 20 s, 45°C for 30 s, and 72°C for 60 s. The PCR products were separated on a 1% agarose gel by electrophoresis. The PCR products showing a clear, single amplicon of the correct size were excised from a 1% agarose gel, purified using the NucleoSpin Gel and PCR purification kit (Macherey-Nagel, Germany), and sequenced using BigDye Terminator v3.1 (Applied Biosystems, USA) and analyzed on an ABI 3730 DNA Analyzer at the Sequencing Service of the Department of Biology, LMU München. The sequences obtained were analyzed using Geneious 6.1 software (Biomatters Ltd.) (Kearse et al., 2012). Each gene was compared against the GenBank BLAST database to verify their homology and was aligned against cnidarian orthologous sequences available from GenBank. Additionally, the DNA

sequences were translated to amino acid sequences and submitted to CDART (Geer et al., 2002) to confirm the presence of each gene's corresponding accurate conserved domain to assure sequence affiliation to a particular gene. Only high quality sequences were chosen for specific qPCR primer design.

1.2.5 qPCR primers

Primers for qPCR were designed from the above-mentioned DNA sequences using Primer3 (Untergasser et al., 2012). All of the guidelines for qPCR primer design (Rodriguez et al., 2015) were followed. pcrEfficiency (Mallona et al., 2011) was used for primer efficiency predictions, and only the primers that showed 100% *in silico* PCR efficiency were chosen for further experimentation. The specificity and efficiency of the selected primers were verified with qPCR using cDNA as a template (Appendix 1.6.4), and the sequence identity of these amplicons as well as the PCR efficiency were confirmed prior to performing the experimental qPCR assays. Details of all the qPCR primers designed for this study can be found in Table 1.1

Table 1.1 Primers designed for qPCR with amplicon characteristics.

No.	Gene Symbol	Primer Sequences (5' to 3')	Size (bp)	Amp. Tm(°C)	Mean efficiency	
					Thermal	Low pH
1	*ACTB*	for: CCAAGAGCTGTGTTCCCTTC	107	83.8	2.01	1.97
		rev: CTTTTGCTCTGGGCTTCGT				
2	*TUBA*	for: AGATGCCGCCAATAACTACG	100	81.3	2.04	1.96
		rev: TGTGCATTGATCAGCCAGTT				
3	*TUBB*	for: ATGACATCTGTTTCCGTACCC	115	80.5	2.04	1.99
		rev: AACTGACCAGGGAATCTCAAGC				
4	*EF1A*	for: TCGCAGGCTGATTGTGCTGT	283	82.5	1.97	1.96
		rev: GTTGTCTCCATGCCATCCAGA				
5	*RPL12*	for: GCTAAAGCAACTCAGGATTGG	141	80.5	2.02	1.97
		rev: CTTACGATCCCTTGGTGGTTC				
6	*GAPDH*	for: GCACAACAAACTGTCTTGCACC	128	80.2	2.01	1.96
		rev: CTTTGCAGAAGGTCCATCAAC				
7	*SRP54*	for: TGGATCCTGTCATCATTGC	184	79.5	2.05	1.97
		rev: TGCCCAATAGTGGCATCCAT				
8	*HSP70**	for: CCCCCTTATACTCCACTTCAAC	274	83.5	2.01	2.02
		rev: GGTGTATTTCAACACGGCAAAG				

Note: * the target gene in this study

1.2.6 Quantitative Real-time RT-PCR (qPCR)

The qPCR was performed on a Rotor-Gene Q 2plex system (Qiagen, Germany) using KAPA SYBR FAST universal mastermix (Peqlab, Germany) in 15 µl reactions containing 1 µl of diluted cDNA, 7.5 µl of 2X mastermix, and 250 to 400 nM of each primer. The two-step qPCR included an initial denaturation step of 3 min at 95 °C followed by 40 cycles of 95 °C for 10 s and 60 °C for 20 s. A non-template control was always included in each assay. A melting curve analysis was performed at the end of each qPCR to confirm amplification specificity (Appendix 1.6.4). Further, the amplified PCR products were also checked by agarose gel electrophoresis after each assay for confirmation (Appendix 1.6.5).

1.2.7 Data Analysis

After qPCR, the raw, non-baseline corrected fluorescence data were analyzed using LinRegPCR (Ramakers et al., 2003). This program performs baseline correction and linear regression analysis and calculates the quantification cycle (Cq) values and amplification efficiency for each amplification curve. These Cq values were used for further analysis.

To assess the expression stability across each experimental condition and to rank the candidate RGs accordingly, four different methods were used, namely the comparative ΔCt method (Silver et al., 2006), geNorm (Vandesompele et al., 2002), BestKeeper (Pfaffl et al., 2004), and NormFinder (Andersen et al., 2004). All of these approaches use different assumptions to yield rankings for the most stably expressed RGs.

Briefly, the comparative ΔCt is a simple approach that relies on the relative gene expression of a pair of genes within each sample to give an idea about the best reference gene. GeNorm measures the per gene average pairwise standard deviation (SD) of the Cq values to determine a stability value (*M*) and eliminates candidate genes with the lowest transcript stability (highest *M* value) in a stepwise manner to return only two candidate genes with the highest stability (lowest *M* values). GeNorm also determines the optimum number of RGs needed for normalization (see ref. for further details) (Vandesompele et al., 2002). NormFinder, on the other hand, selects the best reference gene by considering intra- and inter-group variation, rather than overall stability across the different sample groups (Andersen et al., 2004). NormFinder also determines the best combination of two genes depending on inter-group stability. GeNorm and NormFinder require relative quantities (RQ) as an input rather than Cq values directly.

BestKeeper uses the Cq values directly to rank the candidate genes based on the SD of the Cq values and carries out repeated pairwise correlation analysis to select the gene that is showing the lowest SD and is highly (and significantly) correlated with the remaining genes to select the best reference gene.

In addition to these methods, RefFinder, a web tool integrating all four methods described above, was used to determine the 'overall final ranking' of the RGs (http://www.leonxie.com/referencegene.php).

1.2.8 Reference gene validation and expression of the heat-shock protein 70 (*HSP70*) gene

The heat shock protein 70 gene (*HSP70*) was used as a target to validate the selected reference genes and to analyze the stress-induced differential expression. *HSP70* is one of the members of the heat shock protein family that functions as a molecular chaperone and is involved in protein biogenesis as well as stress responses. *HSP70* gene expression has been used as an indicator of a coral's stress status (van Oppen and Gates, 2006), and its response to thermal stress (Haguenauer et al., 2013; Lõhelaid, H et al., 2014) and air exposure (Teixeira et al., 2013) have been investigated in octocorals. The response of this gene to low seawater pH has not been investigated so far, despite the potential resilience of octocorals to decreased oceanic pH (Gabay et al., 2014). Gene expression analysis was performed using the method described by Pfaffl et al. (Pfaffl et al., 2002) implemented in REST 2009. Cq values, taking into account the mean PCR efficiency, were obtained from LinRegPCR. Initially, expression ratios were calculated for the target gene using one reference gene at a time to demonstrate their effect on the estimation individually, whereas the final analysis of target gene expression was performed using the two best RGs for a more accurate normalization, as described previously (Vandesompele et al., 2002). The statistical significance of the gene expression was tested using randomization and bootstrapping with 5000 iterations, and standard errors were calculated with the Taylor algorithm implemented in REST 2009. The data are represented as the mean ± SE, and REST $p < 0.05$ was considered statistically significant. This study conforms to the MIQE guidelines (Bustin et al., 2009).

3 Results

1.3.1 Selection, amplification and sequencing of the reference genes

Single bands of the expected size were obtained after performing PCRs using degenerate primer pairs and cDNA as a template. The sequence identities to the first GenBank Blast-match ranged from 77% for *RPL12* to 86% for *ACTB* (Appendix 1.6.2). cDART (**c**onserved **D**omain **A**rchitecture **R**etrieval **T**ool) confirmed the presence of conserved domains that belong to the targeted HKGs. Three other octocorals belonging to different genera were also sequenced using these primer pairs for comparison with varied success rates, and all of the sequences generated will be submitted to the European nucleotide archive.

1.3.2 Primers for qPCR

Gene-specific primers for qPCR were designed using nucleotide sequences obtained from *S.* cf. *cruciata*. All of the primer sets yielded a single PCR product, which ranged between 100 bp and 283 bp (Table 1.1) and belong to the species of interest. In addition, each primer pair yielded products displaying single peaks in their melting profile, suggesting primer specificity (Appendix 1.6.4, 1.6.5). LinRegPCR indicated a mean amplification efficiency value during each assay ranging between 96% and 106% (Table 1.1) for the selected RGs as well as the target gene, suggesting a very efficient qPCR system for the species and genes under study.

1.3.3 Expression profiling of candidate reference genes

The expression profiles of all the candidate RGs exhibited slight variability and different levels of abundance under both experimental conditions. Overall, the range of observed Cq values was between 13.73 (*TUBA*) and 25.93 (*SRP54*), irrespective of the type of abiotic stress. The remaining 5 RGs were expressed at moderate levels, with mean Cq values of 19.42, 21.83, 18.77, 20.15, and 22.59 during thermal stress, and 15.31, 18.76, 16.01, 19.16, and 19.70 during pH stress for *ACTB, TUBB, EF1A, RPL12,* and *GAPDH*, respectively. The variability in the transcript abundance during pH stress was less compared to thermal stress (Figure 1.1). The target gene, as expected, showed high variability indicated by large boxes in Figure 1.1.

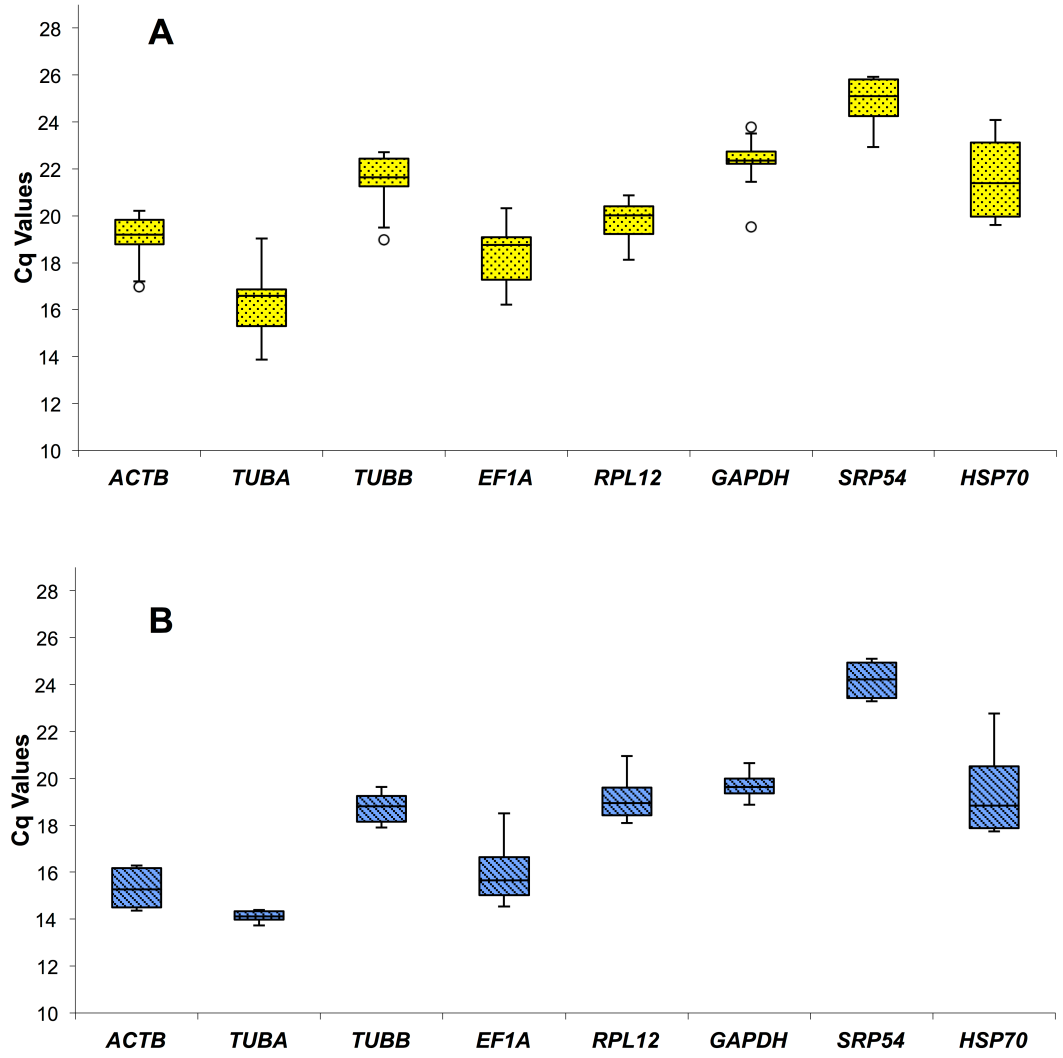

Figure 1.1 Distributions of the reference genes Cq values

Box plot representing the expression levels of reference and target genes for (A) during thermal stress and (B) during low pH stress. Each box corresponds to 25% and 75% percentile while the line across the box represents the median. The whiskers indicate the maximum and minimum values, whereas the hollow circles indicate the outliers.

The coefficient of variation (CV) value can be utilized as a first gross evaluation for the stability of RGs during multiple treatments. In general, during thermal stress, low CV values (CV < 6%) were observed for all of the candidate RGs indicating low variability. Similarly, during pH stress, CV was low for most of the genes (CV < 6%) except for *EF1A*, which exhibited high variability across the samples (CV=8.45%) (Table 1.2). There is an apparent variability in the expression of all the selected HKGs, suggesting

existent spatial and temporal alterations along with changes in the environmental conditions.

Table 1.2 Descriptive statistics of candidate reference gene Cq values.

Genes	Thermal Stress					pH Stress				
	Min Cq	Max Cq	Mean	SD	CV (%)	Min Cq	Max Cq	Mean	SD	CV (%)
ACTB	18.73	20.21	19.42	0.49	2.53	14.35	16.30	15.31	0.79	5.13
TUBA	15.19	19.04	16.63	0.93	5.61	13.73	14.40	14.11	0.24	1.69
TUBB	21.18	22.71	21.83	0.57	2.63	17.90	19.65	18.76	0.65	3.47
EF1A	17.21	20.32	18.77	0.90	4.79	14.54	18.52	16.01	1.35	8.45
RPL12	19.20	20.88	20.15	0.55	2.73	18.09	20.97	19.16	0.97	5.05
GAPDH	21.79	23.78	22.59	0.55	2.42	18.88	20.65	19.70	0.56	2.85
SRP54	24.14	25.93	25.24	0.59	2.32	23.29	25.10	24.19	0.80	3.32

Note: Minimum Cq value (Min Cq), Maximum Cq value (Max Cq), Mean, Standard deviation (SD), and Coefficient of variation (CV) are shown in the table.

1.3.4 Expression stability of candidate reference genes

1.3.4.1 ΔCt and geNorm analysis

ΔCt and geNorm are based on pairwise comparisons but employ different procedures and yield different outcomes. The most stable gene determined by the ΔCt method during thermal stress was *RPL12* followed closely by *TUBB*, whereas *TUBA* was determined as the least stable RG. For low pH stress, *ACTB* was the most stably expressed RG and *EF1A* was found to be highly variable. Additionally, *TUBB* was consistently detected as the second most stable candidate reference gene in both the treatments using this method.

geNorm analysis for the thermal stress experiment indicated *TUBB* and *GAPDH* as the most stable (*M* value for best gene combination 0.31), whereas *TUBA* was the least stable gene. In the pH stress samples, the same set of candidate RGs was found to be the most stable (*M* value for best gene combination 0.19), whereas *EF1A* was the least stable gene. Figure 1.2 shows the gene ranking according to their expression stability, and Table 1.3 indicates the *M* values.

Additionally, geNorm also determined the optimal number of RGs required for accurate normalization. In both the experimental conditions, V2/3 were less than 0.15, the threshold value (Figure 1.3), indicating that two RGs are required to accurately normalize gene expression in both treatment groups.

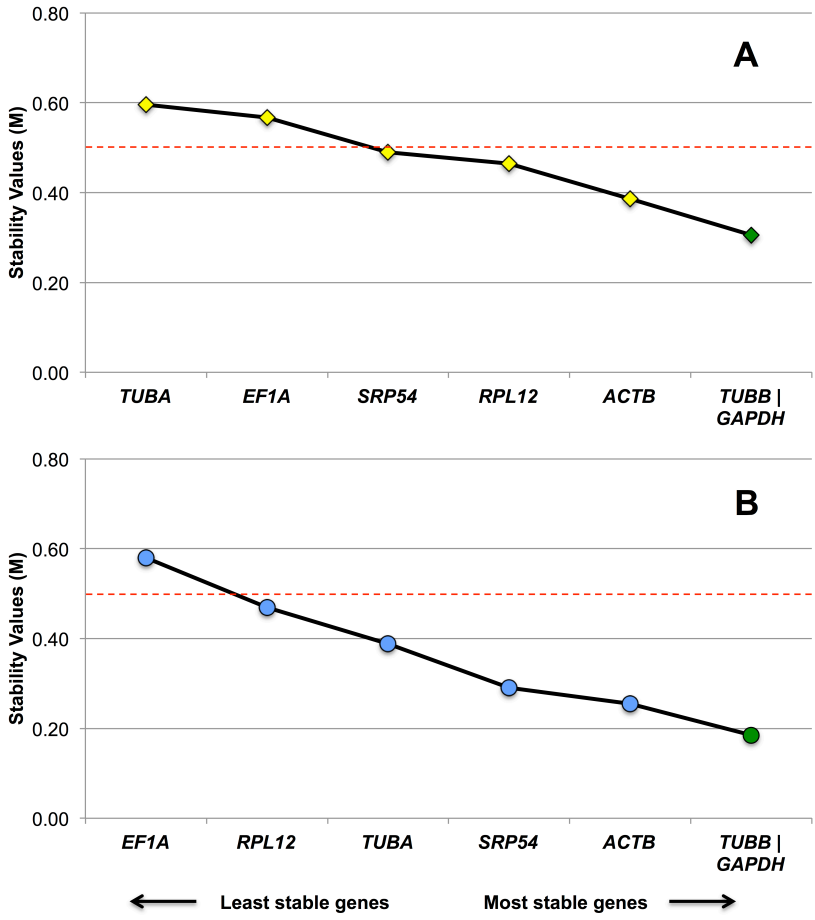

Figure 1.2 Expression stability of the candidate genes determined by geNorm

Genes on the X-axis and Stability value M on the Y-axis for (A) thermal stress and (B) pH stress. Genes were ranked from the least stable (left) to the most stable (right) based on the *M* value. The dotted line represents the threshold *M* value (0.50).

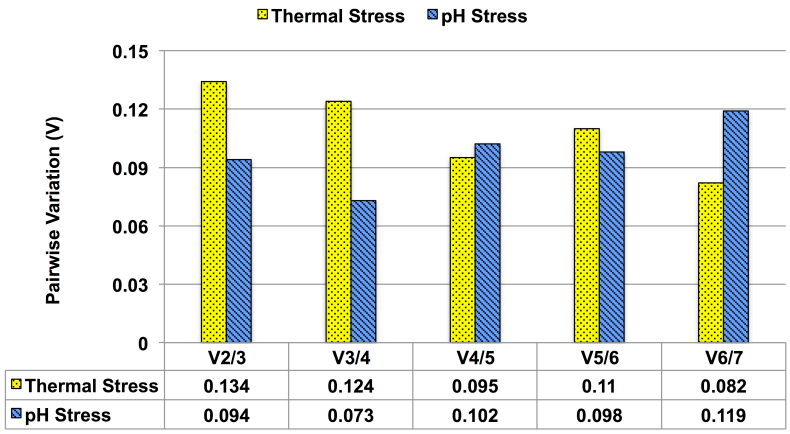

Figure 1.3 Pairwise variation analysis of the putative reference genes by geNorm

The pairwise variation (V_n / V_{n+1}) was analyzed between the normalization factors NF_n and NF_{n+1} to determine the optimal number of reference genes required for accurate normalization.

A value below threshold 0.15 denotes that additional reference genes will not markedly improve normalization.

1.3.4.2 BestKeeper and NormFinder analysis

For thermal stress, BestKeeper and NormFinder determined a different order of gene stability rankings, with *ACTB* (SD=0.41) and *RPL12* (Stability value = 0.126) top-ranked by these methods, respectively. Additionally, BestKeeper selected *EF1A* as the least stable RG, whereas NormFinder selected *GAPDH* as the least stable reference gene, in disagreement with the other three methods. *SRP54* was the third best gene for normalization as determined by both programs. Additionally, NormFinder recommended *RPL12* and *SRP54* as the best combination of reference genes for normalization (combined stability values = 0.085) based on the analysis of intra and inter-group variation (Figure 1.4).

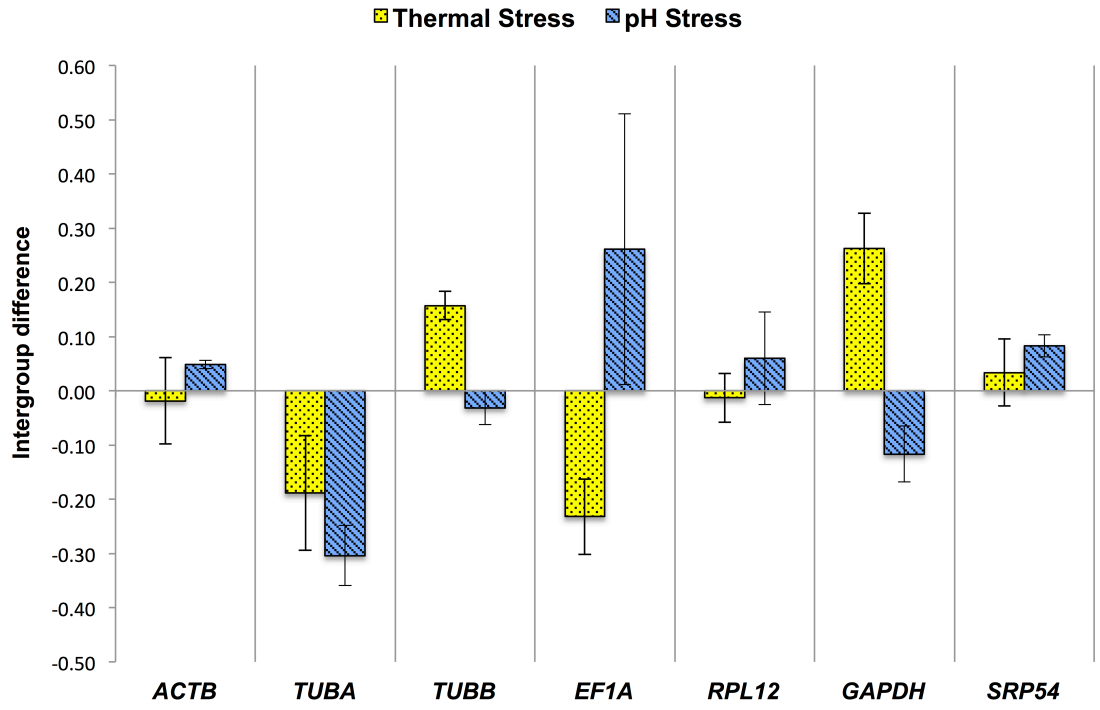

Figure 1.4 NormFinder analysis estimates of intra and intergroup variations

Inter-group variation is represented on the Y-axis and genes on the X-axis. Errors bars show the intra-group variations for (A) thermal stress and (B) low-pH stress. Intergroup differences closer to zero and with minimal error (intragroup variations) depict higher expression stability.

For pH stress, NormFinder found *ACTB* as the most stable gene in agreement with the ΔCt method, whereas *TUBA* was determined as the least stable. The recommended best

combination of genes during this type of abiotic stress was *ACTB* and *TUBB* (combined stability values = 0.062); BestKeeper rankings based solely on SD were not congruent with NormFinder. BestKeeper ranked *TUBA* as the most stable gene, whereas *EF1A* was the least stable and the only gene showing an SD higher than 1. However, considering the coefficient of correlation (r), *TUBB* closely followed by *ACTB* were the most stable genes, and *TUBA* was found unsuitable due to its low r value (r=0.781) (Appendix 1.6.3).

1.3.4.3 RefFinder

The comprehensive stability ranking derived by RefFinder for thermal stress from most stable to least stable reference gene was as follows: *RPL12* > *TUBB* > *ACTB* > *GAPDH* > *SRP54* > *EF1A* > *TUBA* (Table 1.3). Similarly, for pH stress the stability ranking was as follows: *ACTB* > *TUBB* > *SRP54* > *RPL12* > *GAPDH* > *EF1A* >*TUBA* (Table 1.4). Table 1.3 and 1.4 summarize the stability values and gene ranking determined by all 5 of the methods mentioned above.

Table 1.3 Gene Stability values and Rankings for thermal stress experiments.

Gene	ΔCt		geNorm		BestKeeper		NormFinder		RefFinder	
	Rank	Avg. SD	Rank *	*M* value	Rank **	SD	Rank	Stability Value	Rank	Stability Value
ACTB	4	0.57	3	0.39	1	0.41	2	0.126	3	2.63
TUBA	7	0.67	7	0.6	6	0.63	5	0.290	7	6.48
TUBB	2	0.54	1	0.31	5	0.50	4	0.209	2	2.34
EF1A	5	0.66	6	0.57	7	0.66	6	0.324	6	5.69
RPL12	1	0.52	4	0.46	4	0.45	1	0.089	1	2.00
GAPDH	6	0.67	1	0.31	2	0.41	7	0.345	4	3.03
SRP54	3	0.55	5	0.49	3	0.45	3	0.137	5	3.08

Table 1.4 Gene Stability values and Rankings for pH stress experiments.

Gene	ΔCt		geNorm		BestKeeper		NormFinder		RefFinder	
	Rank	Avg. SD	Rank *	*M* value	Rank **	SD	Rank	Stability Value	Rank	Stability Value
ACTB	1	0.44	3	0.26	5	0.70	1	0.097	1	1.86
TUBA	6	0.70	5	0.39	1	0.20	7	0.39	5	3.66
TUBB	2	0.46	1	0.19	3	0.59	2	0.10	2	2.06
EF1A	7	0.86	7	0.58	7	1.05	6	0.38	7	7.00
RPL12	5	0.59	6	0.47	6	0.74	4	0.18	6	5.23
GAPDH	4	0.52	1	0.19	2	0.47	5	0.21	3	2.38
SRP54	3	0.49	4	0.29	4	0.75	3	0.16	4	3.46

Note: * geNorm finds two most stable genes instead of one.
** BestKeeper ranking is based on standard deviation alone.

Overall, as expected, the best reference gene varied depending on the treatment (*RPL12* in thermal and *ACTB* in pH stress), whereas the *SRP54* gene, predominantly ranked as the third best gene during both treatments, is suitable for both abiotic stress experiments alongside *ACTB* showing an overlap. *TUBA* and *EF1A* were found to be the least stable during both of the treatments, rendering them unsuitable for the normalization of the qPCR assay for this system. *TUBB* during thermal stress and *GAPDH* in both of the treatment groups exhibited high overall ranking by virtue of an apparent high ranking in geNorm and BestKeeper analysis. However, further analysis established *TUBB* unsuitable in thermal stress and *GAPDH* in both of the treatments (discussed below). For further confirmation, the expression of the three least stable reference genes when normalized using the three most stable genes was clearly observed to exhibit changes in the expression of the least stable gene due to the experimental treatments (Appendix 1.6.6).

1.3.5 Validation of candidate reference genes and the differential expression of *HSP70*

Heat-shock protein 70 gene (*HSP70*) was utilized as a proxy for analyzing normalization-bias introduced by individual candidate reference genes in gene expression quantification. The initial evaluation using a single gene for normalization clearly indicated that the *HSP70* gene is under regulation due to both thermal and pH stress with significant changes in its expression pattern in both of the treatments ($p<0.05$) (Fig 5). The *HSP70* transcripts were up-regulated in the thermal stress samples and down-regulated in the pH stress samples. However, as expected, the magnitude of *HSP70* up/down regulation determined by qPCR varied considerably in both of the experimental groups depending on the reference gene used for normalization. The fold change estimates ranged between 4.2 and 10.10-fold for thermal stress and -2.2 to -6.7-fold during pH stress depending on the RG used for normalization.

In the thermal stress samples, the three best RGs, *RPL12, SRP54*, and *ACTB*, when used independently as normalizer to quantify the expression changes of the target gene-*HSP70*, the fold changes in gene expression were inter-comparable and exhibited significant up-regulation (~7.4±0.4-fold, $p<0.05$). Use of the best 2 RGs (*RPL12*+*SRP54*) confirmed the observed estimate (7.5-fold, $p<0.001$) (Fig. 6). Additionally, the least stable genes as defined by RefFinder, i.e., *TUBA* and *EF1A*, tended to underestimate the *HSP70* gene transcript levels. Moreover, NormFinder's low

ranking genes such as *GAPDH* (7th) and *TUBB* (4th) resulted in overestimating the expression (thermal stress, Figure 1.5).

In the pH stress samples, all seven RGs showed a similar pattern when used individually for normalization i.e., down-regulation of *HSP70* was noted. However, the best genes, *ACTB*, *TUBB*, and *SRP54*, indicated a fold difference of comparable magnitude (~ -3.45±0.35-fold, $p<0.05$) (Figure 1.5). A decrease in the expression levels was clearly evident (-3.51-fold) when the two best RGs, (*ACTB* and *TUBB*) were utilized together to calculate the gene expression of the target gene (Figure 1.6). On the other hand, the least stable genes, *TUBA* (7th) and *EF1A* (6th), produced unreliable results by either overestimating or under representing the *HSP70* gene response to pH stress (Figure 1.5), respectively, when compared to the estimates by the two most stable genes in each experimental group.

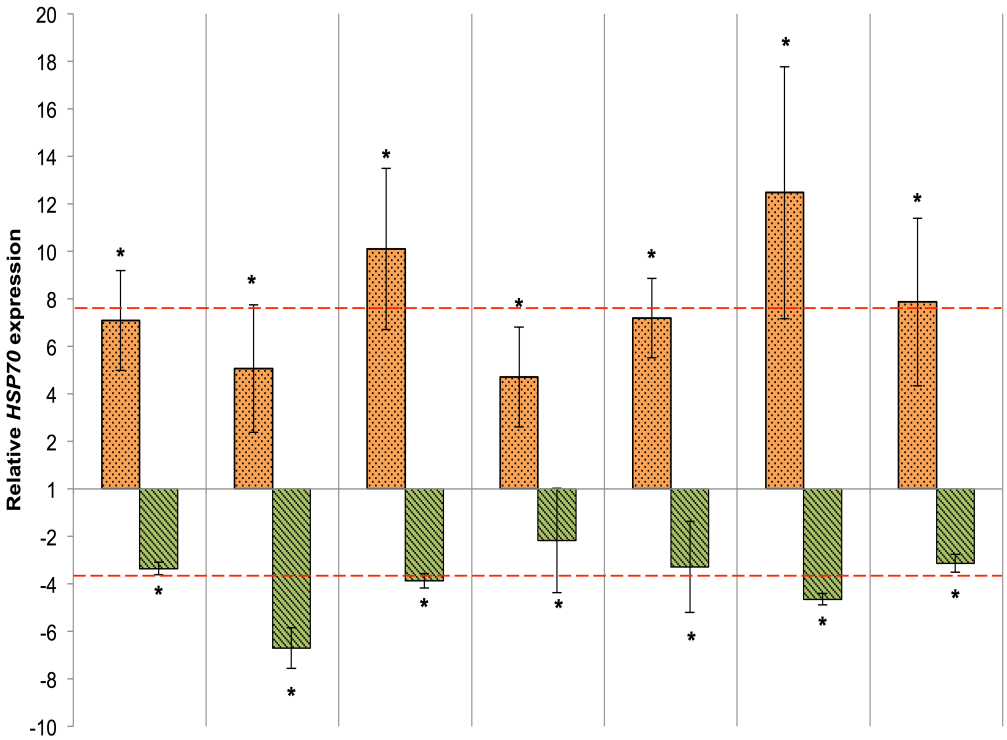

Figure 1.5 Comparison of the relative expression of the *HSP70* gene in both of the treatment groups using each RG separately for normalization

Relative expression ± SE of target gene normalized with each candidate reference gene individually during **(A)** thermal stress and **(B)** low pH stress is represented. The X-axis represents the gene names, and NormFinder gene ranks are shown in the brackets (Thermal/low pH stress). The dotted red line represents the gene expression levels obtained using the best pair of reference genes according to NormFinder for each treatment (refer to Fig 6). REST2009 was used for the analysis. (* indicate REST $p<0.05$, 5000 iterations).

NormFinder clearly yielded more comparable results, as shown above. Hence, the NormFinder-determined best pairs of RGs (thermal= RPL12 and SRP54, pH stress= *ACTB* and *TUBB*) were used for the final analysis of *HSP70* transcript levels. Thermal stress resulted in a 7.5-fold increase in *HSP70* expression ($p \leq 0.001$), whereas the expression was 3.5-fold decreased in low-pH treated samples relative to the control group ($p \leq 0.05$) (Figure 1.6).

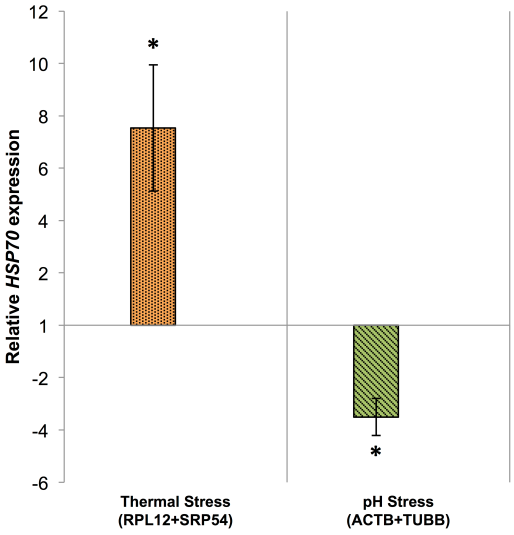

Figure 1.6 Relative expression of the *HSP70* gene normalized using a combination of the two best RGs

The NormFinder-determined best combination of RGs during thermal stress (*RPL12* + *SRP54*) and pH stress (*ACTB* + *TUBB*) used for the final analysis. The relative expression (fold change) values are depicted as the mean ± SE. REST2009 was used for the analysis. (* indicate REST $p \leq 0.05$, 5000 iterations).

1.4 Discussion

The genus *Sinularia* is a widely studied genus among octocorals with respect to population genetics (Bastidas et al., 2001), bleaching and symbiont loss (Strychar et al., 2005; Sammarco and Strychar, 2013), cell culture (Khalesi et al., 2008), calcification (Jeng et al., 2011), and various secondary metabolites (Lakshmi and Kumar, 2009). Additionally, there are studies employing mRNA-pool profiling techniques using an informatics-based analysis of kinetic profiles (Hoover et al., 2007; Hoover et al., 2008). However, despite ecological as well as pharmacological importance, *Sinularia* has not been studied so far with respect to gene expression changes during climate change scenarios using the qPCR method. To our knowledge, this study is the first detailed determination of expression stability of seven candidate genes to be utilized for the normalization of gene expression in the genus *Sinularia* as well as octocorals, in general, subjected to different abiotic stresses.

One of the most essential facets of a successful qPCR assay is the stability of RGs over a spatio-temporal scale, between different samples, treatments, conditions, etc. However, finding such ideal RGs requires validation under those experimental conditions because a universally appropriate RG is nonexistent.

The abiotic stressors or treatments chosen for the current study exhibit different modes of impact at the physiological and hence molecular levels on coral cells. Thermal stress, one of the major consequences of global warming, can result in mass coral bleaching (Hoegh-Guldberg et al., 2007) from disrupted coral-dinoflagellate symbiosis (Weis, 2008). Additionally, the acidification of seawater is reported to reduce the calcification rate in corals, leading to compromised organismal fitness (Doney et al., 2009; Chan and Connolly, 2013).

Previously, *ACTB* and *RPL12* were found to be stably expressed in symbiotic and aposymbiotic *Anthopleura elegantissima* sea anemones using cDNA microarrays (Rodriguez-Lanetty et al., 2008). *ACTB* was also found to be the second most stable gene in a scleractinian coral subjected to excess temperature and nutrients (Pagarigan and Takabayashi, 2008). In present study, *ACTB* was the only gene, alongside novel *SRP54*, which overlapped in both treatment groups, ranking the best in low-pH and third in thermal stress samples. Hence, *ACTB*, a cytoskeletal structural proteins gene, is a widely used RG that shows promise here as well. Similarly, a novel gene, *SRP54*, a signal recognition particle encoding gene responsible for recognizing and targeting specific proteins to the endoplasmic reticulum in eukaryotes (Luirink and Sinning, 2004), was detected as a suitable RG due to its stable expression for normalization during both of the treatments. On the contrary, *TUBA,* involved in cytoskeleton modulation, was found to be one of the least stable genes in both of the treatments and in thermal stress, respectively. Likewise, despite securing a second rank in both of the treatments, *TUBB* was found unsuitable and exhibited erroneous estimates in the thermal stress validation, but was suitable for pH stress. *RPL12*, on the other hand, was not found among the top 3 in the low-pH treatment despite ranking as the best RG for thermal stress. Moreover, *EF1A* was conjointly ranked lower by most of the methods in both of the treatment groups and hence is unsuitable for the normalization of gene expression. *RPL12* (for example, in pH treatment), *TUBB* (in thermal stress) and *GAPDH* (in both treatments) should be cautiously used as a reference based on their apparent variability and instability in expression, as shown earlier in different systems (Thorrez et al., 2008; Kozera and Rapacz, 2013). These observations signify the need

for the proper validation of RGs for specific treatment groups independently. The target gene *HSP70* is under strong regulation in both of the treatment groups apparent from the observed high magnitudes of changes (discussed below); however, the high variability from an actual change when less stable genes are used suggests that these RGs are likely to introduce greater error if the magnitude of the changes in gene expression is less than *HSP70* in this case, and hence capable of completely contradicting the conclusion as demonstrated previously (Dheda et al., 2005; Ferguson et al., 2010).

Gene stability rankings differ depending on the program used due to their different algorithms and analytical procedures (De Spiegelaere et al., 2015). Therefore, each strategy needs to be carefully evaluated while analyzing the actual stability of RGs for a particular experimental scenario. In the present study, differences in the stability rankings of RGs were evident. The geNorm results were found unreliable for thermal stress, as evident from the normalized *HSP70* expression values. The RGs ranked the best by geNorm seemingly exaggerate the actual expression levels of the *HSP70* gene estimated using the two best RGs. This observation is consistent with previous findings by Robledo et al (Robledo et al., 2014) who also found the geNorm results unreliable; however, geNorm was found useful for pairwise variation (*V*) analysis to detect the optimum RG required for the accurate normalization of gene expression.

BestKeeper recommends the SD threshold as 1, above which the gene can be considered inconsistent (Pfaffl et al., 2004), whereas geNorm assumes an expression stability *M* value of 0.05 as a threshold (Vandesompele et al., 2002). Hence, both of these methods were found legitimate for eliminating the worst RGs. For example, the geNorm analysis demonstrated that *TUBA* and *EF1A* during thermal stress and *EF1A* during pH stress are the least stable ($M > 0.05$), whereas BestKeeper eliminated *EF1A* during pH stress (SD>1), similar to geNorm.

NormFinder has advantages over other programs by taking into account intra and intergroup differences. In this study, the NormFinder results were relatively more congruent with the final cumulative rankings for the best RGs in both of the treatment groups. NormFinder determined *RPL12* and *ACTB* as the most stable reference genes during thermal and pH stress, respectively. Additionally, this approach also allowed the assessment of inter-group variation (Figure 1.4), based on which the best combination of two RGs is determined. Therefore, we found the NormFinder ranking the most useful for the current study, corroborating the findings of Robledo et al (Robledo et al., 2014),

as this ranking benefits from the intra and inter-group comparison and results in the most conservative and accurate estimates of gene expression. As reported previously (Robledo et al., 2014), we also observed that the ΔCt, Bestkeeper and NormFinder results correlate better to each other than to the results obtained by geNorm. Notably, NormFinder proposed totally different pairs for both of the treatment groups that were also found valid. Hence, the choice of RG also depends on the treatment, accentuating the need and benefits of proper validation.

To account for the discrepancies in the RG rankings among the different methods used, the RefFinder platform was used as a complementary tool that incorporates information from all four of the methods described above to establish a final comprehensive ranking of RGs per all seven genes during each treatment. Although RefFinder suffers from a few disadvantages, it yields an overall final stability ranking of the candidate RGs (De Spiegelaere et al., 2015). However, careful interpretation is necessary as the ranking of a less stable gene might get enhanced, for example, *TUBB* (during thermal stress) and *GAPDH* (in both treatments) ranked by geNorm as the best RG, leading to their increased RefFinder overall rankings, which could lead to an inaccurate determination of transcript abundance if these genes were to be used as normalizers. Additionally, RefFinder considered BestKeeper's SD but not the coefficient of correlation (r) and *p* value (second important criteria) for ranking the RGs, which wrongly resulted in a better ranking of unsuitable RGs (for example, *GAPDH* in thermal stress and *TUBA* during pH stress) (Appendix 1.6.3). These observations clearly highlight the need for careful validation of algorithms used for RG ranking and empirical determination of stable and/or suitable RGs for qPCR.

Environmental stress results in major cellular and physiological changes in corals. For example, changes in the expression patterns of the genes responsible for metabolic pathways, biomineralization, oxidative stress response, apoptosis, and membrane transporters have been reported (Kaniewska et al., 2012); however, the stress responses of soft corals are generally poorly understood. To our knowledge, this is one of the first studies on octocoral *Sinularia* providing insights on the *HSP70* gene expression pattern during simulated ocean warming and acidification scenarios using qPCR.

The observed increase in *HSP70* gene expression is congruent with previous studies on other octocorals that showed a similar trend for the *HSP70* gene during thermal stress (Haguenauer et al., 2013; Lõhelaid, H et al., 2014), further demonstrating the likelihood of an octocoral host resisting future changing thermal conditions as suggested by

Madeira, et al. (Madeira et al., 2015). Contrary to thermal stress, the noticeable decrease in the expression levels of the *HSP70* gene under low-pH conditions was incongruent with the previous findings that suggested no differential expression in *Acropora digitifera* larvae (Nakamura et al., 2012). Similarly, studies on sea urchin larvae and amphipod have reported a slight decrease or no significant change in *HSP70* expression during acidification stress (Hauton et al., 2009; O'Donnell et al., 2009). The changes in the external pH resulting in acid/base imbalance are unlikely to result in cytoplasmic protein denaturation. Hence, *HSP70* gene induction to refold denatured proteins is not necessary, unlike during thermal stress. Clearly, the focus here is on suppressing metabolism to reduce excess energy investment on unnecessary pathways, diverting it to important ones such as ion transport and energy production (Vidal-Dupiol et al., 2013), which explains the down-regulation of *HSP70*. This finding clearly suggests stress-specific differential responses in *S.* cf. *cruciata* by mounting an adequate response to acute heat stress, whereas energy prioritization is the strategy under elevated CO_2 conditions, contributing to resilience potential.

1.5 Conclusions

We provide the first systematic validation of suitable RGs for ocean acidification- and warming-induced abiotic stress related studies on the octocoral *Sinularia* cf. *cruciata* using the qPCR technique. The experimental condition-dependent validity of RGs was observed, wherein *RPL12* during acute thermal stress and *ACTB* during low pH stress were detected as ideal RGs for accurate normalization. *SRP54*, a new reference gene not widely used, was found among the most stably expressed genes in either treatment and is an interesting target to complement the other "treatment-specific" genes. We also show a stress-dependent differential response of the octocoral on *HSP70* transcriptional levels and highlight their specific strategies for potential resilience. We expect these results will provide the basis for future investigations directed towards increasing our understanding of the mechanisms involved in octocoral stress responses and their resilience to adverse future ocean conditions.

1.6 Appendix

Appendix 1.6.1 Description of candidate reference genes and degenerate primers used.

Appendix 1.6.2 BLAST results for selected HKGs sequenced using degenerate primers.

Appendix 1.6.3 BestKeeper results.

Appendix 1.6.4 Melting curves for all of the selected references and target gene amplicons.

Appendix 1.6.5 Gel image showing the amplification for all of the genes under study.

Appendix 1.6.6 Comparison between the least stable RGs and the most stable RGs

Appendix 1.6.1. Description of candidate reference genes and degenerate primers used.

Sr. No.	Gene Symbol	Gene Name	Cellular Function	Primer Sequence (5' to 3')	Length (bp)	Reference
1	*ACTB*	β-Actin	Cytoskeleton structure protein	F- TCYGGWATGTGYAARGCYGG	1046	*
				R- TACTCCTGCTTGGARATCCACA		
2	*TUBA*	α-Tubulin	Cytoskeleton structure protein	F- RGTNGGNAAYGCNTGYTGGGA	1196	[1]
				R- CCATNCCYTCNCCNACRTACCA		
3	*TUBB*	β-Tubulin	Cytoskeleton structure protein	F- GGWGCWGGBAAYAACTGGGC	519	[1]
				R- VGGCATRAAGAARTGRAGACG		
4	*EF1A*	Elongation factor-1α	Translation factor	F- ATGGGAAAAGGNTCNTTCAAATATGC	638	This study
				R- GTTCCAATTCCTCCAATYTTGTA		
5	*RPL12*	Ribosomal protein L12	Ribosomal protein	F- TTGCYCCNAAGATYGGTCC	319	This study
				R- CCAAGGATCTCCTTNACWGTKCC		
6	*GAPDH*	Glyceraldehyde 3-phosphate dehydrogenase	Glycolysis and gluconeogenesis	F- ATGTTYGTRATGGGTGTNAA	320	This study
				R- ACACGGAANGCCATNCCAGT		
7	*SRP54*	Signal recognition particle 54	Protein translocation	F- GTGCNGATACATTCAGAGCWGGTGC	534	This study
				R- CTTCCAATTTTAGYTCATTNACCTT		

Note: * *ACTB* primer set was personal communication Dr. Oliver Voigt.

1. Rokas A, Krüger D, Carroll SB. Animal Evolution and the Molecular Signature of Radiations Compressed in Time. Science. 2005;310:1933-8. doi: 10.1126/science.1116759.

Appendix 1.6.2: BLAST results for selected HKGs sequenced using degenerate primers.

Organism	Gene	BLAST hit (Acc. No.)	Query cover	E value	% Similarity	Subclass
S. cf. *cruciata*	*ACTB*	*Scleronephthya gracillimum* (AY672589)	99%	0.0	86%	Octocorallia
S. cf. *cruciata*	*TUBA*	*Seriatopora hystrix* (HM147129)	99%	0.0	81%	Hexacorallia
S. cf. *cruciata*	*TUBB*	*Scleronephthya gracillimum* (AY703828)	99%	7e-141	85%	Octocorallia
S. cf. *cruciata*	*EF1A*	*Scleronephthya gracillimum* (AY682093)	100%	0.0	85%	Octocorallia
S. cf. *cruciata*	*RPL12*	*Anthopleura elegantissima* (DQ314616)	71%	3e-37	77%	Hexacorallia
S. cf. *cruciata*	*GAPDH*	*Urticina eques* (EF012780)	51%	6e-34	84%	Hexacorallia
S. cf. *cruciata*	*SRP54*	*Alligator sinensis* (XM_006015375)	99%	2e-136	81%	Reptilia (Class)

Appendix 1.6.3: BestKeeper output for (A) Thermal Stress and (B) pH Stress.

A: Thermal Stress

CP data of housekeeping Genes:							
Genes	***ACTB***	***TUBA***	***TUBB***	***EF1A***	***RPL12***	***GAPDH***	***SRP54***
	HKG 1	HKG 2	HKG 3	HKG 4	HKG 5	HKG 6	HKG 7
n	6	6	6	6	6	6	6
geo Mean [CP]	19.42	16.60	21.83	18.75	20.15	22.58	25.23
ar Mean [CP]	19.42	16.63	21.83	18.77	20.15	22.59	25.24
min [CP]	18.73	15.19	21.18	17.21	19.20	21.79	24.14
max [CP]	20.21	19.04	22.71	20.32	20.88	23.78	25.93
std dev [± CP]	0.41	0.63	0.50	0.66	0.45	0.41	0.45
CV [% CP]	2.09	3.80	2.28	3.54	2.26	1.83	1.78
min [x-fold]	-1.61	-2.67	-1.57	-2.92	-1.93	-1.73	-2.13
max [x-fold]	1.73	5.42	1.84	2.96	1.66	2.29	1.63
std dev [± x-fold]	1.32	1.55	1.41	1.59	1.37	1.33	1.36
BestKeeper vs.	HKG 1	HKG 2	HKG 3	HKG 4	HKG 5	HKG 6	HKG 7
coeff. of corr. [r]	0.758	0.925	0.811	0.906	0.857	0.531	0.829
p-value	0.001	0.001	0.001	0.001	0.001	0.023	0.001

B: pH Stress

CP data of housekeeping Genes:							
Genes	***ACTB***	***TUBA***	***TUBB***	***EF1A***	***RPL12***	***GAPDH***	***SRP54***
	HKG 1	HKG 2	HKG 3	HKG 4	HKG 5	HKG 6	HKG 7
n	6	6	6	6	6	6	6
geo Mean [CP]	15.29	14.10	18.75	15.96	19.14	19.69	24.18
ar Mean [CP]	15.31	14.11	18.76	16.01	19.16	19.70	24.19
min [CP]	14.35	13.73	17.90	14.54	18.09	18.88	23.29
max [CP]	16.30	14.40	19.65	18.51	20.97	20.65	25.10
std dev [± CP]	0.70	0.20	0.59	1.05	0.74	0.47	0.75
CV [% CP]	4.60	1.39	3.14	6.54	3.87	2.37	3.12
min [x-fold]	-1.89	-1.29	-1.79	-2.60	-2.04	-1.73	-1.83
max [x-fold]	1.97	1.22	1.85	5.61	3.46	1.90	1.86
std dev [± x-fold]	1.61	1.14	1.49	2.03	1.65	1.37	1.67
BestKeeper vs.	HKG 1	HKG 2	HKG 3	HKG 4	HKG 5	HKG 6	HKG 7
coeff. of corr. [r]	0.985	0.781	0.935	0.946	0.945	0.878	0.948
p-value	0.001	0.0027	0.001	0.001	0.001	0.001	0.001

Appendix 1.6.4 Melting curves for all of the selected references and target gene amplicons.

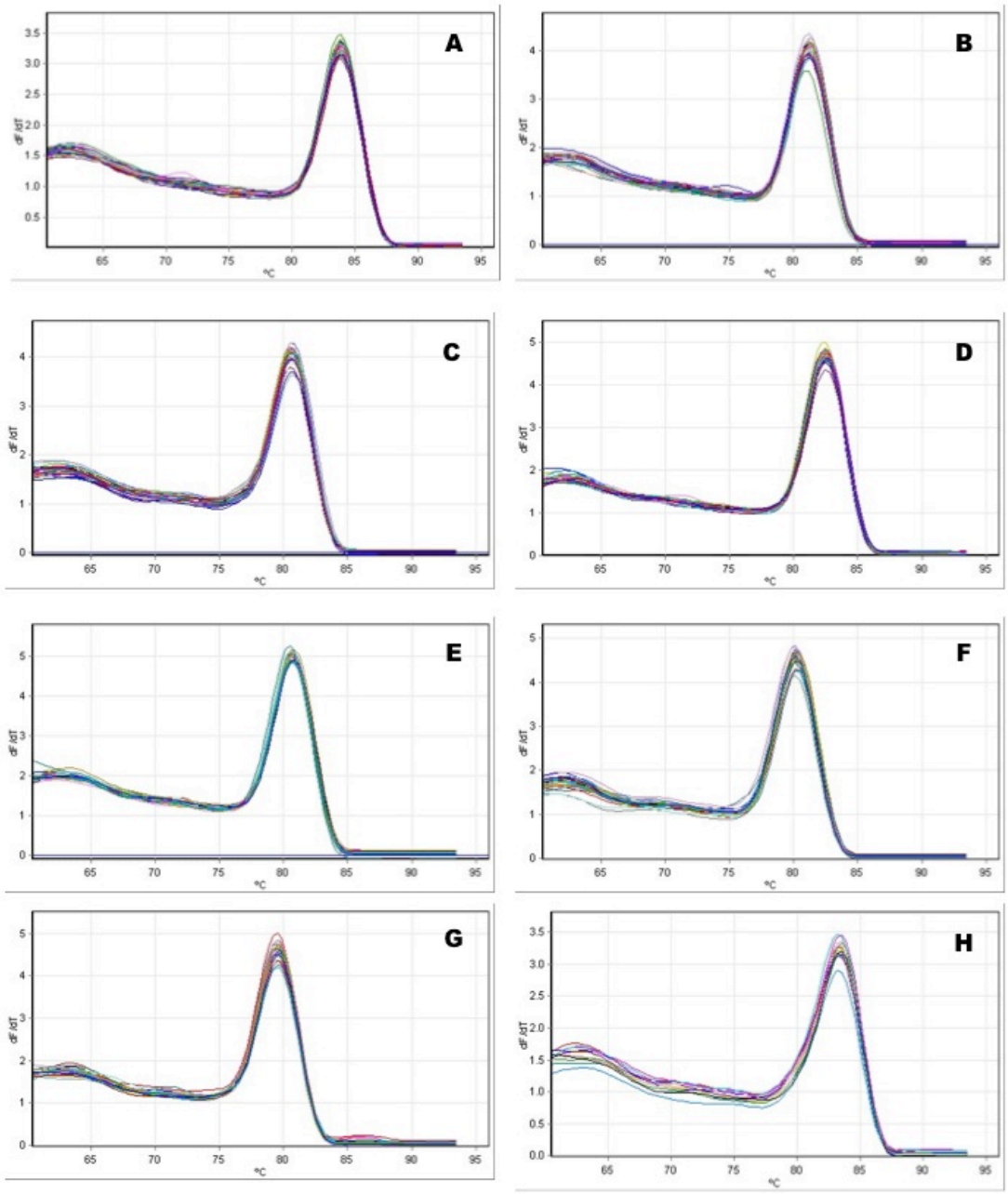

Figure S1: Melting Curves for seven candidate reference genes and the target gene: (A) *ACTB*, (B) *TUBA*, (C) *TUBB*, (D) *EF1A*, (E) *RPL12*, (F) *GAPDH*, (G) *SRP54*, and (H) *HSP70*.

Appendix 1.6.5 Gel image showing the amplification for all of the genes under study.

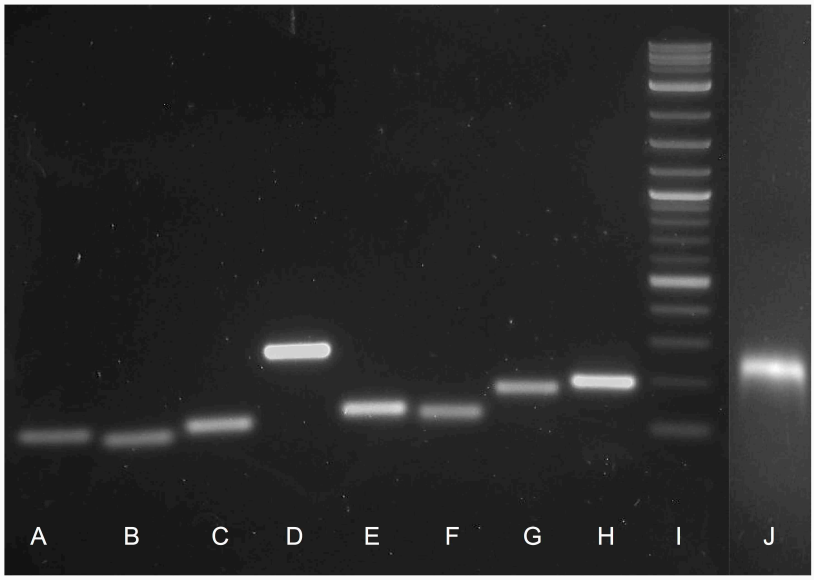

Fig S3: Gel image for candidate reference and target genes, (A) *ACTB*, (B) *TUBA*, (C) *TUBB*, (D) *EF1A*, (E) *RPL12*, (F) *GAPDH*, (G) *SRP54*, (H) *COI*, (I) 2-Log DNA ladder (NEB), and (J) *HSP70*.

Appendix 1.6.6 Comparison between the least stable RGs and the most stable RGs

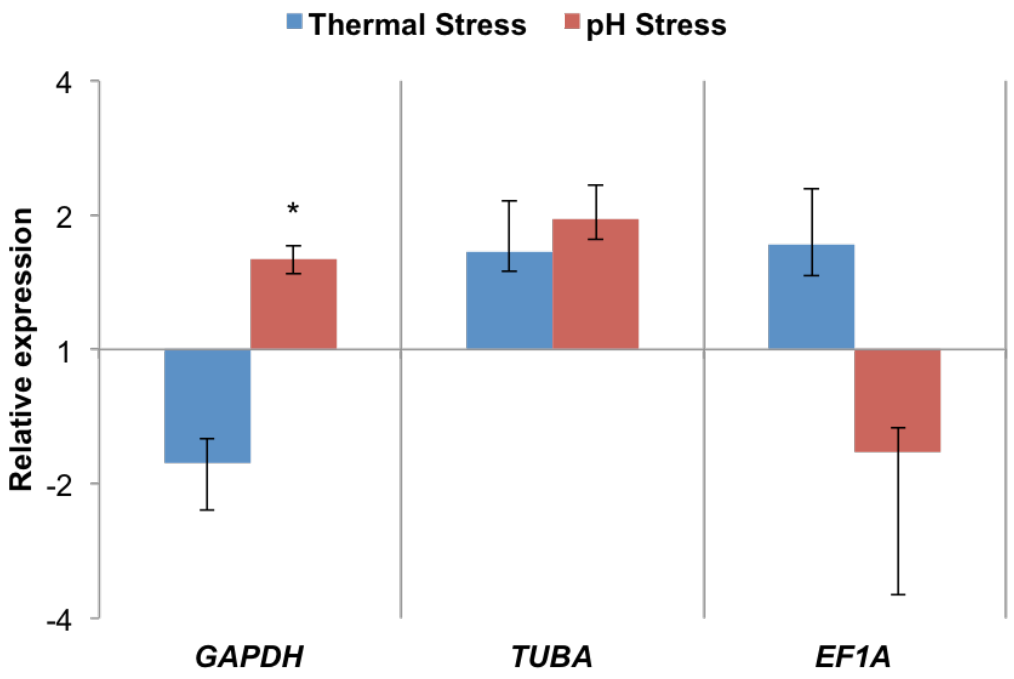

Appendix 1.6 Comparison between the least stable RGs and the most stable RGs

The three least stable RGs (*GAPDH, TUBB, EF1A*) expression was normalized using three best RGs during thermal stress (*RPL12* + *SRP54* + *ACTB*) and pH stress (*ACTB* + *TUBB* + *SRP54*). The relative expression (fold change) values are depicted as the mean ± SE. REST2009 was used for the analysis. (* indicate REST $p \leq 0.05$, 5000 iterations).

CHAPTER 2

Robust Mitochondrial Response to Oxidative DNA Damage in Octocorals

This chapter will be submitted as a standalone publication to the journal 'Global Change Biology'.

Chapter 2

Robust Mitochondrial Response to Oxidative DNA Damage in Octocorals

2.1 Introduction

Since the advent of aerobic life on planet earth 2.5 Gyr (Falkowski et al., 2004), oxidative stress exerted by the production of cellular reactive oxygen species (ROS) has been associated with biological systems (Cadenas, 1989). The accumulation of ROS in the cellular environment when overwhelmed beyond possible quenching capacity results in damage to lipids, proteins and most importantly the DNA. Adverse consequences of global warming and changing oceans have long been implicated in imposing greater oxidative stress as a unifying mechanism for coral bleaching (Lesser, 2006). Warming oceans, acidification accelerated by anthropogenic activities are causing increased stress on coral reef communities, resulting in partial or complete colony mortalities ultimately leading to affecting productivity and growth of these so called "rainforests of the ocean" on a global scale (Hughes et al., 2003; Hoegh-Guldberg et al., 2007). However, despite ever-increasing knowledge about the biology and ecological implications of climate change induced stress on corals, the precise understanding of mitochondrial response that, in general, is known to underpin the process of cell death is still not understood entirely and remains underappreciated in corals.

The energy status of the coral, like every other organism, determines its performance under stressful conditions and is crucial for survival (Lesser, 2013). Being an energy hub, mitochondria are a principle source of ROS, and consequently a major site of oxidative damage. Mitochondrial DNA (mtDNA) is particularly prone to this kind of damage (Sawyer et al., 2001) and genomic integrity of the mtDNA is constantly threatened by endogenous ROS. Besides damaging DNA, these ROS can elicit cellular stress response, which may result in triggering the release of cytochrome c and other

pre-apoptotic protein-signaling cascade, ultimately leading to cell death (Gogvadze et al., 2006; Ott et al., 2007). To cope with the DNA damage, cells posses a number of DNA repair mechanisms for both, nucleus as well as organelles. However, there are multiple DNA repair mechanisms for the nucleus whereas ability of mitochondria appears limited in this respect. Moreover, the fidelity and efficiency of DNA repair for nuclear and organellar DNA is speculated to be differ (Boesch et al., 2011) due to observed 10 to 20 times faster accumulation of mutations for animal mtDNA than the nuclear DNA (nDNA) (Brown et al., 1982; Shigenaga et al., 1994), potentially attributed to less efficient DNA repair mechanism for mitochondria (Fernández-Silva et al., 2003; Boesch et al., 2011). Reports also suggest that the oxidative stress induced mtDNA damage persist longer than the nDNA in human cells (Yakes and Van Houten, 1997). Yet, the high mutation rate for mtDNA among animals is not ubiquitous as the non-bilaterians, such as anthozoans and sponges exhibit unusually slow rate of mtDNA sequence evolution (van Oppen et al., 2001; Shearer et al., 2002; Hellberg, 2006; Huang et al., 2008; Chen et al., 2009).

A typical animal mitochondrial genome encodes 13 protein coding genes, 22 tRNA and 2 ribosomal genes. No DNA repair or oxidative stress related protein-encoding genes are reported in animal mitochondrial genomes so far. However, the octocoral mitochondrial genomes are unique exception encoding a mismatch repair gene (*mtMutS*) not found in any other animal mitochondria studied so far (Pont-Kingdon et al., 1995; Pont-Kingdon et al., 1998). Although the exact function of this gene remains undetermined, its role in maintaining low variations and its involvement in mtDNA repair and gene rearrangements in the octocoral mitochondrial genomes have been proposed (Bilewitch and Degnan, 2011; Brockman and McFadden, 2012). mtDNA is widely known to be more susceptible to damage in presence of oxidative stress of any sort (Sawyer et al., 2001). Therefore, it is interesting to explore the potential benefit of harboring a large gene in a compact mitogenome (~3kb gene, ~16% of mitogenome size, largest among the octocoral mitogenome-encoded genes), the *mtMutS* gene, and its probable role in octocoral response to oxidative stress and the resulting DNA damage.

Like most other animals, in cnidarians as well, the mitochondria are known as a principle source of cellular ROS (Blackstone, 2009), and the role of mitochondria in ROS generation has been studied in sea anemone (Dykens et al., 1992). Moreover, the molecular responses to climate change induced oxidative stress are well documented for

some members of this phylum and are reported to involve heat shock proteins and antioxidant enzymes (Kaniewska et al., 2012; Moya et al., 2012; Hennige et al., 2013; Gibbin et al., 2014; Rosic et al., 2014; Tarrant et al., 2014; Dixon et al., 2015). The ROS generated during oxidative stress imparted by any environmental stress is bound to cause DNA damage (Barzilai and Yamamoto, 2004). There are studies exploring the damage to nuclear DNA in response to oxidative stress and other DNA damaging agents among cnidarians (Lesser and Farrell, 2004; Nesa and Hidaka, 2008; Schwarz et al., 2013; Svanfeldt et al., 2014). Disruption of host mitochondrial integrity in symbiotic *Aiptasia sp*. has been demonstrated post thermal stress using microscopic observations (Dunn et al., 2012). However, susceptibility of mtDNA to the excess ROS generated by electron transport chain (ETC) in its proximity is of prime concern for cellular homeostasis during stress. The mitochondrial response during and/or after oxidative stress ultimately decides the fate of an organism (Turrens, 2003). Nevertheless, despite the uniqueness of octocoral mitochondrial genomes, their response to oxidative stress has never been studied. A combined assessment of mt-genome integrity, potential for mtDNA recovery, the response of *mtMutS* as well as other stress biomarkers genes, (such as heat shock protein 70 *(HSP70),* glutathione peroxidase *(GPX)* and Cu/Zn superoxide dismutase *(CuZnSOD)*) in response to the increase oxidative stress resulting from different climate change related as well as exogenous sources is missing for the members of soft corals (Octocorallia).

Here, we aim to study how octocoral mitochondria respond to different abiotic stressors and an exogenous DNA damaging agent induced oxidative stress. We use a sensitive quantitative real-time PCR based approach to assess the extent of mtDNA damage caused by common climate change-related stressors such as thermal and low-pH, as well as exogenous hydrogen peroxide (H_2O_2), and the capacity of octocoral *Sinularia* cf. *cruciata* to repair damaged mtDNA. We followed the dynamics of mtDNA copy number to understand the associated changes during the mitochondrial recovery process. The gene expression of two mitochondrial and three nuclear genes involved in oxidative stress response was also assessed. This is one of the first attempts to integrate gene expression and mtDNA damage/repair quantification to explore the ability of octocorals to mitigate and resist the climate change-induced oxidative stress events, and represents a first step towards developing fundamental/mechanistic mitochondria-centric/inclusive models of stress tolerance in octocorals.

2.2 Materials and Methods

2.2.1 Coral collection and maintenance

Coral colonies were obtained from a commercial source. They were subsequently cut into several pieces that were allowed to grow independently in a closed circuit seawater aquarium at Molecular Geo- and Palaeobiology lab, LMU Munich. The corals were kept under controlled conditions (25 ± 1 °C, pH 8.2 ± 0.1) with a biweekly exchange of 50% fresh artificial seawater. All the corals were maintained on 12 h light / 12 h dark light-regime provided by LED light (GHL Mitras LX 6200-HV) at a light intensity of 14 ± 2 kLux. Similar light regime was used for both, control as well as experimental systems mentioned below.

2.2.2 Gene identification, sequencing and qPCR primers

Identitities of the organisms under study were confirmed using the *mtMutS* gene (McFadden et al., 2009).

For relative quantification of gene expression using qPCR, reference genes were validated in a treatment-specific manner and those genes found to exhibit stable expression in *Sinularia* cf. *cruciata* during thermal and low-pH stress were used for qPCR normalization (unpublished data). Sequences of stress-related genes were obtained from shallow transcriptomic data (unpublished), their identities were confirmed by BLASTn, BLASTp and CDART, a domain search tool (Geer et al., 2002), and were used for qPCR primer design.

For semi-long run qPCR (SLR-qPCR) and mt-number (detailed below), a large (1057 bp) fragment spanning mitochondrial *COII*-igr-*COI* genes was sequenced using previously reported primers (McFadden et al., 2011) and a new primer binding 100 bp upstream to the 3' end of this large fragment was designed (short fragment). Nuclear *ACTB* gene primers for comparison to determine mtDNA copy number were same as those used for gene expression. Primer designing was performed using Primer3 and Geneious 6.1 was used for sequence analysis (Kearse et al., 2012). Melting curves (Appendix 2.6.1), electrophoresis and sequencing confirmed the specificity of all the

primer pairs used. Sequences obtained will be submitted to European Nucleotide Archive (ENA).

2.2.3 Experimental oxidative stress and DNA damage treatments

To determine the effect of oxidative stress due to rising seawater temperature, decreased pH (both sub-lethal) and hydrogen peroxide (H_2O_2) (acute toxicity) on mtDNA damage, mtDNA copy number variations and gene expression the nubbins of *Sinularia* cf. *cruciata* were exposed to these conditions (see below). All experiments were performed in biological as well as technical triplicates unless otherwise stated and the controls as well as treated sample tissues were preserved in absolute ethanol for DNA extraction or were snap frozen in liquid nitrogen and subsequently stored at -80°C until RNA extraction. Same DNA extracts and concentrations were used for both, mtDNA damage quantification as well as mtDNA/nDNA ratios.

2.2.3.1 Thermal stress

Three *Sinularia* cf. *cruciata* nubbins of similar size were placed in an experimental 10L tank and the temperature in the tank was raised gradually from 26 °C to 34 °C over a period of 2 h and was maintained at 34 °C for 6 h thereafter. Three controls were maintained in a similar tank as the experimental tank but temperature was kept at 26ºC during the course of the experiment.

2.2.3.2 Low pH stress

Three *Sinularia* cf. *cruciata* nubbins were exposed to low seawater pH by pumping carbon dioxide (CO_2) into the seawater of a 10L experimental tank to maintain a stable low pH value of 7.5. The pH was first reduced to 7.5 over a period of 2 h and then maintained at this value for 24 h. The pH value was recorded throughout the experiment and it was observed to be constant at 7.5. Corals were sampled after 24 h exposure. Control samples were maintained under normal pH of 8.2 during the course of experiment and the temperature in both tanks was kept constant at 26 °C.

2.2.3.3 Hydrogen Peroxide treatment:

For this treatment, three independent DNA damage experiments were performed at different times on independently growing nubbins. A 5 mM H_2O_2 concentration was used for acute toxicity and extensive DNA damage. H_2O_2 is potent DNA damaging agent and one of the reactive oxygen intermediates generated during oxidative stress in

mitochondria and is known to remain stable in seawater and to readily diffuse across biological membranes (Lesser, 2011). The experiments were performed in 2L tanks. A tissue sample was taken as a 'time-zero' control. Subsequently, 30% v/v H_2O_2 (Sigma-Aldrich) was added to a final concentration of 5 mM to the seawater. Corals remained in this solution for 30 min. After tissue sampling (Labeled as 'Treatment'), the corals were kept at initial control conditions for recovery. During recovery two tissue samplings were performed each after 1h and 5h (Labeled as 'Rec-time') of the treatment. Additionally, two other octocorals namely, *Sinularia sp.,* and *Briareum sp*., were treated similarly and the recovery was monitored for 1 h.

2.2.4 Total RNA extraction and cDNA synthesis

Total RNA was extracted from control as well as treated samples exposed to thermal and pH stress using Trizol reagent (Invitrogen, USA) following the manufacture's instructions. Contaminating DNA was eliminated from RNA extracts with the help of RQ RNase-free DNase (Promega, USA) according to manufacture's protocol. The treated RNA was further purified using Sodium Acetate- Ethanol precipitation. Purity of RNA was determined using a Nanodrop ND-1000 spectrophotometer (Thermo Fisher Scientific, USA). RNA samples with absorbance at OD260/280 and OD260/230 ratio ~ 2.0 were used for further analysis. RNA integrity was also verified by 1% agarose gel electrophoresis as well as using a Bioanalyzer (Agilent Inc.). RNA extracts with a RIN value ≥ 7.5 were used for cDNA synthesis (data not shown). For each sample, ~1 µg of total RNA was reverse transcribed using ProtoScript® First Strand cDNA Synthesis Kit (NEB, Germany) employing an anchored oligo-(dT) primer in 20 µl reaction according to manufacture's instructions.

2.2.5 Quantitative Real-time RT-PCR (qPCR)

The qPCR was performed on a Rotor-Gene Q 2plex system (Qiagen, Germany) using KAPA SYBR FAST universal mastermix (Peqlab, Germany) in 15 µl reactions containing 1 µl diluted cDNA, 7.5 µl 2X mastermix, and 250 to 400 nM each primer. A two-step qPCR including an initial denaturation step of 3 min at 95 °C followed by 40 cycles of 95 °C for 10 s and 60 °C for 20 s. A non-template control was always included in each assay. Melting curve analysis was performed at the end of each qPCR to confirm amplification specificity and amplification products were also checked by

agarose gel electrophoresis after each assay. Details on the primers used can be found in Table 2.1.

2.2.6 DNA extraction:

Extraction of total DNA from control and treated coral tissues was performed using NucleoSpin Tissue kit (Macherey-Nagel, Germany) following manufacture's instructions. DNA quality and purity was determined using Nanodrop ND-1000 spectrophotometer (Thermo Fisher Scientific, USA), which showed a high quality DNA (A260/A280 > 1.8).

2.2.7 Semi-long run qPCR (SLR-qPCR)

To quantify mtDNA damage a semi-long run quantitative PCR (SLR-qPCR) was performed as described previously (Rothfuss et al., 2010). Briefly, a large fragment (1057 bp) and a small fragment (100 bp) of same mitochondrial region was amplified using KAPA SYBR FAST universal mastermix (Peqlab, Germany) in 15 µl reactions containing 1x mastermix, and 500 nM each forward and reverse primer and 5 ng total DNA. The cycling conditions consists of a pre-incubation step at 95 °C for 3 min followed by 40 cycles of 95 °C for 10 sec, 60 °C for 20 sec for small fragment, and 95 °C for 10 sec, 58 °C for 20 sec and 72 °C for 30 sec for large fragment. The mitochondrial regions, primers and PCR efficiencies are listed in Table 2.2. Each sample was assayed in triplicates, and the amplicon specificity was monitored by melting curve analysis as well as by gel electrophoresis. Cq values and mean PCR efficiency (E) for the primer pair was obtained using LinRegPCR program. Cq values were efficiency-corrected using the formula "efficiency-corrected-Cq = Cq * (log(E) / log(2))" (Kubista M, 2007) and used in the calculation of mitochondrial lesion frequency (MLF) using the formula, "Lesion rate (lesions/10kb) = $(1 - 2^{-(\Delta \text{ long} - \Delta \text{ short})})$ × (10000 [bp] / size of long fragment [bp])" (Rothfuss et al., 2010). Isolated DNA from non-treated controls was used as reference whereas Cqs of the large and small mitochondrial fragments were used for DNA damage quantification.

Table 2.1: Description of gene specific qPCR primers used for gene expression analysis

No.	Gene	Gene Name	Primer Sequences (5' to 3')	Size (bp)	Amplicon Tm (°C)	*E*
	Reference genes primers					
1	*ACTB*	β-Actin	for: CCAAGAGCTGTGTTCCCTTC rev: CTTTTGCTCTGGGCTTCGT	107	83.8	1.97
2	*TUBB*	β-Tubulin	for: ATGACATCTGTTTCCGTACCC rev: AACTGACCAGGGAATCTCAAGC	115	80.5	1.99
3	*RPL12*	Ribosomal protein L12	for: GCTAAAGCRACTCAGGATTGG rev: CTTACGATCCCTTGSTGGTTC	142	80.5	1.97
4	*SRP54*	Signal recognition partical 54	for: TGGATCCTGTCATCATTGC rev: TGCCCAATAGTGGCATCCAT	184	79.5	1.97
	Target gene primers					
1	*HSP70*	Heat shock protein 70	for: GGTGTATTTCAACACGGCAAAG rev: CCCCCTTATACTCCACTTCAAC	274	83.5	1.99
2	*GPX*	Glutathione peroxidase	for: TTTCCTTGCAATCAGTTTGG rev: GGCAGTCGTTGGAGAATATC	252	80.0	2.00
3	*CuZnSOD*	Cu-Zn Superoxide dismutase	for: CCAACTGATACAGAGAGGCATG rev: CATCAACACCAGCATGTACCAC	150	80.3	1.99
4	*COI*	Cytochrome c oxidase subunit 1	for: ACGGCTTGATACACCTATGTTGTGG rev: TACCGAACCAATAGTAGTATCCTCC	200	78.7	1.99
5	*mtMutS*	Mitochondrial *muts* homolog	for: GCATGAGCCCGATACTTCTAGT rev: ACGAAGCAACTTGTTCAATGG	119	81.7	1.98

E represents LinRegPCR amplification efficiency

Table 2.2: Description of qPCR primers used for mtDNA damage and mitochondrial copy number quantification

No.	Gene fragments	Genes	Primer Sequences (5' to 3')	Size (bp)	Tm (°C)	*E*
1	Small mt-fragment	*COI*	f-TAATTCTACCAGGATTTGG r-ATCATAGCATAGACCATACC	97	75.8	1.95
2	Large mt-fragment	*COII-COI*	f-CCATAACAGGACTAGCAGCATC r-ATCATAGCATAGACCATACC	1057	82.3	1.76
3	Nuclear fragment	*ACTB*	f-CTTTTGCTCTGGGCTTCGT r-CCAAGAGCTGTGTTCCCTTC	107	83.5	1.96

E represents LinRegPCR amplification efficiency. f = forward, r= reverese.

2.2.8 Determination of mtDNA copy number

To determine the effect of experimental treatments on mitochondrial degradation, the mtDNA/nDNA ratio (i.e mtDNA copy number) was calculated before and after treatment using qPCR as described above. Equal amount of total DNA was used to amplify nuclear gene (*ACTB*) and one mitochondrial gene (*COI*) in control and treatment samples and the ratios of mtDNA/nDNA were obtained using Livak's method (Livak and Schmittgen, 2001) with non-treated sample served as control and *ACTB* Cq values as reference. Primer details are listed in Table 2.2.

For comparison of initial mitochondrial number among all control samples used during each experiment, which were done at different times during the span of 3 years on nubbins obtained from same colony, a ratio of *COI* versus *ACTB* gene fragment was obtained for each control separately. The geometric mean of these ratios was calculated and each mtDNA/nDNA ratio was divided by this value to obtain relative mitochondrial copy number for control samples in using REST2009 (single time-zero control for each H_2O_2 treatment experiment and triplicate control samples for thermal and low pH treatment each).

2.2.9 Data Analysis

The raw, non-baseline corrected fluorescence data obtained after qPCR baseline corrected using LinRegPCR (Ramakers et al., 2003) and Cq values and amplification efficiency for each amplification curve were calculated using this program. These Cq

values were used for mtDNA damage-repair, mtDNA copy number and gene expression analyses.

Gene expression analysis was performed using the method of (Pfaffl et al., 2002) implemented in REST2009. Cq values corrected by the mean PCR efficiency were obtained from LinRegPCR. Multiple, treatment-specific multiple reference genes were used for normalization (Vandesompele et al., 2002; Bustin et al., 2009). Fold changes in the expression of target or stress related genes (*HSP70, GPX, CuZnSOD, COI and mtMutS*) were calculated using *RPL12, SRP54* and *ACTB* during thermal stress, and *ACTB, TUBB,* and *SRP54* during pH stress, as reference genes. These sets of genes were found to be the most stably expressed reference genes during the respective stress treatments (unpublished data). Statistical significance of gene expression was tested using randomization and bootstrapping with 10000 iterations, and standard errors were calculated with the Taylor algorithm implemented in REST 2009. Data is represented as mean ± SE and REST's p <0.05 was considered as a threshold for statistically significance.

The present study conforms to the Minimum Information for Publication of Quantitative Real-Time PCR guidelines (Bustin et al., 2009).

2.3 Results:

2.3.1 Effect of thermal and pH stress on mtDNA (Sub-lethal treatments)

Significant mtDNA damage was detected during both sub-lethal thermal and low-pH stress. During elevated seawater temperature (6 h exposure), the corals exhibited 1.29 lesions per 10 kb DNA (p <0.05). However, the damage was higher (3.22 lesions per 10 kb DNA; p <0.01) after 24 h exposure to low-pH stress (Figure 2.1A). The mtDNA copy number variation was also monitored for these treatments. The mtDNA copy number variation showed opposite trend, decreasing (mtDNA/nDNA = 0.68, p <0.05) in response to thermal stress and increasing, with respect to the controls during pH stress (mtDNA/nDNA = 1.57, p <0.01) (Figure 2.1B).

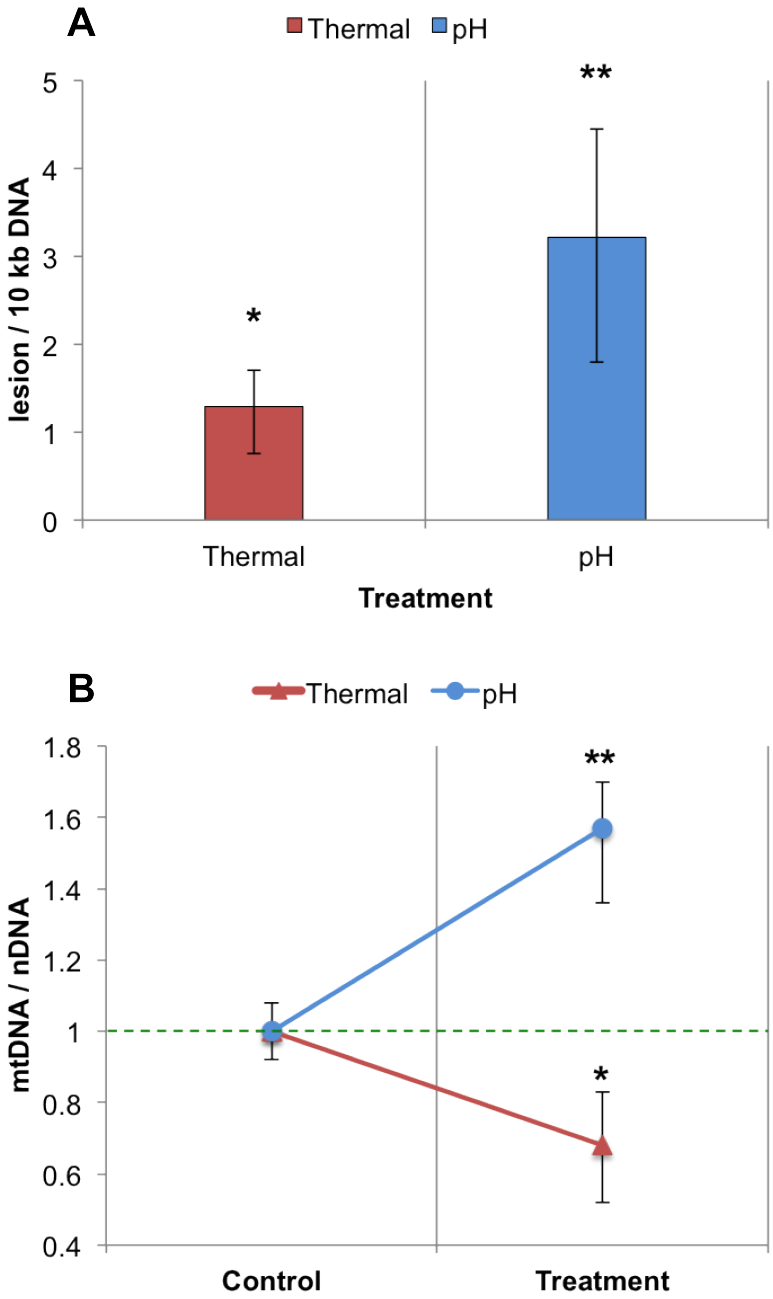

Figure 2.1 Thermal and low-pH stress induced mtDNA damage, recovery kinetics and mitochondrial copy number variation.

(A) Quantification of mtDNA lesion frequency (MLF) per 10 kb DNA by SLR-qPCR amplification of total DNA from *Sinularia* cf. *cruciata* exposed separately to elevated temperature (34 °C) for 6 h and reduced pH for 24 h. (B) In parallel, mitochondrial copy number was determined by amplifying one mitochondrial fragment and normalized using one nuclear fragment. Untreated controls (26 °C or pH 8.2) were used as reference during respective experiments. Data represents the mean ± SE of biological triplicates. * Statistical significant at $p < 0.05$; ** Statistical significant at $p < 0.01$.

2.3.2 Effect of thermal and pH stress on antioxidant defense and mitochondrial genes

HSP70 was strongly induced (>7 folds change; p <0.05) during thermal stress while the expression *GPX* decreased (-6.1 folds) and that of *CuZnSOD* was slightly affected (-1.4 fold). *COI* expression was detected to vary greatly though overall it showed an upward trend with 2.2 folds increase. The *mtMutS* gene was similarly upregulated with a 1.4 fold increase in transcript abundance (Figure 2.2).

Low pH stress resulted in the downregulation of *HSP70* (-1.87 fold, p <0.05), *GPX* (-1.71 fold, p <0.05) and *CuZnSOD* expression decreased. Mitochondrial gene *COI* was also downregulated (-2.8 fold; p <0.05) but the *mtMutS* was significantly upregulated (1.25 fold, p <0.05) (Fig. 2). The expression difference between these two mitochondrial genes is as much as 4 folds (p <0.001).

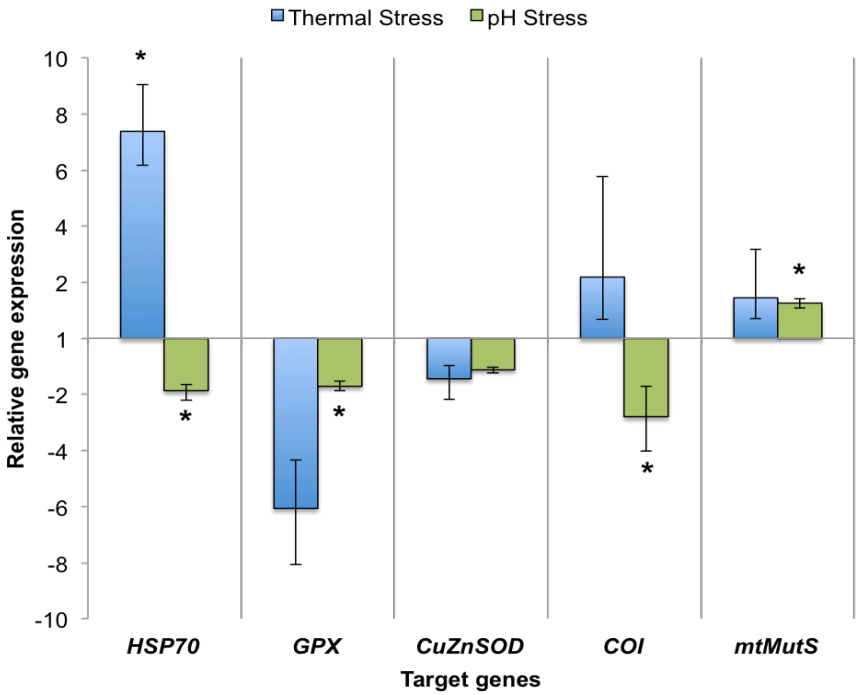

Figure 2.2 Relative expression of stress-related and mitochondrial genes post thermal and low-pH stress.

Changes in transcript levels of 3 stress response gene, *HSP70*, *GPX*, and *CuZnSOD*; and 2 mitochondrial genes, *COI* and *mtMutS* were assessed. Normalization was performed using validated sets of three reference genes namely *ACTB* and *SRP54* during either and *RPL12* and *TUBB* during thermal and pH stress, respectively. Bars represent the mean expression value (fold change ± SE) relative to untreated controls (26 °C or pH 8.2) of three biological replicates. *Asterisks* (*) denote significantly higher or lower expression relative to respective controls (REST; p < 0.05).

2.3.3 Effect of acute H_2O_2 stress on mtDNA and recovery dynamics

The response of octocoral mtDNA to excess acute DNA damage induced by a high concentration of potent DNA damaging agent, H_2O_2, was quantified and subsequent recovery kinetics was monitored.

The first experiments showed a dramatic effect of H_2O_2 treatment on mtDNA damage, inducing 9 lesions per 10 kb. This damage was completely reversed after 1 h recovery and an excess repair was observed as indicated by a negative lesion frequency (-9.6 lesions per 10 kb). Excess repair was still observed after 5 h when the lesion frequency was -6.6 per 10 kb (Figure 2.3A).

On a second experiment performed, the mtDNA damage was not as high as it was observed during the first experiment and only 2.4 lesions per 10 kb were observed after 30 min exposure to H_2O_2. Lesions increased (3.4 lesions per 10 kb) after 1 h recovery and were reverted only after 5 h recovery (-2.4 lesion per 10 kb) (Figure 2.3A).

During the third experiment, the observed lesion frequency was minimum (0.4 lesions per 10 kb) after 30 min exposure. This was followed by damage reversal indicated by lesion frequencies of -1.1 and -4.2 lesions after 1hr and 5 h recovery, respectively. In all experiments the mtDNA damage was reversed and an excess repair was observed within 5 h post-treatment (Fig. 2.3A). An additional experiment performed together with two other soft corals, *Sinularia sp.* and *Briareum sp.*, also exhibited mtDNA damage followed by a damage reversal after 1 hr recovery (Appendix 2.6.2).

2.3.4 mtDNA copy number variations upon acute H_2O_2 induced mtDNA damage

The accumulation of lesions in the mtDNA beyond the threshold levels result in blockage of the transcription as well as replication leading to mtDNA degradation (Alexeyev et al., 2013). We evaluate the impact of H_2O_2 driven mtDNA damage on mtDNA replication after treatment and its recovery as a proxy. Mitochondrial DNA copy number relative to nuclear DNA was monitored during each independent experiment to understand the recovery kinetics and its correlation to the DNA damage extent compared to time-zero control. During first experiment, the mtDNA copy number decreased to almost half with respect to the control after 30 min H_2O_2 exposure

indicating degradation of severely damaged mtDNA during the treatment. This was rapidly reversed after 1 h recovery to 2 folds excess with respect to the time-zero control. mtDNA copy number remained high (1.7 X control) after the remaining recovery period (Figure 2.3B). During the second experiment however, mtDNA copy number increased during the 30 min treatment. It remained 1.5 fold higher after 1 h recovery and subsequently returned to a value equivalent to the time-zero control. No degradation was observed. During the third experiment, there was no detectable increase or decrease during the treatment or the recovery period and mtDNA copy number ranged from 0.97 to 1.1 during the course of experiment (Figure 2.3B).

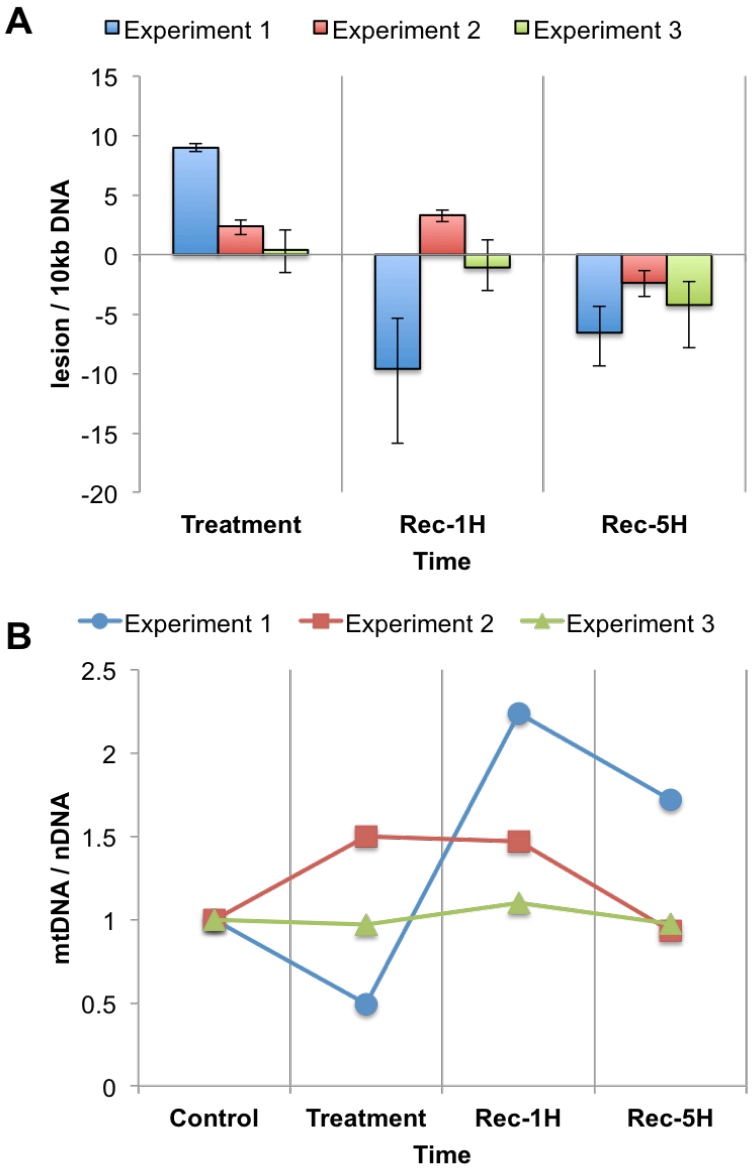

Figure 2.3 Hydrogen peroxide induced mtDNA damage, recovery kinetics and mitochondrial copy number variation.

(A) Quantification of mtDNA lesion frequency (MLF) per 10 kb DNA by SLR-qPCR amplification of total DNA from *Sinularia* cf. *cruciata* exposed to 5 mM H_2O_2 for 30 min (designated as 'Treatment') followed by recovery for 1 hr and 5 hr (designated as 'Rec-1H' and 'Rec-5H', respectively). Data represents the mean ± s.e.m. of three replicates. **(B)** In parallel, mitochondrial copy number variation was determined by amplifying a mitochondrial fragment and normalized using a nuclear fragment. Non-treated time-zero corals were used as a reference sample during respective experiments. Three independent experiments performed at different times.

2.3.5 Comparison of mtDNA copy number among experimental control samples

To further understand the reasons for differential responses of mtDNA damage and mtDNA copy number of genetically identical coral under similar initial conditions at different times, the mtDNA/nDNA ratios of the controls (time-zero) tissue DNA were compared with each other aiming to find a probable correlation. The mtDNA copy number was found lowest for the control samples of experiment1 and highest during the third H_2O_2 experiment. The difference between first and third experiment was 5.5 fold mtDNA copies and 5.2 fold difference in mtDNA copy number between first and second experiment. The thermal and pH stress mtDNA copy numbers where found to be similar to the second and third H_2O_2 experiment rather than those observed for the first one (Figure 2.4).

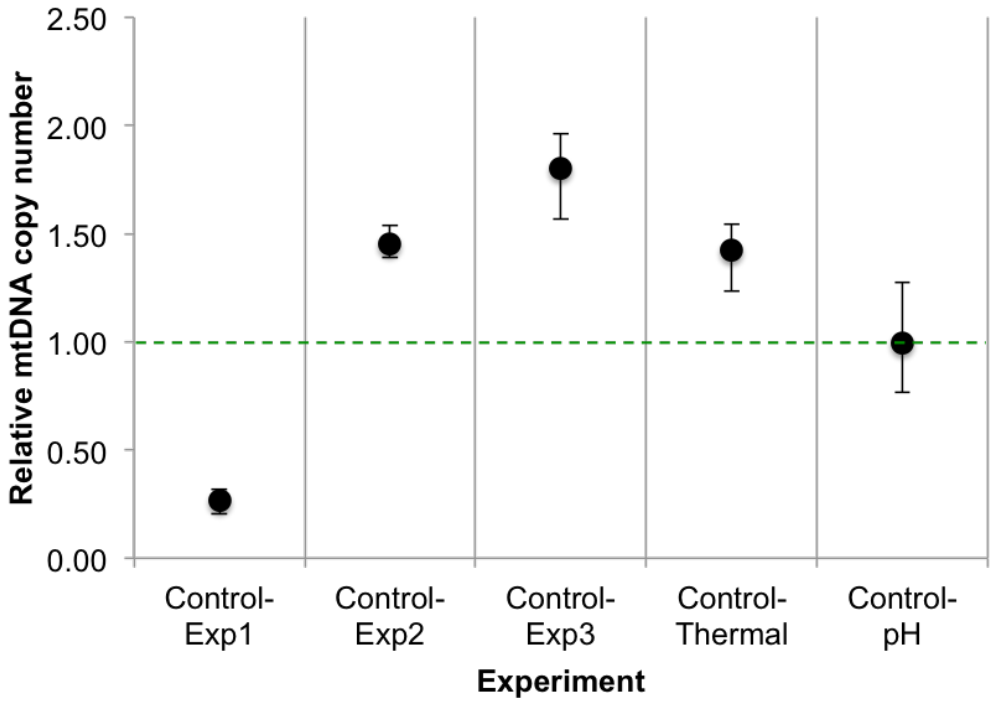

Figure 2.4 Comparison of initial mtDNA copy numbers among experimental controls.

Initial mitochondrial copy number variation was determined by amplifying a mitochondrial fragment and normalized using a nuclear fragment. The differences in the Cq values of mitochondrial gene versus nuclear gene were calculated using $2^{-\Delta Cq}$. The geometric mean of the values obtained for all controls served as a baseline (represented by the dotted line in figure), which was used to calculate the ratios. Time-zero controls for H_2O_2 experiments and untreated controls (in triplicate) for thermal and pH stress were used for comparison. Data represents the mean ± SE.

2.4 Discussion

Octocorals are unique members of the Phylum Cnidaria, especially with respect to their unique mitochondrial genomes, which encode an additional ~3 kb putative mismatch repair gene (Pont-Kingdon et al., 1995), a bacterial homolog. While most studies on coral stress response focus on coral-dinoflagellate symbiosis, calcification, bleaching, heat and acidification stress (Hoegh-Guldberg et al., 2007), the investigations on mtDNA damage, repair and gene expression during climate change-related environmental stress are lacking. This study is the first of its kind in this context. Here, the importance of the *mtMutS* gene during stress response was demonstrated and shown that the host mitochondria are capable of reverting the extensive oxidative damage to mtDNA.

Oxidative stress in marine ecosystems is a well-known phenomenon with adverse effects on marine organisms (Lesser, 2006). Corals exhibit a typical stress response at cellular level to a variety of insults imparted by various environmental stresses. Thermal and low-pH stress has long been implicated in exerting oxidative stress on corals (DeSalvo et al., 2008; Soriano-Santiago et al., 2013), and the reef-building or hard corals response to the increased temperature, as a zooxanthellate host system, has been extensively studied (Lesser, 2006; Lesser, 2011). Studies exploring the response of octocorals to such environmental stresses have recently started to emerge (Haguenauer et al., 2013; Sammarco and Strychar, 2013; Teixeira et al., 2013; Lõhelaid, H et al., 2014; Lõhelaid, Helike et al., 2014; Woo et al., 2014), exploring the physiological as well as transcriptomic changes. However, response of several key genes responsible for antioxidant defenses such as, *CuZnSOD, GPX*, along with mitochondrial genes, has not been investigated so far.

Different studies have shown upregulation of heat shock protein gene *HSP70* in response to thermal stress in octocorals as well as other cnidarians, pointing towards the existence of a conserved mechanism among cnidarians to mitigate heat stress (Rodriguez-Lanetty et al., 2009; Lõhelaid, H et al., 2014). The results of present study corroborate this observation and further highlight the importance of the *HSP70* during thermal stress response in this group of organisms as exhibited by a very strong induction of *HSP70* in the octocoral *Sinularia* cf. *cruciata*. Interestingly, we found a significant down-regulation of *HSP70* gene in acidified seawater in contrast to the previous studies that found either an increase in expression (Moya et al., 2015) or no

differential expression of this gene in early life stages of acroporid corals under ocean acidification conditions (Nakamura et al., 2012). Studies on other invertebrates (non-cnidarian) have reported either a decrease or no significant change in *HSP70* expression during stress induced by seawater acidification (Hauton et al., 2009; O'Donnell et al., 2009). It implies that the *HSP70* gene induction is not required during low-pH stress, as the external pH changes resulting in acid/base imbalance may not necessarily result in denatured cytoplasmic proteins, unlike heat stress during which refolding of denatured proteins require assistance. The coral might try to compensate for the stress by suppressing unnecessary metabolic pathways, investing energy into the important ones, which explains down-regulation of *HSP70*.

GPX gene, encoding glutathione peroxidase, a key antioxidant enzyme that catalyzes the conversion of harmful H_2O_2 to H_2O with the help of reduced glutathione, plays an important role in ROS detoxification (Halliwell, 2006). Surprisingly, *GPX* was downregulated during both thermal and low-pH treatments. Depletion of the glutathione pool during initial hours of exposure to stress could be the reason for the observed decrease in *GPX* expression (Sagara et al., 1998; Downs et al., 2000). Furthermore, the sea anemone genome has found to contain 12 *GPX* isozyme genes (Goldstone, 2008), hence it is also possible that the *GPX* isozyme gene assessed here does not participate in oxidative stress response at this stage and or under circumstances studied here. Additionally, another gene involved in antioxidant defense *CuZnSOD,* occurs predominantly in the cytosol of eukaryotes (Halliwell, 2006), remained relatively unaffected during both stress conditions. Nonetheless, because three different members of *SOD* multigene family have been described in sea anemone along with several isoforms of *CuZnSOD,* it is likely that the other *SODs* or their isoforms are involved in scavenging superoxide radicals under these conditions (Plantivaux et al., 2004; Richier et al., 2005).

Mitochondrial DNA integrity is a prerequisite for cellular homeostasis as it encodes the most crucial component of electron transport chain (ETC) involved in oxidative phosphorylation and energy production. The energy budget plays a crucial role in corals for survival during environmental stress (Lesser, 2013). Therefore, it's necessary to appreciate the changes in mitochondrial gene expression during oxidative stress as a proxy to understand its impact at cellular as well as organismal levels. Hence, to identify the impact of climate change exerted oxidative stress on mitochondria of the host, the expression of one key gene, cytochrome c oxidase subunit I (*COI*)- a crucial

component of complex IV of ETC, and other unique genes, *mtMutS*, with putative mtDNA repair function were assessed for changes in expression. Earlier it has been shown that the thermal stress adversely affects *ATPase* gene expression, also a component of Complex IV in *Aiptasia sp*., correlating to compromised mitochondrial structure and functionality (Dunn et al., 2012). It is also evident here from the observed lesions and decreased mtDNA copy number during thermal stress. However, no negative effect on *COI* and *mtMutS* gene expression likely due to low level of mtDNA damage suggests less compromised mitochondrial integrity in *Sinularia* cf. *cruciata* in response to acute short-term thermal stress.

In contrast, during low-pH stress, a significant reduction in *COI* gene transcripts indicates severely compromised mitochondrial integrity by this treatment. This is also supported by observed higher number of mitochondrial lesions than thermal stress. Here it is interesting to note that the observed increase in mtDNA copies implies that the damaged mitochondria were retained, and replicated, which could recover under favorable conditions rather than destined to degradation, using complementation of mitochondrial function by fusion, sharing DNA when mutation load is low, as observed in animals (Kazak et al., 2012) discussed below in detail. The changes in seawater pH result in changing the carbonate chemistry thereby elevating the oxidative stress and DNA damage has been reported previously in marine organisms (Lesser, 2006; Wang et al., 2009). Prolonged exposure to oxidative stress results in reduced expression of mitochondrial genes shown previously in several studies on other animals (Austin et al., 1998; Crawford et al., 1998; Schwarze et al., 1998; Morel and Barouki, 1999) corroborates observed *COI* downregulation during pH stress. Despite that the *mtMutS* gene was significantly overexpressed suggesting an increased need of *mtMutS* gene product during low-pH stress that indeed resulted in mtDNA damage. This up-regulation of *mtMutS* was despite the significant down-regulation of *COI* gene as discussed earlier. Mitochondrial genes not involved in energy production pathways (such as the *mtMutS*) are generally co-expressed with the OXPHOS genes (van Waveren and Moraes, 2008). Our observation of *COI* and *mtMutS* upregulation during thermal stress is congruent with these observations. However marine organisms are known to exhibiting metabolic suppression in response to elevated CO_2 (Pörtner, 2008; Kaniewska et al., 2012). Hence, a decrease in *COI* and other stress-response genes expression during a prolonged and coral host-oriented acidification stress is anticipated. However, the decoupling of expression between *COI* and *mtMutS,* and the significant

upregulation of the later during pH stress highlights its importance, likely as a mtDNA repair protein, in the octocoral stress response. Moreover, it is clear from the observed differences in mitochondrial as well as stress-related gene expression changes between thermal and pH stress that the octocorals and their mitochondria exhibit different strategies to tackle the stressors differing in nature.

Another main goal of the present study was to evaluate the capability of octocoral mtDNA to recover from severe mtDNA damage. Hydrogen peroxide (H_2O_2), a principle mediator of oxidative stress, was used as a DNA damaging agent due to its natural occurrence and longer stability in seawater as well as high membrane permeability (Lesser, 2011) allowing it to diffuse freely throughout the cell and causing DNA damage via Fenton reaction (Henle et al., 1996). H_2O_2 is formed photochemically in seawater under natural conditions and its effects have been studied in relation to metabolic activities on stony corals (Higuchi et al., 2009).

Spatiotemporal changes in normal physiological conditions among independently growing coral nubbins over a long period of time may have resulted in variable initial impact of H_2O_2 induced mtDNA damage evident from different MLF after each treatment. Nonetheless, observed complete recovery along with an excess repair within 5 h is noteworthy. Excess repair is likely when the basic low-level mtDNA lesions present under normal physiological state (time-zero controls) are also reversed due to an induced process of damage recovery. Increase in mtDNA copy number can also lead to observed excess repair (e.g. Experiment 1 recovery). Likewise, a strong correlation is evident between mtDNA copy number and MLF. Processes such as mitochondrial fission, fusion and degradation, discussed below in detail, are underpinning the observed fluctuations in mtDNA copy number and can be correlated to quantity/extent of mtDNA damage. It has been previously shown that higher incidence of lesions leads to mtDNA degradation (Shokolenko et al., 2009), much like during first experiment where mtDNA copies reduced to half. In such stress situations cell survival depends on mitochondrial fusion, whereby cross-complementation of undamaged mtDNA, along with sharing of RNA, lipid and protein components, results in rescuing two mitochondria leading to maximized oxidative capacity during environmental stress and recovery (Youle and van der Bliek, 2012). Moreover, the lesions represent a blockage in the replication and transcription and hence the presence of efficient mtDNA repair machinery is likely to help in its rapid recovery by complementing the replication process (Li, 2008). The second H_2O_2 experiment somewhat mimics the pH stress in

terms of both MLF and mtDNA copy number changes during treatment, where retention mtDNA copies with low damage (less MLF), perhaps below threshold, is evident. Least MLF and unchanged mtDNA copies during third experiment provide an example of redundancy discussed below.

The mitochondrial copy number can vary based on energy requirements of the cells and/or oxidative stress conditions (Lee and Wei, 2005). It has also been suggested that cells with low mtDNA number are more susceptible to mtDNA damage and that high copy numbers confers buffering via redundancy (Meyer and Bess, 2012). The observation of higher initial mtDNA copies during last two H_2O_2 experiments in association with minimum fluctuations in MLF and mtDNA copy number during treatment indicates that the higher initial mtDNA/nDNA ratio is essential to mitigate the oxidative stress from its onset. It remains to be elucidated, however, what affects the initial mt-number under normal physiological conditions in octocorals. Polyp density (polyp number per unit surface area) may differ (Clayton, 1985) over a period of time and it is likely that this parameter was variable during the independent experiments spaced apart in time. Mitochondrial number also varies greatly depending on metabolic activity and energy requirements of cells and tissues (Dunn et al., 2012). Polyp as a functional unit of colony is metabolically very active, and hence likely to have high mitochondrial numbers. Consequently any differences in polyp density are likely to result in differences in mitochondrial numbers. The particular state of coral prior to the experiments could have affected the initial mtDNA/nDNA ratios of the independent experiments. However, further studies would be needed to understand the normal level of variations in mtDNA copy numbers in corals to undercover the causes of this variation. However, the initial as well as stress-affected mtDNA copy number variation remains underappreciated among corals and our present study signifies its importance during coral stress response assessment.

Recently, it has been shown that the human MutS homolog 5 (hMSH5) protein localizes in mitochondria, binding to mtDNA, interacting with DNA Polymerase gamma (POLG), and it's overexpression leads to efficient repair of oxidative lesions (Bannwarth et al., 2012). It is tempting to speculate that the elevated transcript levels of *mtMutS* gene during prolonged pH stress and mtDNA damage observed in our study indicates its role in enhancing the replication fidelity and/or DNA repair capabilities of host mitochondria during oxidative stress response. We are, however, aware that the evident mtDNA repair observed in the current study is a multifactorial phenomenon

involving other, still unexplored, molecular mechanisms in need of detailed future investigations. In this respect, functional studies of the *mtMutS* gene are still required, as is the characterization of other, if any, associated proteins involved in mtDNA repair in octocorals. The gene expression of nuclear encoded mitochondrial genes, such as *POLG*, mitochondrial DNA-directed RNA polymerase (*POLRMT)*, mitochondrial single-stranded DNA binding proteins *(mtSSB)* and mitochondrial transcription factor A (*TFAM)*, along with several other key players responsible for the maintenance of mitochondria deserved to be investigated. Alongside, comparisons of mtDNA repair capacity among different classes of cnidarians will clearly aid in advancing our understanding of the biology of coral stress response.

2.5 Conclusions

Here we present, for the first time, a mitochondria-centric view and emphasize its importance during global climate change scenarios among corals; by investigating mtDNA damage, repair, mtDNA copy number variations coupled with gene expression. We demonstrate the stress-specific gene expression strategies and upregulation of *mtMutS* gene during acidification stress. Additionally, we show that octocoral host mitochondria are capable of reversing the acute toxic stress-caused mtDNA damage, hence demonstrating their resilience potential. Recent evidences suggest that the corals are capable of acclimating to thermal stress via physiological plasticity (Bellantuono et al., 2012), transcriptome changes (Bay and Palumbi, 2015; Seneca and Palumbi, 2015) and/or by developing successful associations with more heat-tolerant symbionts (Keshavmurthy et al., 2014). There are also studies showing that the octocoral tissue can act as a barrier to resist adverse effect of lowered pH (Gabay et al., 2013; Gabay et al., 2014). Considered together all these evidences along with their resilient mitochondria point towards a potential for acclimation and positive future for some octocorals in changing future oceans.

2.6 Appendix

2.6.1 Melting Curves

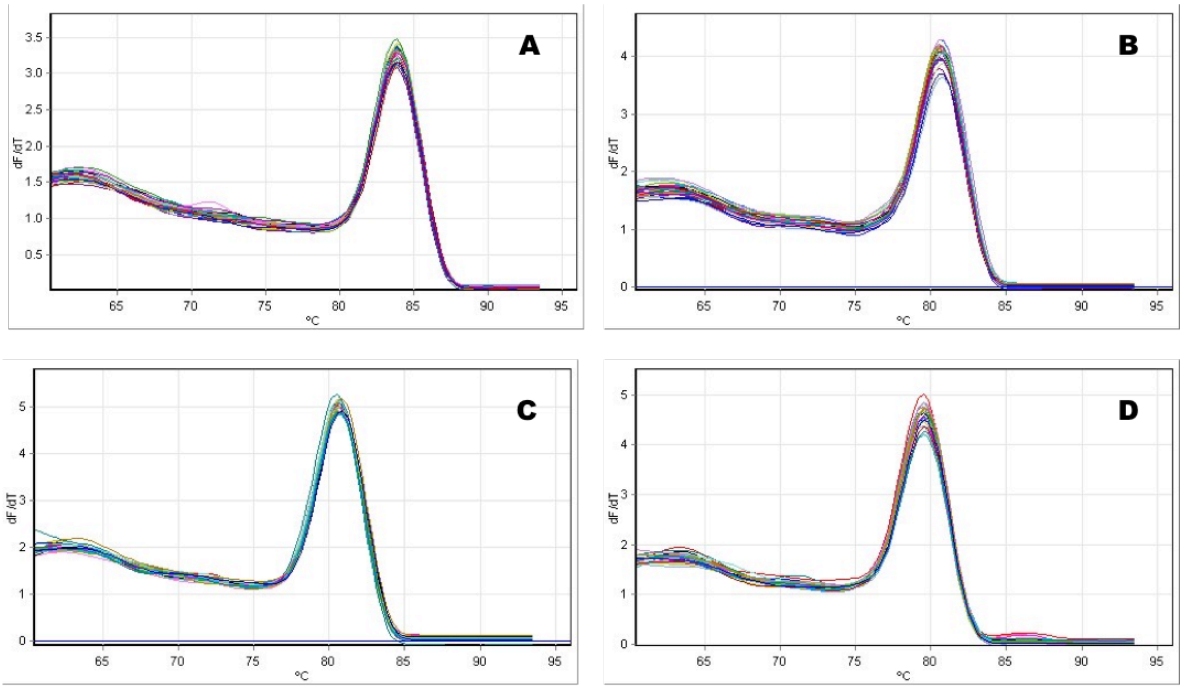

Appendix 2.6.1A: Melting curves for the reference genes : (A) *ACTB*, (B) *TUBB*, (C) *RPL12*, and (D) *SRP54*.

2.6.1 Melting Curves (continued)

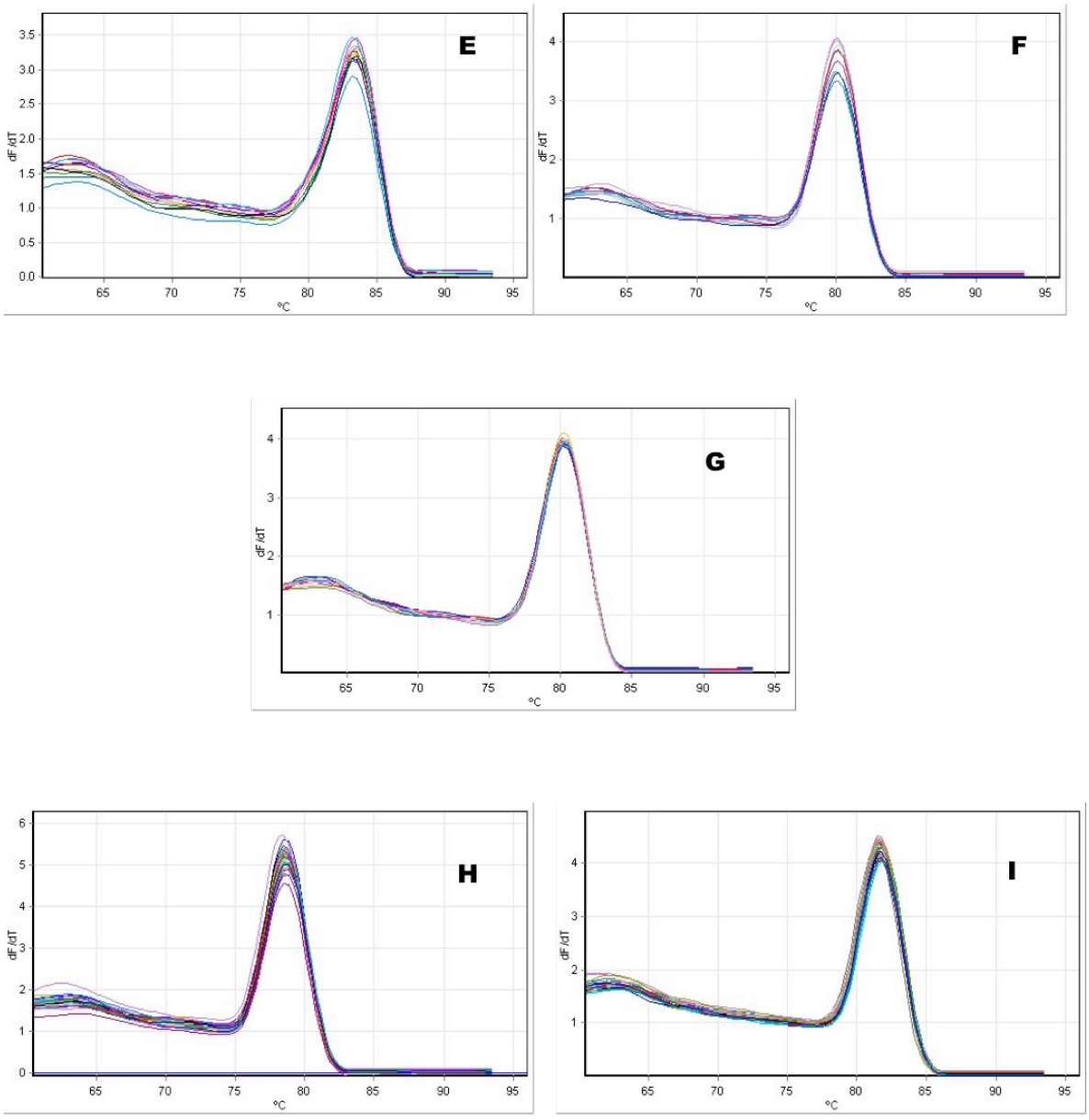

Appendix 2.6.1B Melting curves for the target genes: (E) *HSP70*, (F) *GPX*, (G) *CuZnSOD*, (H) *COI,* and (I) *mtMutS*.

2.6.1 Melting Curves (continued)

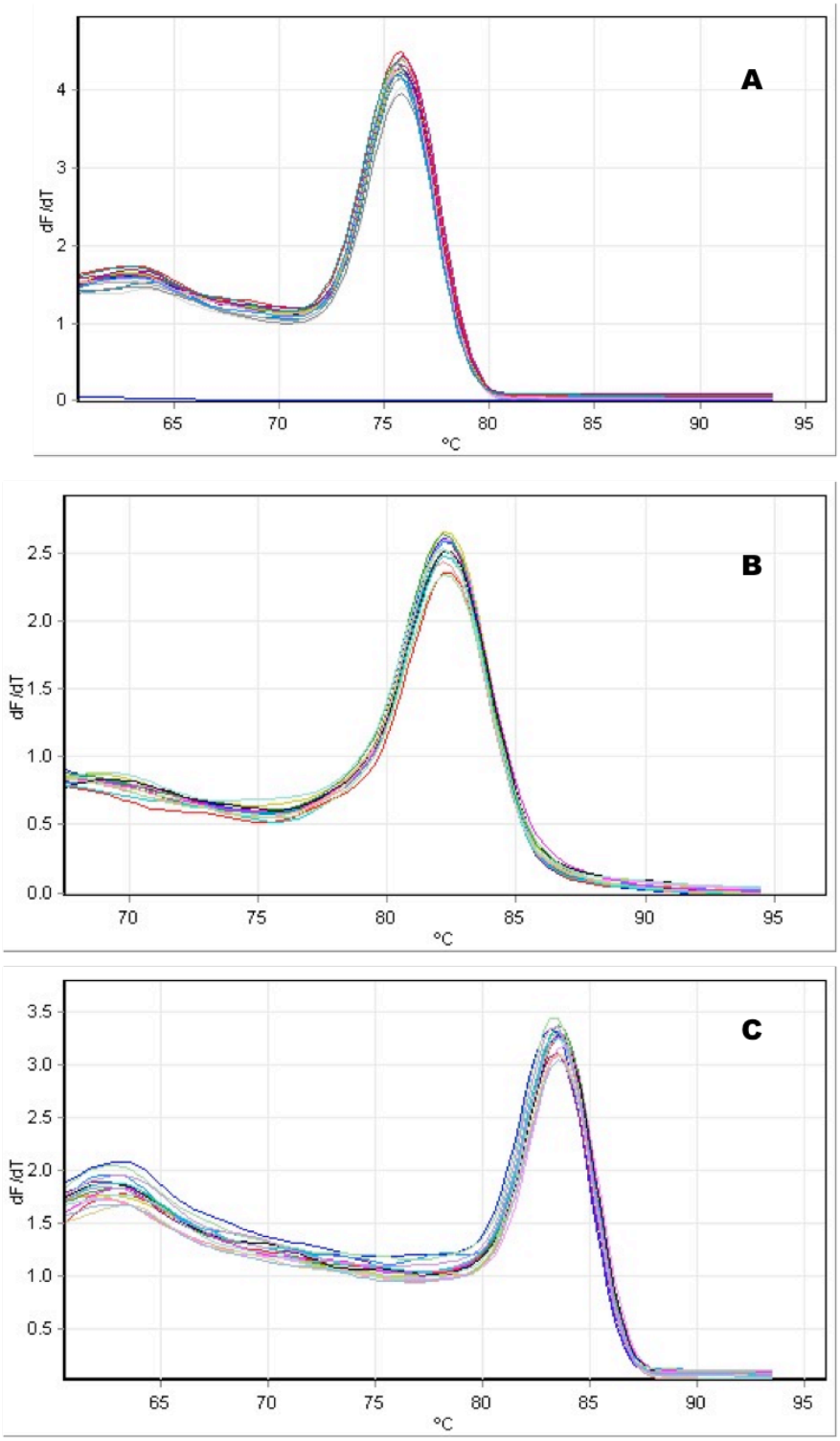

Appendix 2.6.1C: Melting curves for (A) Small mitochondria fragment (*COI*), (B) Large mitochondrial fragment (*COII-COI*) (C) Nuclear gene fragment (*ACTB*).

Appendix 2.6.2 mtDNA damage in other octocoral species after exposure to 5mM hydrogen peroxide for 30 min.

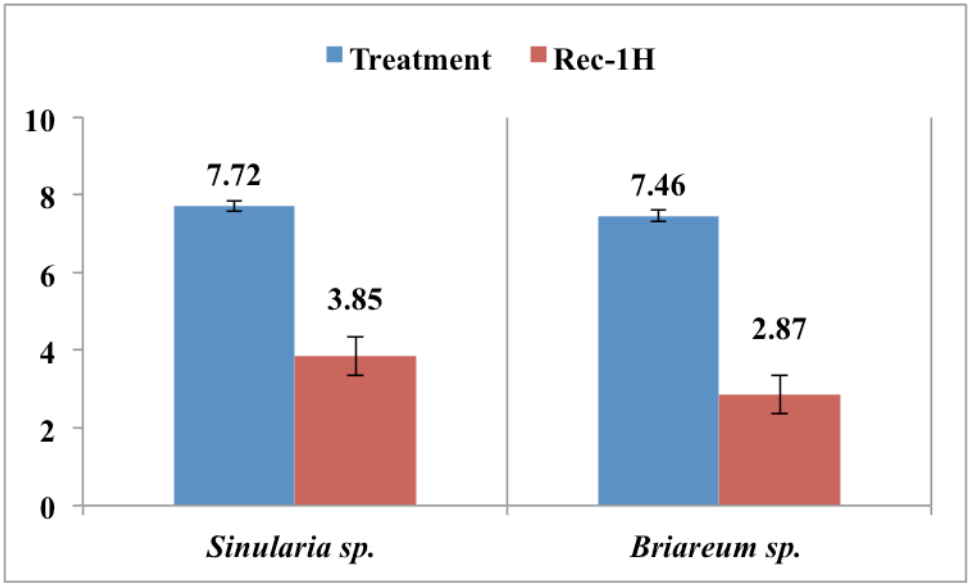

Two octocoral species (*Sinularia sp. and Briareum sp*.) were exposed to 5 mM H2O2 for 30 min (Treatment) and MLF was quantified followed by 1 h recovery (Rec-1H) and quantification.

CHAPTER 3

Mitochondrial RNA Processing in Absence of tRNA Punctuations: Lessons from Octocorals

This chapter will be submitted to 'Molecular Biology and Evolution (MBE)' journal.

Chapter 3

Mitochondrial RNA Processing in Absence of tRNA Punctuations: Lessons from Octocorals

3.1 Introduction

The great diversity of animals emerged from the ancestors of simplest members of the animal kingdom such as sponges and corals i.e., the non-bilaterians. Two major evolutionary events occurred early in the animal history forging the majority of animals, as we know them today: the origin of multicellularity, and the origin of bilateral symmetry. Multiple genomic changes accompanied these morphological transitions, and the genome sequencing projects give us a glimpse into these changes (Scientists et al., 2014). Undoubtedly, these transitions also correlate with multiple changes in mitochondrial genome (mitogenome) architecture and organization (Lavrov, 2007). The metazoan mitochondrial genome underwent reductive evolution, transferring most of its genome content to the nucleus (Berg and Kurland, 2000; Adams and Palmer, 2003). The majority of these alterations in mitogenome content include loss of ribosomal protein genes, and some tRNA genes, changes in the genetic code, disappearance of introns, and further compaction of mitochondrial DNA (mtDNA). As an aftermath, a quintessential animal mitochondrial genome harbors only 13 genes encoding essential energy pathway proteins, 2 ribosomal RNA genes and 22 transfer RNA genes. This composition is invariable among bilaterians in terms of gene content (Boore, 1999). However, alterations in mitogenome content, size and organization are more prominent and peculiar among most basal, multicellular, non-bilaterian animal members of the tree of life. The mitogenomes of non-bilaterian metazoan phyla comprise several novelties compared to typical animal mitogenomes. These include, the presence of group I introns in sponges and scleractinians (van Oppen et al., 2002; Rot et al., 2006; Szitenberg et al., 2010; Erpenbeck et al., 2015), additional protein coding genes and/or unknown ORFs and gene duplications in anthozoans (Pont-Kingdon et al., 1995; Flot and Tillier, 2007; Park et al., 2011; Lin et al., 2014), linear mitogenomes in calcisponges and

medusozoans (Voigt et al., 2008; Lavrov et al., 2013), among other. Therefore, as a hotspot of mitochondrial genome diversity, early branching animals present a unique opportunity to understand evolution of mitochondrial genome architectures as well as the fundamental processes governing its functionality and maintenance from a bottom-up perspective i.e., from early-branching to modern animals.

The significantly reduced but extremely crucial repertoire of genes present in animal mitogenomes is fundamental to its functions, and to gain deeper understanding of these processes it is essential to understand the expression and processing of mitochondrial gene transcripts. The information available so far on the mitogenome transcription originates from bilaterian members of animal kingdom (Coucheron et al., 2011; Mercer et al., 2011; Mounsey et al., 2012). The canonical animal mitogenome is known to transcribe symmetrically as polycistronic precursors spanning the entire heavy (H-) and light (L-) strands (Temperley et al., 2010). The tRNAs act as punctuation marks whereby the 22 tRNA interspersed throughout the mitogenome are recognized and cleaved off at 5' and 3' ends by mitochondrial RNase P and RNase Z, respectively (Ojala et al., 1981; Rossmanith, 2012). The genes within these precursors are simultaneously liberated for maturation following this mt-tRNA processing. Consequently, most of the mature mitochondrial mRNAs are monocistronic units with the exception of *ATP8-ATP6* and *ND4L-ND4*, which are known to exist as bicistronic elements. All messagers end with the post-transcriptional addition of 40-45 adenosines for maturation, which also completes the stop codon at 3' end of mRNA in most cases (Nagaike et al., 2008). The animal mt-mRNAs are either devoid of the untranslated regions (UTRs), or tend to have very short UTRs, consisting of 1-2 nucleotides flanking the mature mRNAs (Temperley et al., 2010). All these studies are, however, confined to a small number of vertebrates. To our knowledge, the exploration of mature mitochondrial mRNA transcripts and characterization of UTRs is still lacking for the non-bilaterian animals.

Among non-bilaterians, octocorals (Anthozoa: Octocorallia) are unique members due to their atypical mitochondrial genome organization. As many as five different gene arrangements have been reported among the octocorals studied so far (Brugler and France, 2008; Uda et al., 2011; Brockman and McFadden, 2012; Figueroa and Baco, 2015), all with an exceptionally reduced complement of transfer RNAs (a single $tRNA^{Met}$ gene) and the presence of additional gene, a unique mismatch repair gene (*mtMutS*) (Pont-Kingdon et al., 1995; Pont-Kingdon et al., 1998), closely related to the

non-eukaryotic *MutS7* lineage from epsilon-proteobacteria or DNA viruses (Bilewitch and Degnan, 2011). This gene has been speculated to have a role in the slow rate of mtDNA evolution (Shearer et al., 2002; Hellberg, 2006), intramolecular recombination and genome rearrangements (Brockman and McFadden, 2012), and predicted a self-contained mismatch repair function (Bilewitch and Degnan, 2011). Considering the mutation pressure as a key factor leading to reduced genome content in metazoan mitochondria (Lynch et al., 2006), the occurrence of such a large gene occupying almost 16% of the mitogenome in octocorals is somewhat surprising. The presence of mRNA transcript suggested its availability for translation into a protein product (Bilewitch and Degnan, 2011). However, 20 years after its discovery (Pont-Kingdon et al., 1995) and despite of being extensively used for phylogenetic studies as an the only rapidly evolving mitochondrial marker among octocorals (McFadden et al., 2011), a thorough understanding of transcriptional processing and maturation of *mtMutS* gene remains uninvestigated.

Octocoral mitogenomes contain a single gene for tRNA located subsequent to *COIII* on the L-strand. Cleavage of this tRNA from the precursor RNA will only "liberate" *COIII* mRNA at its 5' end. In such a scenario, that is, How the individual mitochondrial gene mRNAs are released for maturation from the long polycistronic precursors in the absence of punctuation marks (i.e. tRNAs) in octocoral mitochondria remains a mystery, as to date, no information on mitogenome transcription pattern, description of the mature mt-mRNA transcripts, and their 5'and 3' UTRs (if any) is available for non-bilaterian metazoans.

In absence of knowledge on precise boundaries of the mRNA in octocoral mitogenomes, despite all the novelties they confers, the understanding of biology and evolution of animal mitochondria remain incomplete. Here we characterize the mitogenome transcription of an early branching non-bilaterian, the octocoral *Sinularia* cf. *cruciata.* (Alcyoniidae: Octocorallia). We describe the 5' and 3' boundaries and UTRs of mature mitochondrial mRNAs and thoroughly characterize the transcription of the *mtMutS* gene. Our results provide the first glimpse of unique features and complexity of non-bilaterians mitochondrial transcriptome.

3.2 Materials and methods

3.2.1 Specimens

Coral colonies were obtained from a commercial source and maintained in a closed circuit seawater aquarium at Molecular Geo- and Palaeobiology lab, LMU, Munich. Two species of the genus *Sinularia* were used for current investigation. *Sinularia* cf. *cruciata* was utilized for the majority of the experiments, whereas additionally, a second *Sinularia sp*. was used for RT-PCR screening, RHAPA and antisense mRNA detection (see below). All the references to the nucleotide positions refer to the full mitochondrial genome of *Sinularia piculiaris* (GenBank accession NC_018379) (Kayal et al., 2013). The mitogenome of *S.* cf. *cruciata* was completely sequenced (Appendix 3.6.4), whereas the regions investigated here for the other *Sinularia sp*. were also sequenced, both were found predominantly conserved with respect to *S. piculiaris*.

3.2.2 Total RNA extraction and cDNA synthesis

TRIzol reagent (Invitrogen, USA) was utilized for the extraction of total RNA as per the manufacture's instructions. RNA was dissolved in 100 µl DEPC treated water and contaminating DNA was eliminated from RNA extracts by performing a DNase (RQ1 RNase-free DNase, Promega, USA) treatment at 37 °C for 30 min. Treated RNA was purified after inactivation of the DNase and its purity of RNA was determined using a Nanodrop ND-1000 spectrophotometer (Thermo Fisher Scientific, USA). RNA samples with absorbance at OD260/280 and OD260/230 ratios ~ 2.0 were used for further analysis. RNA integrity was also verified by 1% agarose gel electrophoresis as well as using a Bioanalyzer (Agilent Inc.). RNA extracts with a RIN value ≥ 7.5 were used for cDNA synthesis (data not shown). These extracts were stored at -80 °C until use.

3.2.3 Reverse-transcription PCR (RT-PCR)

RNA extracts were PCR controlled in order to detect amplifiable levels of small DNA fragments. Only RNA extracts devoid of any amplification were used in RT-PCR experiments. For each sample, ~1 µg of total RNA was reverse transcribed using ProtoScript® II First Strand cDNA Synthesis Kit (New England Biolabs, USA) employing an anchored oligo-(dT) primer in 20 µl reactions according to manufacture's instructions.

RT-PCR sequencing primers were designed using the published mitochondrial genomic sequence of *Sinularia piculiaris,* GenBank accession NC_018379.1 (Kayal et al., 2013). Screening for the presence of the polycistronic mRNAs was done using the primers enlisted in Table 3.1.

Table 3.1: RT-PCR screening for mature mRNA transcripts spanning two or more genes

Sr. No.	Primer Pair Forward/Reverse	Regions	Length (bp)	igr+Gene*	RT-PCR	
					DNA	cDNA
1	C2-18173/C1-839	*COII-COI*	1051	951	☑	☒
2	C1-743/12S-2240	*COI-12S*	1498	658	☑	☒
3	N1-3534/CB-4128	*ND1-CYTB*	595	479	☑	☑
4	CB-4539/N6-4995	*CYTB-ND6*	457	152	☑	☑
5	CB-4539/N3-5623	*CYTB-ND6-ND3*	1085	*ND6*+182	☑	☒
6	N6-4972/N3-5623	*ND6-ND3*	652	182	☑	☑
7	N6-4972/N3-5841	*ND6-ND3*	870	400	☑	☑
8	N6-4972/N4L-6141	*ND6-ND3-ND4L*	1170	*ND3*+291	☑	☑
9	N3-5520/M-6801	*ND3-ND4L-mtMutS*	1282	*ND4L*+638	☑	☑
10	N3-5520/M-7220	*ND3-ND4L-mtMutS*	1701	*ND4L*+1057	☑	☑
11	N3-5520/M-8298	*ND3-ND4L-mtMutS*	2779	*ND4L*+2135	☑	☑
12	N3-5520/M-8838	*ND3-ND4L-mtMutS*	3319	*ND4L*+2675	☑	☑
13	M-8725/16S-9408	*mtMutS-16S*	683	259	☑	☑
14	16S-10966/N2-11765	*16S-ND2*	800	639	☑	☒
15	N2-12177/N5-12636	*ND2-ND5*	458	118	☑	☑
16	N5-12973/N4-15325	*ND5-ND4*	2353	989	☑	☒
17	N4-14818/C3-16480	*ND4-COIII*	1663	599	☑	☒
18	N4-15725/A6-17060	*ND4-COIII-ATP6*	1336	*COIII*+226	☑	☒

☑ Positive amplification

☒ No amplification

Primer codes= first part indicates the gene name and the number indicates 5' end of primer corresponding to *S. piculiaris* mitogenome (NC_018379)

Asterisk (*) indicates bps into the gene downstream to the igr

3.2.4 Analysis of 5’ and 3’ ends

Two different approaches were used for analyzing the transcript ends of mature mitochondrial mRNA species.

3.2.4.1 Circularized RT-PCR (cRT-PCR)

Isolation of mRNA from total RNA was performed using Dynabeads® mRNA purification kit (Invitrogen). 100 ng of polyA-selected mRNA as well as total RNA were circularized using T4 RNA ligase I (New England Biolabs) following the manufacture’s protocol. The circularized RNA was purified and used for cRT-PCR and 5’/3’ end screening using the method described by (Slomovic and Schuster, 2013). cDNA synthesis was performed as described above using gene-specific reverse primers (listed in Table 3.2).

Table 3.2: Primers used in this study

A. Primers used in 5' and 3' RACE Amplification				
Gene	**5'RACE**	**Sequence**	**3'RACE**	**Sequence**
COI	C1-839*	ATCATAGCATAGACCATACC		
	C1-1144	CATAGTGGAAGTGAGCTACTAC		
CytB-ND6	CB-4128*	GCTCCCCAAAAGGACATTTGTC		
ND3-ND4-mtMutS	N3-5623	CACATTCATAGACCGACACTT	N4L-6092	GCCATTATGGTTAACTATTAC
	M-6402	ACGAAGCAACTTGTTCAATGG	M-6384	ATTGAACAAGTTGCYTCGTTACTTG
	M-6740	CCGGGTTACTTTGTCCCTGTCCG	M-8636	TGATTCGCCAGTTCGGTGCT
			M-6676	CAGCCATGAATGGGCATAG
			M-8079	GCATTAAGCGGGGCTATTGCGG
COII	C2-18173	CCATAACAGGACTAGCAGCATC		
B. Primers used in cRT-PCR				
Gene	**3' Facing**	**Sequence**	**5' Facing**	**Sequence**
COI	C1-1324	TACTCGGATTTCCCTGATGC	C1-251	AACCAATTTCCGAATCCTCCG
CytB-ND6	N6-4972	TTTGGTTAGTTATTGCCTTT	CB-4128*	GCTCCCCAAAAGGACATTTGTC
ND3-ND4-mtMutS	M-8636	TGATTCGCCAGTTCGGTGCT	M-6801*	TTAAACCTACCCCCGAGTCC
ND2-ND5	N5-14131	GCTCAGTTTGGAAGTTTGGC	N2-11765*	ACATCGGGAGCCCACATA
ND4	N4-15725	TTTTGGGCAACTTTCTCC	N4-14543	CAGAGACCACTCTAACGCTTGTTG
COII-ATP6-ATP8	C2-18173	GGTTGAAGGTCACTCGTAGGTATC	A6-17060	GGGTTCGCAATGATTAGTAATGGAATGT

C. Gene-specific primers used for RT for cRT-PCR analysis		
Gene	**Primer**	**Sequence**
ATP6	A6-17104	TTAGCAGCCAATCGAACACC
ND4	N4-15325	GCGTCTACCTGTCTGCAAGT
mtMutS	M-8838	CATTTCGGGATGGTAGCTCC

Asterisk (*) indicates the other primers used for RT during cRT-PCR

3.2.4.2 Rapid amplification of cDNA ends (5'and 3' RACE)

First strand synthesis was performed to obtain the template for 5' and 3' RACE PCRs using SMART™ RACE cDNA Amplification Kit (CLONETECH Inc.) following the supplier's protocol. Approximately ~1 µg of total RNA was used for cDNA synthesis to obtain two separate pools of 5'-RACE-Ready cDNA and 3'-RACE-Ready cDNA. RACE PCR reactions were the performed using different gene-specific primers and adaptors primers as per the supplier's instructions (see Table 3.2).

3.2.5 Cloning, sequencing and sequence analysis of amplified products

Amplified products were either extracted from the 1% agarose gel or purified using NucleoSpin Gel and PCR Purification Kit (MACHEREY-NAGEL, Germany) and cloned using a TOPO TA Cloning Kit (Invitrogen). The clones obtained were PCR amplified, precipitated and sequenced using ABI BigDye v3.1 sequencing chemistry on an ABI 3730 DNA Analyzer Sequencing instrument. Sequences obtained were edited and aligned to the mitogenomes of *S. piculiaris* (NC_018379) analyzed using Geneious® 6.1.6 software (Biomatters) (Kearse et al., 2012). mtDNA sequences from the other two *Sinualria* species were also aligned for comparison.

3.2.6 Detection and quantification of alternative polyadenylation (APA)

RNase H alternative polyadenylation assay or RHAPA (Cornett and Lutz, 2014) was employed to determine and quantify alternative polyadenylation of the *mtMutS* mRNA transcripts. For the first time, we coupled this assay with quantitative real-time PCR technique (qPCR) for accurate estimation of the abundance of alternative transcripts. Primers used for removing the 3' end poly(A) tail was 5'-CATTTCGGGATGGTAGCTCC-3', which hybridized to *mtMutS* mRNA between positions 8819-8838. This DNA-RNA hybrid was digested with the help of RNase H resulting in a truncated *mtMutS* mRNA with an associated loss of the 3'region adjacent to the poly(A) tail. This RNA was purified using RNA Clean & Concentrator™ kit (Zymo Research) and reverse transcribed using oligo(dT) as described above. A control RT-PCR using primers binding to the adjacent regions of the RNase H digested site ensured the successful digestion of the 3' including and poly(A) tail of mature, full mRNA species. This was followed by a quantitative real-time PCR (qPCR) assay to determine abundance-levels of transcript upstream and downstream of digested mRNA region. Primer details can be found in Appendix 3.6.1.

3.2.7 Strand-Specific RT-PCR

Strand-specific RT-PCR was performed as described previously (Ho et al., 2010) for the detection of antisense RNA transcripts of the *ATP6* gene in both *Sinularia* species. Earlier, we observed one of the clones containing a RACE adaptor ligated at 3'end of 5' RACE-ready cDNA suggesting the presence of antisense transcript for *ATP6* gene, also noted previously in porcine brain (Michel et al., 2000). Two antisense strand-specific primers were used for cDNA synthesis (AAR1. 5'-TTACTCCTACTGCCCATATTG-3' and AAR2. 5'-TGTAGTTCGGATAATTGGGGG-3'), whereas sense strand specific primer (SAF. 5'-TTAGCAGCCAATCGAACACC-3') as well as an anchored oligo(dT) employed separately for first strand synthesis. For RT-PCR, AAR1-SAF primer pair was used.

3.2.8 Experimental treatment

Three coral nubbins of *Sinularia* cf. *cruciata* were exposed to two different stress conditions, such as thermal stress (temperature=34 °Cfor 6 h) and low-pH stress (pH =7.5 for 24 h). Primers binding to different *mtMutS* gene regions, like 5' region, central region and 3'end region were used for qPCR to determine the relative abundance of transcript having these regions among mRNA variants. *COI* was used as proxy for comparison and stress-specific sets of three reference genes were used for normalization of gene expression during each condition (Thermal stress= *RPL12+SRP54+ACTB* and low-pH stress= *ACTB+TUBB+SRP54*). (For primer details see Appendix 3.6.2).

3.2.9 Quantitative Real-time RT-PCR (qPCR) and data analysis

Rotor-Gene Q 2plex system (QIAGEN) was utilized for the qPCR analysis. The KAPA SYBR FAST universal mastermix (Peqlab) was used in 15 µl reactions containing 1 µl diluted cDNA, 7.5µl 2X mastermix, and 250 to 400 nM each primer. A two-step qPCR including an initial denaturation step of 3 min at 95 °C followed by 40 cycles of 95 °C for 10 s and 60 °C for 20 s. A non-template control was always included in each assay. Melting curve analysis was performed at the end of each qPCR to confirm amplification specificity and amplification products were also checked by agarose gel electrophoresis after each assay.

Fluorescence data obtained after qPCR was analyzed using LinRegPCR, which determines Cq values and PCR efficiencies (Ruijter et al., 2009). Using these values

further analysis of gene expression and statistical tests were performed using REST 2009 (QIAGEN) as described previously (Pfaffl et al., 2002).

3.3 Results

3.3.1 RT-PCR screening for mature mRNA transcripts spanning two or more genes

In the absence of tRNA punctuation marks, to determine the presence of mature polycistronic mRNA transcripts, we conducted RT-PCR using primers for adjacent protein coding gene regions, away from protein start/stop codons, and amplifying parts of both genes and their intergenic regions (IGRs). Amplification was observed using all primer pairs for all the gene-regions screened using DNA as a template. However, using cDNA as a PCR template, mitogenomic regions spanning two adjacent genes were amplified for most but not all genes, suggesting the presence of several bicistronic as well as tricistronic mature mRNA transcripts (see Table 3.1). The regions spanning *COI-12S*, *CytB-ND6-ND3*, *16S-ND2*, *ND5-ND4*, *ND4-COIII*, and *COII-COI* did not yield any detectable PCR products, suggesting most other regions screened are parts of polycistronic transcription units. These results allowed us locate the boundaries of the mature mRNA transcripts.

3.3.2 Characterization of 5' and 3' ends of *mtMutS* gene mRNA

5'-RACE mapped the 5' end of the *mtMutS* gene upstream of *ND3* start codon with a long 31bp 5'UTR suggesting that this gene is transcribed as a tricistronic unit together with *ND3* and *ND4L* (Figure 3.1). Using several *mtMutS*-specific primers we were unable to detect any alternate 5' end using RACE PCR. However, when cRT-PCR was employed, an internal *mtMutS* 5'end was detected at 6565-position which is 389bp downstream of the annotated *mtMutS* start codon, indicating that either a monocistronic *mtMutS* species encompassing two out of four protein domains exist, or a sign of existence of truncated polyadenylated transcripts. An additional single thymine, which is not present in the DNA sequence of any *Sinularia* species as determined visually by BLAST search, was detected at 5' end of the message. The region flanking this start position is highly conserved in the genus with no substitutions in the vicinity of this 5'end. Hence, this thymine residue indicates the potential RNA editing of *mtMutS*

internal transcript. When sequenced with the opposite primer, a 3'end for this transcript was observed at a position 8962, which is 187bp upstream to the annotated stop codon. This transcript ended with UAA clearly followed by a polyA-tail. The stop codon, however, is not in frame. Hence, if or how it is used during translation as a termination signal remains unknown.

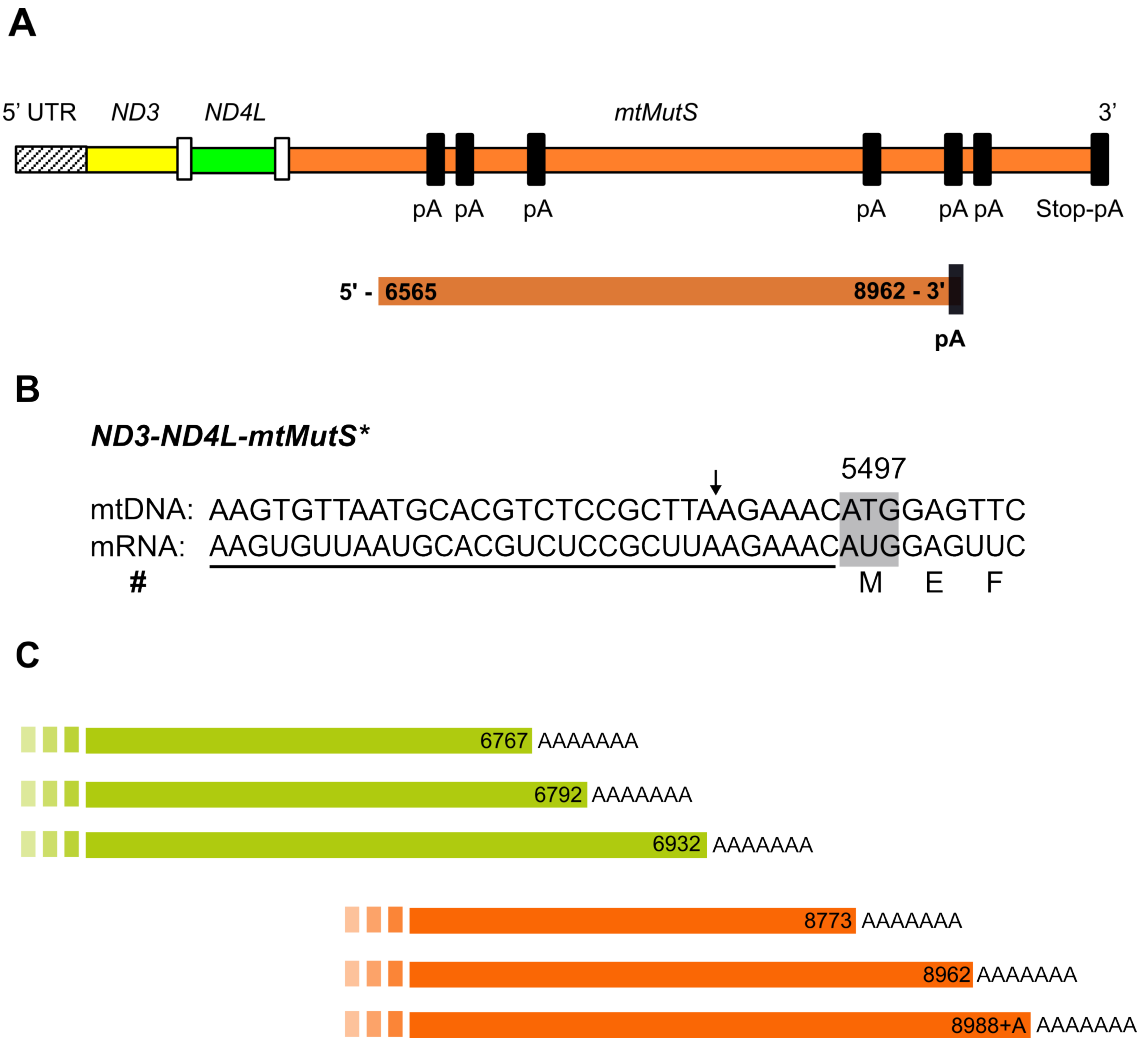

Figure 3.1 The *mtMutS* mRNA transcript variants.

(A) Schematic of the *mtMutS* gene as a tricistronic transcription unit with different poly(A) tail positions (not to scale) shown as dark blocks. pA=poly(A)-tail. Below is the internal transcript. **(B)** The 5' end of *ND3-ND4L-mtMutS* tricistronic transcript. The 5' UTR region is underlined. Shaded box depicts start codon. Arrow above indicates 11bp deletion in *S.* cf. *cruciata* compared to *S. piculiaris*. # indicates detection using both, RACE and cRT-PCR methods. **(C)** Alternatively polyadenylated *mtMutS* mRNAs. Position of the poly(A) start is indicated.

Surprisingly, at least 6 different 3' ends were detected for the *mtMutS* gene mRNA using both methods. These were found to end at position 6767, 6792, 6932, 8773, 8962 (described above), and 8989 besides the annotated in-frame stop codon at position-9150

(Figure 3.1). These messages end in with two types of codon before polyadenylation, such as GAA and UAA. Only one of them (i.e., 8989) was found to complete UAA-stop codon by with the addition of poly(A) tail. Notably, none of these end-codons are in-frame, as observed earlier for the internal transcript. Full *mtMutS* gene as per annotation along with different possible regions spanning from *ND3* 5'-end until *mtMutS* 3'-end were screened using RT-PCR confirmed the presence of all possible transcript variant described above (See Appendix 3.6.3 for details).

Additionally, the gene-specific cRT-PCR yielded several unprocessed precursor RNAs spanning 3'*mtMutS*-5'*16S*-5'*ND3* regions. Several clones containing similarly structured pre-mRNAs were observed suggesting a strong presence of unprocessed pre-mRNAs/rRNAs of various lengths for this particular region. 5'RACE detected a truncated *16S* transcript starting at a position 10684 further corroborating the presence of unprocessed RNA in the sample.

3.3.3. Mapping the ends of other mitochondrial protein coding gene mRNAs

Along with the *mtMutS* gene, the mRNA and/or mature transcriptional units of several other protein coding genes were mapped. The *COI* mRNA was start precisely at position 1 and has a 4bp 5'UTR upstream to this start codon. We also detected the 3'end this gene, which was unknown due to the absence of proper stop codon at the 3' end of *COI* gene. The *COI* mRNA terminates at a position 1590 after creating a stop codon (UAA) by addition of the last A during polyadenylation for maturation of the mRNA. This suggests that the polyadenylation takes place after the first TA nucleotides (nts) immediately following the annotated (uncertain) 3' end in *Sinularia spp*. This may also occur in other octocorals in which the precise *COI* stop codon is not known, however, this needs to be confirmed in others members also. This confirms that the *COI* is a monocistronic gene expressed as a single unit.

Three different 5' ends for the *CytB* mRNA were detected. One of these 5'ends initiated at position 3683, exactly two codons (6bp) downstream from the annotated start, without any 5'UTR. The other two were downstream from this 5'end at positions 3926 and 3970. The first two messengers were detected using both the methods whereas the third one was observed with only with cRT-PCR.

As suggested by the initial RT-PCR screening, the *CytB* mRNA was found to continue into the *ND6* gene. Consequently, no 3'end could be detected for *CytB* mRNA

suggesting it to be a bicistronic unit co-expressed with *ND6* gene. A polyadenylated *ND6* mRNA 3'end was detected with an 8bp 3'UTR. However, as reported previously in other animals (Slomovic et al., 2005), the possible presence of variable length mRNA extending further can not be excluded, as apparent from the RT-PCR results indicating amplification of the region spanning *ND6-ND3-ND4L* mRNA.

Solely based on cRT-PCR, the mature mRNA ends were detected for the *ND2-ND5* dicistronic unit and for the *ND4* gene. Only the 5'end for the former could be detected, which has a single base as 5'UTR before the start codon at position 11185, not 11158 as it is annotated. Similarly, a 12bp 5'UTR was detected for the *ND4* mRNA along with a 44bp 3'UTR after the stop codon at position 15879.

Initial RT-PCR results indicated the presence of a *COII-ATP8-ATP6* tricistronic mRNA. End mapping corroborated this observation. *COII* mRNA was found to contain a 3bp 5'UTR whereas an 83bp long 3'UTR was detected after the stop codon of *ATP6*. The ends of the protein coding genes *ND1* and *COIII* remain undermined, which most likely are monocistronic messages based on initial RT-PCR results. For more details on UTRs of the mature mt-mRNAs see Figure 3.2.

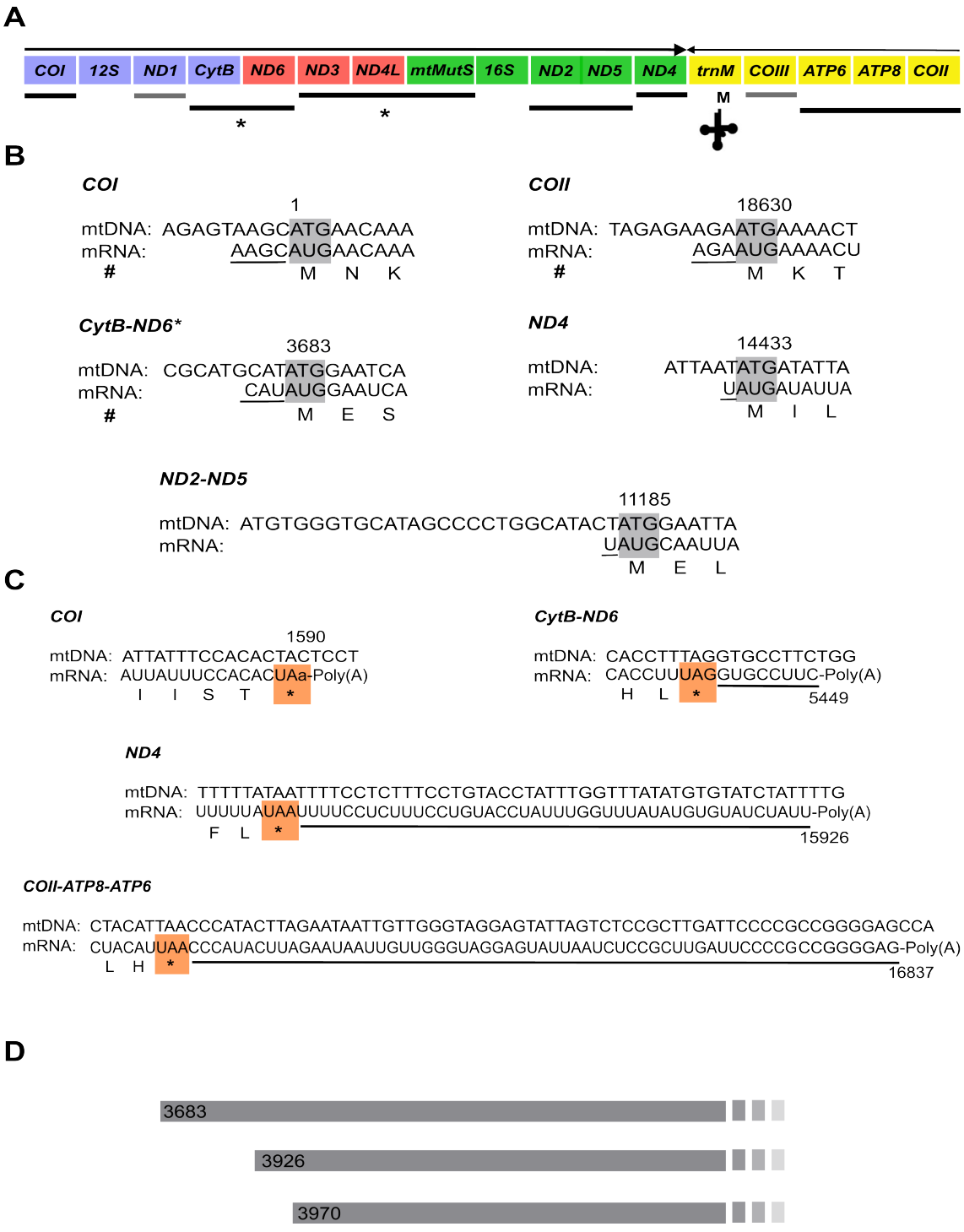

Figure 3.2 Mapped 5' and 3' ends of mature mitochondrial mRNAs.

(A) Schematic representation of *Sinularia* mito-transcriptome arrangement. Arrows above show transcription orientation. Lines below denote the transcription units (mono- and polycistronic transcripts). Asterisk (*) shows the transcription units for which alternate ends were detected. **(B)** Summary of 5' end mapping for mt-mtRNAs. The 5' UTR regions are underlined. Shaded boxes depict start codons. # indicates detection using both, RACE and cRT-PCR methods. Nucleotide positions of the first base of start codons are indicated. **(C)** Summary of 3' end mapping for mt-mtRNAs. The 3' UTR regions are underlined. Colored boxes show stop codons. Nucleotide positions of the last base of stop codons are indicated. **(D)** Alternative starting positions of *CytB-ND6* mRNA.

3.3.4 Detection and quantification of alternatively polyadenylated for *mtMutS* messengers

Further confirmation of alternative polyadenylation of *mtMutS* messengers in the normal mt-mRNA pool was attained using RHAPA method.

Real-time PCR based quantification of different variants using primer pairs binding the 5'region (immediate downstream of the start codon), the central region and the 3'region (cleaved off with RNase H) (2 primer pairs each) suggested a variable expression levels of these parts of the *mtMutS* gene. The central region, which includes partial domain III region of *mtMutS,* was 6.35±0.3 fold more abundant than the 3'end whereas the transcript containing the 5'part was 1.8±0.15 fold higher relative to the extreme 3'end of the *mtMutS* mRNA transcript (Figure 3.3). This observation suggests the existence of different variants of the same gene under normal conditions in the mature mt-mRNA pool of octocorals.

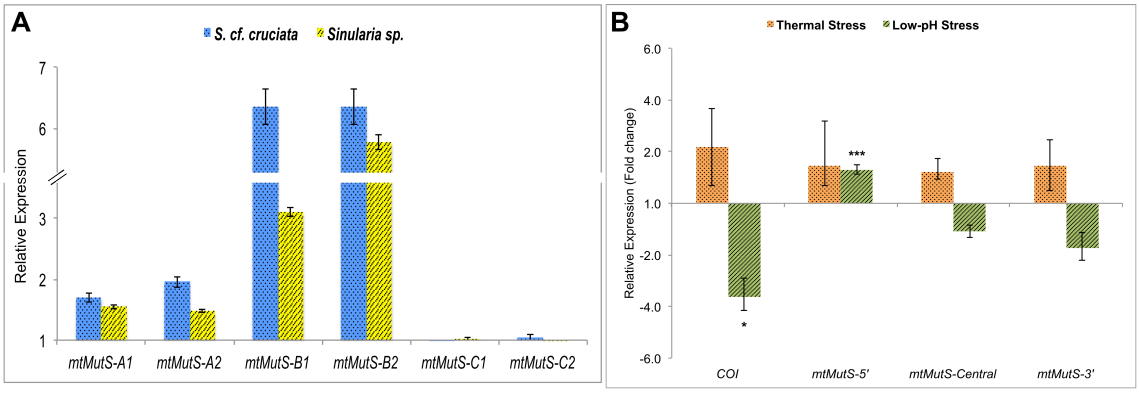

Figure 3.3 Relative quantification of mRNA transcript abundance.

(A) Quantification alternatively polyadenylated *mtMutS* transcripts. *ACTB* gene served as reference. Comparison was performed against 3' region cleaved-off after RNase H digestion (*mtMutS*-C1, C2). Data shows relative expression ± SD of technical triplicates for two *Sinularia* species. **(B)** Changes in transcript levels of mitochondrial genes *COI* and *mtMutS* (5', central and 3' part) were assessed. Normalization was performed using validated sets of three reference genes (Thermal stress= *RPL12+SRP54+ACTB*, and low-pH stress= *ACTB+TUBB+SRP54*). Bars represent the mean expression value (fold change ± SE) relative to untreated controls (26 °C or pH 8.2) of three biological replicates. * Statistical significant at $p < 0.05$; *** Statistical significant at $p < 0.001$.

We further investigated the gene expression pattern of these 3 regions under two stress conditions. The three primer pairs binding 5', central and 3' parts of *mtMutS* gene indicated comparable relative expression values during thermal stress conditions suggesting a balanced expression of different *mtMutS* variants and/or a full mRNA.

Slight upregulation was observed for both *mtMutS* as well as *COI* genes without any significance difference. On the contrary, during exposure to low-pH conditions, the 5'end portion was detected as significantly upregulated (1.3±0.1; $p<0.001$) indicating its preferential expression. The *COI* gene was also found to be significantly downregulated under this condition (-3.6±0.6; $p<0.05$). Surprisingly, the central and 3'end regions did not show any significant differential expression and were slightly downregulated (-1.35 and -2.1 fold, respectively) as opposed to the 5'part of the gene (Figure 3.3), indicating the higher presence of alternatively polyadenylated *mtMutS* mRNAs coding for only the first protein domain.

3.3.5 Antisense *ATP6* mRNA

We detected the presence of an antisense mRNA transcript complementary to *ATP6* gene coding strand using 5'RACE approach. Five different starting points were determined for these antisense transcripts at positions 16849, 16891, 16895, 16896, and 16932. The reverse primer used for PCR was specific to the antisense strand and bind the heavy strand at the position 17060, which indicates that this antisense transcript is longer than 200bp, polyadenylated (i.e. reverse transcribed using anchored oligo-dT), and lacking open reading frames (ORFs). Therefore, this RNA species can be categorized as long noncoding RNA (lncRNA) (Rinn and Chang, 2012).

Antisense strand-specific RT-PCR as described earlier resulted in the successful amplification of an internal region after strand-specific reverse transcription further corroborating the presence of the *ATP6* lncRNA (lnc*ATP6*).

3.4 Discussion

Using different experimental approaches we describe, for the first time, the complex mitogenome expression patterns present in early branching animals. The precise ends of most mature mt-mRNAs were assessed for the first time in octocorals. Most mature protein-coding mRNAs detected were bicistronic or tricistronic units, with the exception of *COI*, *ND4* and putatively, *ND1* and *COIII*. The occurrence of polycistronic mature mRNAs potentially stems from the paucity of tRNA punctuation marks in octocoral mitogenome. The majority of mature transcription units were detected to possess 5' and 3' UTRs, contrary to what is known for bilterians in general. Moreover, occurrence of alternative polyadenylation (APA) of the *mtMutS* mRNA transcript, long non-coding antisense *ATP6* RNA (lnc*ATP6*) and unprocessed mRNA intermediates indicate very

distinctive ways of mitogenomes expression. These novel features detected provide a glimpse into a unique and complex mitochondrial transcription mechanism for early branching members metazoan.

Evolution of specific mechanisms for expression of the mitogenome was necessitated by the reduced gene repertoire and compact nature of this crucial cell organelle with its own genome evolved from the α-proteobacterium-like ancestor (Gray, 1993; Dyall et al., 2004). In cnidarians, which harbor only 16±2 genes contrary to a typical animal mitogenome containing 37 genes in total, reduction in gene content, but not the genome size, is remarkable to some extent. Our understanding of the mitogenome transcription/expression patterns and regulation is currently limited to a handful of bilaterian members of the animal kingdom (Stewart and Beckenbach, 2009; Coucheron et al., 2011; Mercer et al., 2011). However, such attempts are lacking for non-bilaterians. Information on the mitochondrial transcriptomes of three sea anemones (Emblem et al., 2014) have added to our understanding the potential complexity of mitochondrial transcription and highlighted the need for a better understanding of the evolutionary processes leading to different strategies of mitochondrial transcription and regulation.

Processing of mt-tRNAs interspersed in the mitogenomes of animals holds a key to liberating protein-coding mRNAs from polycistronic precursors leading to their maturation and availability for translation (Ojala et al., 1981). Most studies so far have reported that majority of processing events adhere to tRNA punctuation model except for the occurrence bicistronic transcription units like *ATP8-ATP6* and *ND4L-ND4* apparently due to overlapping ORFs in animals (Stewart and Beckenbach, 2009; Temperley et al., 2010; Coucheron et al., 2011). In cnidarians, however, presence of only one or two tRNA genes in the mitogenomes point towards the utilization of an unknown mechanism of mRNA maturation or existence of a different post-transcriptional regulatory system for mitochondrial gene expression. Our observation of 4 polycistronic units comprising 10 (out of 14) different genes is staggering, and suggests a potentially unique mt-mRNA processing as well as gene expression mechanism in octocorals. Our findings may also apply to other early branching animals with a paucity of mt-tRNA genes.

The untranslated regions (UTRs) flanking the mature mRNA transcripts play a crucial role in post-transcriptional regulation of gene expression (Mignone et al., 2002). However, in the case of mitogenomes, the mature mRNA transcripts are generally

devoid of, or having only few (≤3) nucleotides as UTRs (Temperley et al., 2010). The presence of 5'UTRs for transcriptional units such as *COI*, *ND3-ND4L-mtMutS*, *ND2-ND5*, *ND4*, and *COII-ATP8-ATP6* mRNA, as well as, 3'UTRs for *CytB-ND6*, *ND4*, *COII-ATP8-ATP6* suggests a putative role of these UTRs in tight regulation of these genes and represent, to our knowledge, the first report of the presence of long UTRs in mature mt-mRNAs.

Different studies have detected at least five diverse mitogenome arrangements in octocorals all of which appear to preserve four conserved gene blocks and the inversion or translocation of one these blocks led to five mitogenome arrangements (Brockman and McFadden, 2012; Figueroa and Baco, 2015). It has been suggested that the occurrence of the genes in conserved clusters is selectively advantageous, for instance, as the genes can be co-transcribed and processed in a similar way (Dowton and Campbell, 2001; Brockman and McFadden, 2012). However, the evidence on selection favoring a particular mitochondria gene order is sparse in cnidarians, as they exhibit high diversity of mitogenome arrangements with no sharing of gene boundaries, particularly in subclass Hexacorallia (Brockman and McFadden, 2012). Our results indicate that the transcriptional units possess genes from two distinct adjacent gene blocks (e.g. the polycistronic transcription units *CytB-ND6* and *ND3-ND4L-mtMutS*), contradicting the hypothesis of co-transcription as a selective force in keeping these genes together in conserved blocks in the mitochondria of octocorals. Moreover, it also indicates that different mitogenome rearrangements detected so far in octocorals may have different mature mt-mRNA transcript structures and transcription patterns, highlighting the potential complexity of mitochondrial transcription among non-bilaterians, and the need for research in order to better understand mitochondrial evolution in these animal groups.

The *mtMutS* gene present in octocorals is thought to underpin several peculiar processes not present in typical animal mitochondria. The presence of such a large gene seemingly uninvolved in energy production, within a streamlined organelle genome dedicated to this task is mysterious as well as interesting. The second largest gene in *Sinularia piculiaris* mitogenome, *ND5* 1818bp long is known to be the most tightly regulated protein-coding gene in other animals (Bai et al., 2000). Thus it could be hypothesized that the transcription of *mtMutS* is tightly regulated as well. Consistent with this hypothesis we observed distinct *mtMutS* variants resulting from the use of different polyadenylation site internal to the full *mtMutS* gene. It clearly indicates the presence of

alternative polyadenylation (APA) occurring in octocoral mitochondria. Primary function of RNA polyadenylation in plants mitochondria and bacteria is to promote RNA degradation (Mohanty and Kushner, 2011), whereas in mammals the poly(A) tails provide stability to the mature mRNA and create the stop codon, if it is not complete (Nagaike et al., 2008). Polyadenylated truncated transcripts destined to degradation have also been detected in mammals (Slomovic et al., 2005); however, the abundance of such messengers is low and they are generally difficult to detect using standard methods. All the *mtMutS* variants reported here were readily detectable indicating their potential functional role.

Interestingly, the transcripts detected were differentially expressed. Under normal conditions a transcript variant encompassing Domain III and V of *mtMutS* (position 6565-8962) was more abundant than either the 5'or 3'end regions. These domains are central to the structure of the *mutS* gene (Domain III) and display ATPase functionality (Domain V) (Obmolova et al., 2000; Bilewitch and Degnan, 2011). Under low-pH conditions, stringent upregulation ($p < 0.001$) was detected only for the 5'end mRNAvariant; whereas, downregulation was found for the central and 3'regions. The Domain I, encoded in the 5'-end variants, possess the conserved residues responsible for mismatch recognition (Bilewitch and Degnan, 2011). The overexpression of this variation may be interpreted as a necessity for increased mismatch recognition in the mitochondria. Exposure to thermal stress, however, did not result in differential expression. All mRNA variants were expressed in equal abundance or there was no alternative polyadenylation. The method used doesn't allow distinguishing between these possibilities. Alternative polyadenylation plays a crucial role in regulating the gene expression (Lutz and Moreira, 2011). Hence, the occurrence of alternative polyadenylation for the *mtMuts* gene mRNA is a novel finding in octocoral mitochondria serving a putative regulatory function for *mtMutS* gene expression. The precise start and end points of each *mtMutS* mRNA variant deserved to be determined to better understand how the start-stop codons are chosen during translation. Additionally, protein studies need to be conducted in order to corroborate the localization and functionality of these transcripts and their products.

Long noncoding RNAs (lncRNAs) have been recently described in the mitochondria of mammals, primarily for *ND5*, *ND6* and *CytB,* and are shown to interact with their mRNA complement, which may have roles in stabilizing the mRNA and/or blocking the access of mitochondrial ribosome, thereby inhibiting translation (Rackham et al.,

2011). The presence of a lncRNA transcript for *ATP6* (lnc*ATP6*) in *Sinularia* mitochondria is striking, and indicated that the regulation of mitochondrial expression using lncRNAs evolved early in Metazoa and is ancient.

The dependency of mitochondrial biogenesis on the nuclear genome is evident, as more than 99% of mitochondrial proteome is nuclear DNA-encoded including mt-tRNAs, which are imported in mitochondria after their expression in the cytosol (Salinas-Giege et al., 2015). Loss of mt-tRNAs in cnidarians is suggested to be genuine and occurred in association with loss of nuclear-encoded mt-aminoacyl-tRNA synthetases (Haen et al., 2010). This scarcity of mt-tRNAs in octocoral mitochondria, thus, indicates a greater dependency on nuclear encoded tRNAs than for bilaterian mitochondria. However, the retention of a single mt-tRNA for formyl-methionine suggests the bacteria-like characteristic and reflects its very specific mitochondrial function. Nevertheless, the general paucity of tRNAs and varied rearrangements in mitogenomes indicate a highly complex and perhaps a unique system for mRNA processing in cnidarian mitochondria.

3.5 Conclusions

Recent studies on the human mitochondrial transcriptome revealed an unexpected complexity in expression, processing, and regulation of mt-mRNAs (Mercer et al., 2011; Rackham et al., 2012). Our results shed first light on a potentially more complex nature of these processes in the mitochondria of early branching animals by virtue of their “special" and diverse mitogenomes. Overall, mitochondrial mRNA processing in octocorals appears to be drastically different from bilaterians likely due to the lack of tRNAs as punctuation marks. The presence of polycistronic mature mRNAs for the majority of genes agrees with this hypothesis. The occurrence of alternately polyadenylated transcripts for the *mtMutS* gene, the existence of 5’ and 3’ UTRs, and the presence of lnc*ATP6* transcripts are additional features highlighting the complexity of the post-transcriptional modifications used by early branching metazoans. More research will contribute to better understand the mitobiology of early branching animals from functional perspective. This will certainly only increase our knowledge on the evolutionary innovation that shaped the evolution of these organisms.

3.6 Appendix

Appendix 3.6.1 qPCR primers used for quantification of alternative transcripts.

Appendix 3.6.2 Quantitative real-time PCR (qPCR) primers for gene expression.

Appendix 3.6.3. Positive PCR amplification of cDNA using primers binding different regions of *ND3-ND4L-mtMutS* transcription units.

Appendix 3.6.4 *Sinularia* cf. *cruciata* mitogenome sequencing results.

Appendix 3.6.1 qPCR primers used for quantification of alternative transcripts.

No.	Gene	Gene Name	Primer Sequences (5' to 3')	Amplicon Size (bp)
A.	**Reference gene primers**			
1	*ACTB*	β-Actin	for: CCAAGAGCTGTGTTCCCTTC rev: CTTTTGCTCTGGGCTTCGT	107
B.	**The *mtMutS* gene primers**			
1	*mtMutS*-A1	6284-6402	for: GCATGAGCCCGATACTTCTAGT rev: ACGAAGCAACTTGTTCAATGG	119
2	*mtMutS*-A2	6284-6740	for: GCATGAGCCCGATACTTCTAGT rev: CCGGGTTACTTTGTCCCTGTCCG	457
3	*mtMutS*-B1	6676-6961	for: CAGCCATGAATGGGCATAG rev: TSGAGCAAAAGCCACTCC	286
4	*mtMutS*-B2	6676-6801	for: CAGCCATGAATGGGCATAG rev: TTAAACCTACCCCCGAGTCC	126
5	*mtMutS*-C1	9014-9095	for: GGTGCCAGTTTGTTCAAGC rev: ATGTCCTGGGGTTCTCTTCC	82
6	*mtMutS*-C2	9014-9149	for: GGTGCCAGTTTGTTCAAGC rev: TTACTCAGTTCCACTGTC	136

The nucleotide positions indicated for different *mtMutS* primers are as per *S. piculiaris* (NC_018379) mitogenome

Appendix 3.6.2 Quantitative real-time PCR (qPCR) primers for gene expression.

No.	Gene	Gene Name	Primer Sequences (5' to 3')	Amplicon Size (bp)
A.	**Reference genes primers**			
1	*ACTB*	β-Actin	for: CCAAGAGCTGTGTTCCCTTC rev: CTTTTGCTCTGGGCTTCGT	107
2	*TUBB*	β-Tubulin	for: ATGACATCTGTTTCCGTACCC rev: AACTGACCAGGGAATCTCAAGC	115
3	*RPL12*	Ribosomal protein L12	for: GCTAAAGCRACTCAGGATTGG rev: CTTACGATCCCTTGSTGGTTC	142
4	*SRP54*	Signal recognition partical 54	for: TGGATCCTGTCATCATTGC rev: TGCCCAATAGTGGCATCCAT	184
B.	**Target gene primers**			
1	*COI*	Cytochrome c oxidase subunit 1	for: ACGGCTTGATACACCTATGTTGTGG rev: TACCGAACCAATAGTAGTATCCTCC	200
2	*mtMutS*-5’	6284-6402	for: GCATGAGCCCGATACTTCTAGT rev: ACGAAGCAACTTGTTCAATGG	119
3	*mtMutS*-Central	8726-8838	for: GCCCTCTCAATATGGCATTG rev: CACTTCGGGATGGTAACTCC	113
4	*mtMutS*-3’	9014-9149	for: GGTGCCAGTTTGTTCAAGC rev: TTACTCAGTTCCACTGTC	136

The nucleotide positions indicated for different *mtMutS* primers are as per *S. piculiaris* (NC_018379) mitogenome.

Appendix 3.6.3. Positive PCR amplification of cDNA using primers binding different regions of *ND3-ND4L-mtMutS* transcription units.

Sr. No.	Primer Pair Forward/Reverse	Region	Position	Length (bp)
1	M-6177/M-9150	Complete *mtMutS*/Start-Stop codons	6177-9149	2972
2	N4L-6092/M-8838	*ND4L-mtMutS*	6092-8838	2746
3	N3-5520/M-7220	*ND3-ND4L-mtMutS*	5520-7220	1700
4	N3-5520/M-6801	*ND3-ND4L-mtMutS*	5520-6801	1281
*	**Primers**	**Sequence (5'---> 3')**		
1	M-6177	ATGAATCAGATACCTATGC		
2	M-9150	TTACTCAGTTCCACTGTC		
3	N4L-6092	GCCATTATGGTTAACTATTAC		
4	M-8838	CACTTCGGGATGGTAACTCC		
5	N3-5520	ACTACTTATCGTCAGCGGAAC		
6	M-7220	AGGCAATAAGTCCAATTGATATTCTGCTCG		
7	M-6801	TTAAGCCAACCCCCGAGTCC		

Appendix 3.6.4 *Sinularia* cf. *cruciata* mitogenome sequencing results.

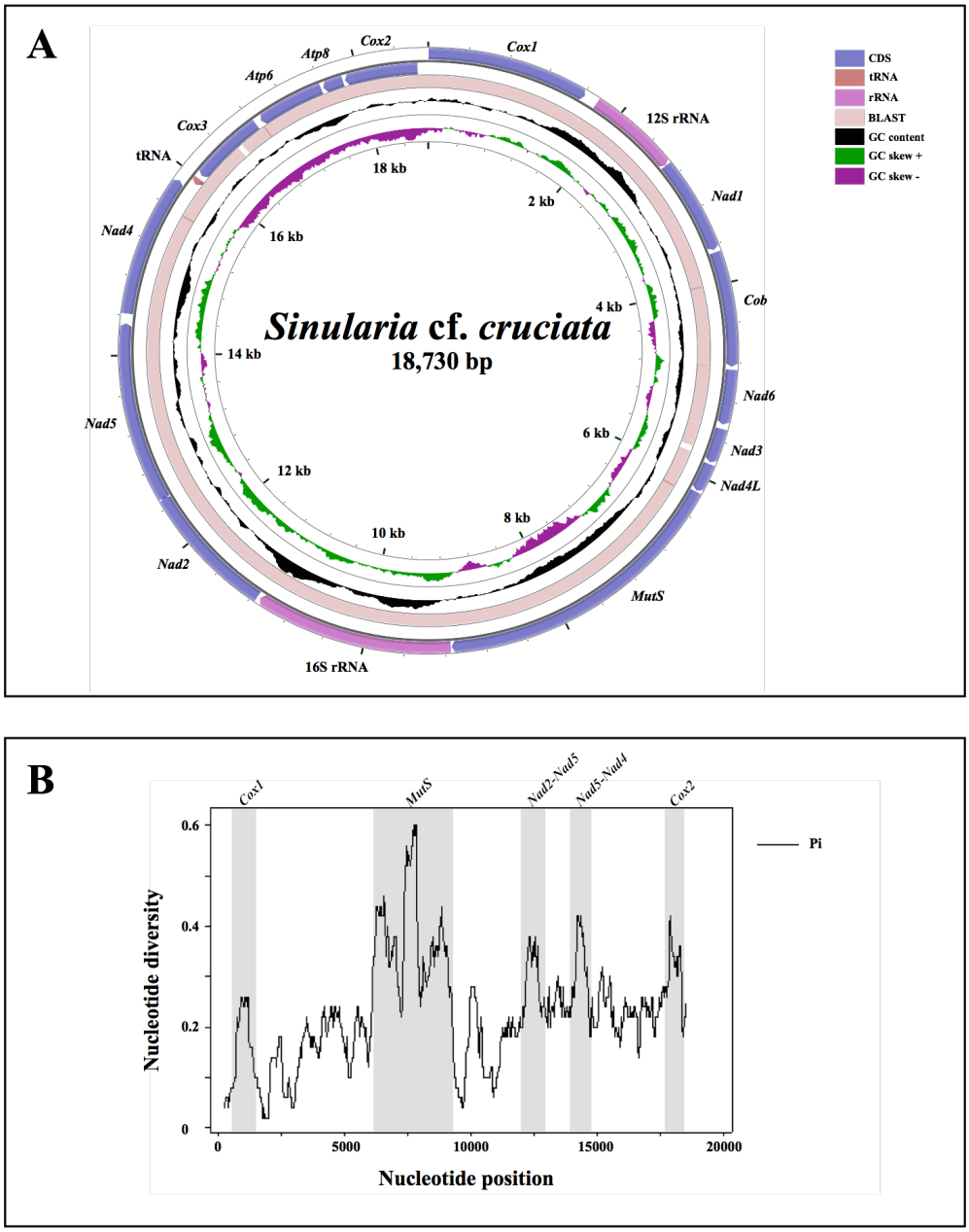

Figure 3.6.4.A The complete mitogenome of *Sinularia* cf. *cruciata* and genomic comparisons with *Sinularia peculiaris*. A: Graphical view of the mitochondrial genome of *Sinularia* cf. *cruciata* with genome size and gene annotations. GC content is shown in black, GC skew is plotted for the entire sequence in green (GC skew +) and purple (GC skew -). The inner pink ring shows the BLAST hit detected by the *blastn* search against *Sinularia peculiaris* mitogenome. B: Sliding window analysis of the complete mitogenomes of *Sinularia* cf. *cruciata* and *Sinularia peculiaris*. Nucleotide diversity across the genome is shown by the black line in a window of 500 bp (25 bp steps). Grey panels show the most variable regions across the two *Sinularia* species.

Table 3.6.4.B Mitochondrial genome organization of *Sinularia* cf. *cruciata*

Species	Gene	Feature	Position		Codon		Strand	Length (bp)	IGRs
			Start	Stop	Start	Stop			
Sinularia cf. *cruciata*	*COI*	CDS	1	1613	ATG	TA	H	1613	135
	12S	rRNA	1749	2673			H	925	4
	NDI	CDS	2678	3649	ATG	TAG	H	972	27
	CytB	CDS	3677	4843	ATG	TAA	H	1167	30
	ND6	CDS	4874	5431	ATG	TAG	H	558	44
	ND3	CDS	5476	5829	ATG	TAG	H	354	19
	ND4L	CDS	5849	6142	ATG	TAA	H	294	13
	mtMutS	CDS	6156	9137	ATG	TAA	H	2982	9
	16S	rRNA	9147	11114			H	1968	31
	ND2	CDS	11146	12519	ATG	TAG	H	1374	-13
	ND5	CDS	12507	14324	ATG	TAA	H	1818	97
	ND4	CDS	14422	15870	ATG	TAA	H	1449	56
	tRNA-Met	tRNA	15927	15997			L	71	39
	COIII	CDS	16037	16822	ATG	TAG	L	786	64
	ATP6	CDS	16887	17594	ATG	TAA	L	708	24
	ATP8	CDS	17619	17834	ATG	TAA	L	216	22
	COII	CDS	17857	18618	ATG	TAA	L	762	112

CHAPTER 4

Alternate Strategies for the Construction of DNA Heteroduplex Plasmid Substrates for *in vitro* Mismatch Repair Assays

This chapter will be submitted as a standalone publication to DNA repair journal and is formatted accordingly.

Chapter 4

Alternate Strategies for the Construction of DNA Heteroduplex Plasmid Substrates for *in vitro* Mismatch Repair Assays

4.1 Introduction

Maintaining integrity of the genetic material is a fundamental cellular process. And cells exhibit a vast repertoire of DNA repair mechanisms. Mismatch repair (MMR) is a pivotal DNA repair mechanism that acts upon wrongly incorporated (mismatching) bases during DNA replication increasing replication fidelity by 20-400-fold (Marinus, 2012). Moreover, it aids in correcting mismatches arising from other biological sources and helps to avoid illegitimate recombination and their detrimental effects on the cell and the organism (Jiricny, 2013). Since MMR malfunction is linked to development of various types of cancers (Modrich and Lahue, 1996; Hsieh and Yamane, 2008), it is important to gain a precise understanding of the pathways leading to mismatch correction, and of the proteins involved and their activities *in vitro* as well as *in vivo*.

In vitro DNA mismatch repair assays greatly facilitate the rapid assessment of MMR activity detection and/or its deficiency in various cellular/organellar extracts (Thomas et al., 1995; Corrette-Bennett and Lahue, 1999; Mason et al., 2003). MMR assay utilizes an overlapping restriction endonuclease site with a mismatch, which upon repair restores either of the sites available to be cleaved by one of the restriction enzymes, thus indicating a mismatch repair. The prerequisite for these assays is the availability of appropriate amounts of substrate containing defined mismatched lesions. Several methods have been described so far to prepare different heteroduplex substrates for MMR assays. In general, they involve the annealing of a single-stranded f1 phage DNA to an identical double stranded plasmid containing a single base mutation (Thomas et al., 1995; Corrette-Bennett and Lahue, 1999). This requires access to such specialized phages bearing a mismatch on a complementary strand of double stranded DNA

plasmids, their culturing and maintaining. This is generally technically demanding and consuming, involving multiple preparative steps, and may lead to low starting substrate yield. Another difficulty of using phage DNA is the lack of unique restriction sites limiting its utility. These limitations reduce the usability MMR assays to only specialized laboratories. Other methods involve the preparation of plasmid variants using several site-directed mutagenesis steps and the treatment of each batch of substrate with nicking endonucleases followed by a chromatographic and/or streptavidin bead-based purifications (Tsai-Wu et al., 1999; Wang and Hays, 2000). Consequently, difficulties are commonplace during the preparation of specific MMR substrates containing a single defined lesion and a single nick acting as a strand discrimination signal (Larson et al., 2002). Yet these substrates are essential to assess the actual biological response of MMR proteins.

Here we describe two simple and efficient strategies for the producing large quantities of G/T and A/C heteroduplex substrates with high purity and reproducibility for *in vitro* MMR assays. We used a commonly available and easily accessible high copy number plasmid pGEM-T with multiple cloning sites (MCS), for the development of these methods. These strategies can be used in parallel providing methodological choice and involve the use of routine standard laboratory methods and reagents (e.g. restriction enzymes). The first strategy is modified from (Wang and Hays, 2000) and utilizes the nicking endonucleases; whereas the second strategy involves the use of "bacterial packaging cell lines" which secrete the phagemid DNA in culture medium without the need of helper phage, producing large amounts of ssDNA which can later be annealed to linear double-stranded plasmid DNA to obtain heteroduplex substrates. Both these strategies are integrated and can be utilized interchangeably. In addition, these methods will help to increase accessibility of MMR assays to more laboratories. Although, the strategies described here lead to the production of G/T and A/C mismatches, they can be easily adapted to produce various kinds of substrates with different lesions such as base/base mismatches, insertion/deletion substrates, and substrates with DNA loops, among others. Hence, these strategies are highly flexible to modifications and can be easily adapted according to specific requirements.

4.2 Materials

4.2.1 Reagents, and Enzymes

Restriction enzymes *Sac*I, *Sma*I, *Nde*I, *Nco*I, nicking endonucleases Nt.*Bbv*CI, Nb.*Bbv*CI Nt.*Bsp*QI as well as special enzymes such as Klenow DNA polymerase, Calf Intestinal Alkaline Phosphatase (CIP), and T4 polynucleotide kinase were purchased from New England Biolabs (USA). T4 DNA ligase was acquired from Promega (USA). The Plasmid-safe DNase was purchased from Epicentre biotechnologies (USA). All the other chemicals were from Sigma-Aldrich (USA).

4.2.2 Kits, Plasmids and Oligonucleotides

Plasmid extraction was performed using peqGOLD plasmid miniprep kit II (Peqlab). NucleoSpin Gel and PCR clean-up kit (Macherey-Nagel, Germany) was utilized for enzymatic reaction cleanup. The pGEM-T easy vector was obtained from Promega (USA). The M13cp plasmid used for preparation of bacterial packaging cell line was kindly provided by Dr. A. R. M. Bradbury (Chasteen et al., 2006). Four 43mer oligonucleotides were synthesized by Metabion (Germany) (Figure 4.1).

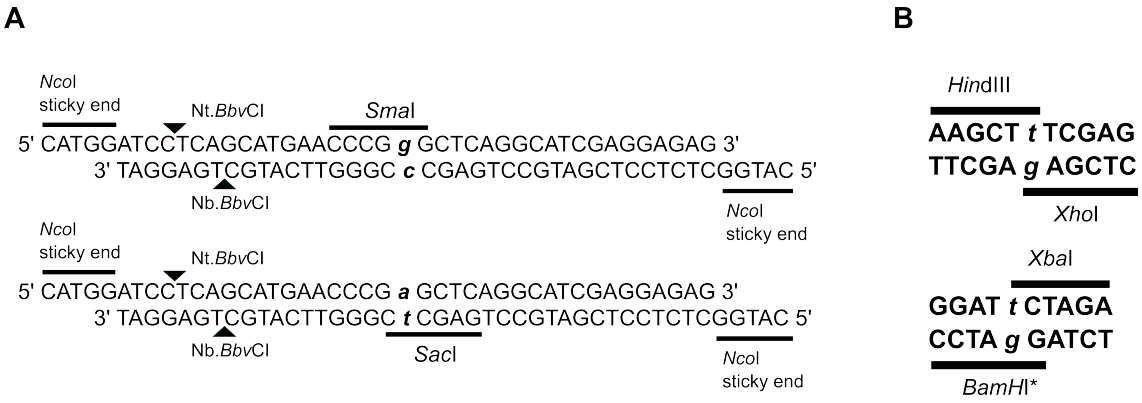

Figure 4.1 Synthetic oligonucleotides used and their features.

(A) The synthetic 43mer oligonucleotide pairs are shown, which upon annealing form a homoduplex with *Sma*I and *Sac*I site each, used in present study. The nicking endonuclease sites and sticky overhangs are also depicted. The nucleotides forming a heteroduplex later are shown in small-bold-italic letters.

(B) Other overlapping restriction site combinations that can be used in current setup instead of *Sma*I-*Sac*I (* indicates that the 6th or 7th nucleotide downstream of the 5'end of synthetic oligos need to be changed in order to use *Xba*I-*Bam*HI combination).

4.3 Results

4.3.1 Preparation of the parent plasmid

The pGEM-T plasmid was modified in order to incorporate the two desired oligonucleotide pairs with unique restriction sites (*Sma*I and *Sac*I) each, not available in the plasmid. This was an optional step dependent on the choice of restriction enzyme sites needed for analysis. Choosing a different oligoduplex pair would eliminate the requirement of this step (see Figure 4.1B for alternative options). In order to delete the preexisting SacI site, 10 µg of the pGEM-T plasmids were double-digested overnight at 37°C with *Nde*I and *Sac*I (10U each). The resulting linear plasmid with overhangs was purified and treated subsequently with Klenow DNA polymerase (10U) to digest the 3' overhang and to fill-in the 5' overhang. The incubation was performed at 25°C for 25 min, and was followed by the addition of EDTA to a final concentration of 10mM, and the enzyme inactivation at 75°C (20 min). This reaction resulted in removal of 10 nucleotides in total, and eliminated the with *Sac*I site. The resultant linear plasmid with blunt ends was purified, self-ligated (re-circularized) using T4 DNA ligase and used to transform into DH5α cells for propagation. The absence of *Sac*I site was confirmed by sequencing and the resulting plasmid was referred as pG*Sac*I-minus.

4.3.2 Construction of separate plasmids with either *Sma*I or *Sac*I sites each

Synthetic oligonucleotides containing one restriction site each for *Sac*I or *Sma*I were mixed in equal amounts, heat denatured and allowed to re-anneal slowly. This process yielded a 39bp double-stranded homoduplex DNA with 4bp overhangs complementary to the overhang generated by *Nco*I (see Figure 4.1A for the features of synthetic oligos). These re-annealed homoduplexes were phosphorylated with the help of T4 polynucleotide kinase (NEB) following the supplier's protocol to facilitate ligation into a linear plasmid with dephosphorylated overhangs (pG*Sac*I-minus).

The pG*Sac*I-minus plasmid from the previous step was digested with *Nco*I, purified and treated with Calf intestinal alkaline phosphates (CIP) following the manufacture's protocol, in order to avoid re-circularization of the *Nco*I-digested plasmid. The re-annealed phosphorylated homoduplex DNA oligos with overhangs were then ligated to

the dephosphorylated pG*Sac*I-minus using T4 DNA ligase (Promega) as per manufacture's instructions. This ligation reaction was transformed into chemically competent DH5α cells by heat shock. The clones obtained after 15 h were PCR amplified and sequenced for confirmation of successful ligation of the desired homoduplexes into the plasmids. Two types of clones were selected for each plasmid construct: those having G nucleotide (nt) on the top strand (pGSM-t) or having G nt at the bottom strand (pGSM-b), in case of *Sma*I construct. Similarly, for *Sac*I construct, clones obtained were pGSA-t or pGSA-b depending on the occurrence of T nt on top or bottom strand, respectively (Figure 4.2). A single cloning and transformation step yielded all four plasmids due to bidirectional cloning with sticky *Nco*I ends.

A

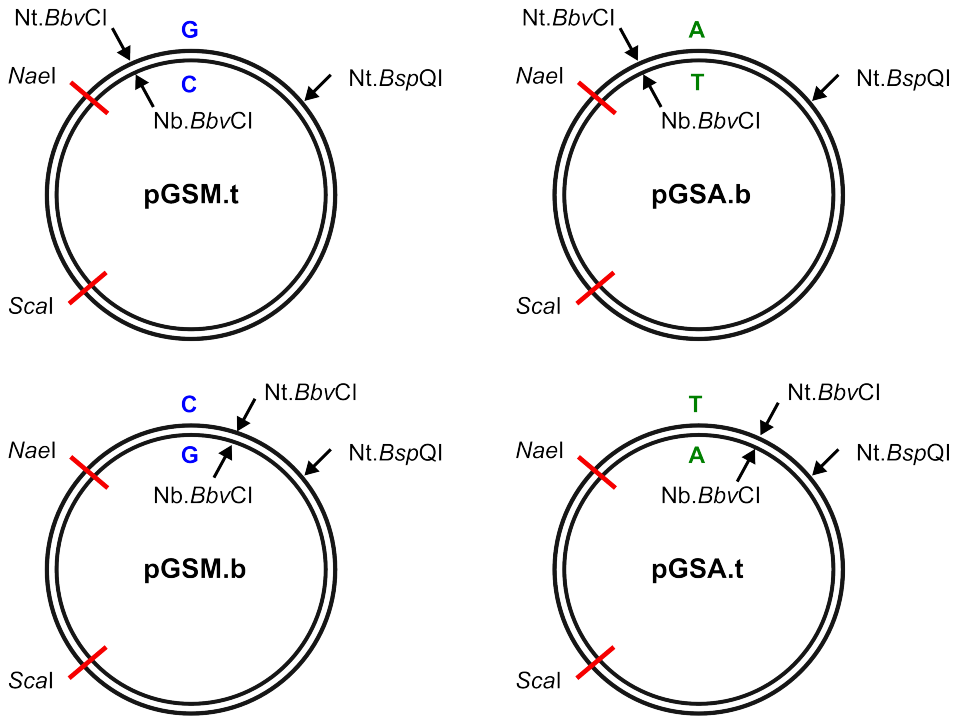

B

i) Nicking endonuclease strategy

(pGSM.t + Nb.*Bbv*CI + ExoIII) + (pGSA.b+*Sac*I or *Nae*I) = G/T mismatch

(pGSM.b + Nt.*Bbv*CI or Nt.*Bsp*QI + ExoIII) + (pGSA.t+*Sac*I or *Nae*I) = G/T mismatch

(pGSM.t + Nt.*Bbv*CI or Nt.*Bsp*QI + ExoIII) + (pGSA.b+*Sac*I or *Nae*I) = A/C mismatch

(pGSM.b + Nb.*Bbv*CI + ExoIII) + (pGSA.t+*Sac*I or *Nae*I) = A/C mismatch

ii) Phagemid strategy

(pGSM.t ssDNA) + (pGSA.b+*Sac*I or *Nae*I) = A/C mismatch

(pGSM.b ssDNA) + (pGSA.t+*Sac*I or *Nae*I) = G/T mismatch

Figure 4.2 Recombinant plasmids and their usage-combinations for heteroduplex preparation.

(A) Four variants of pGEM-T-derived plasmids generated by homoduplex oligonucleotide ligation. The nucleotides leading to formation of heteroduplex later are shown along with important restriction and nicking endonuclease sites.

(B) Different combinations leading to formation of G/T and A/C heteroduplex are shown in the form of equations.

4.3.3 Preparation of ssDNA

Two different strategies were applied to obtain ssDNA from either of the plasmids depending on the mismatch required. The first strategy depends on the use of nicking endonucleases treatment, followed by Exonuclease III digestion. The second strategy, on the other hands, exploits the phagemid properties of the original engineered construct, described below.

4.3.3.1 Nicking endonuclease + Exonuclease III based mismatch repair substrate production

This strategy is modified from the one described earlier by Zhou et al. (Zhou, Bisheng et al., 2009). Both pGSM and pGSA contain two unique nicking endonuclease sites, one site for Nt.*Bsp*QI is inherent to pGEMT plasmid whereas the other nicking site, recognized by either Nt.*Bbv*CI or Nb.*Bbv*CI depending on the strand needs to be digested, was introduced by the oligo-homoduplex ligated to it. The addition of this recognition site adds flexibility as it allows to nick either the top strand or the bottom strand. After nicking the plasmids Exonuclease III digestion results in the complete removal of the nicked strand. The resulting single stranded DNA can then be used for heteroduplex preparation as described in section 4.3.4.

4.3.3.2 Using phagemid to produce ssDNA

The most frequently utilized approaches for the preparation of ssDNA use phagemids, which are derived from the single-stranded bacteriophage M13, fd, or f1, and are capable of replicating as plasmids in bacterial hosts (Blondel and Thillet, 1991). The pGEM-T has properties of phagemid as it contains an f1 origin enabling ssDNA replication and packaging into phage particles. Therefore, it was chosen for the current study to produce ssDNA with the help of a phage display system. However, a novel approach was utilized to overcome the need of a helper phage. DH5α cells were transformed with the plasmid M13cp making them “bacterial packaging cell lines”(Chasteen et al., 2006). M13cp is an M13-based helper plasmid that contains the phage genome without its packaging signal/origin and a chloramphenicol resistant gene. The absence of packaging signal makes it incapable of packaging its own DNA. However, when a phagemid (e.g. pGSM or pGSA which contain f1 origin) is transformed into M13cp containing cells, they replicate the phagemid, producing

ssDNA. (See (Chasteen et al., 2006) for more details). The M13cp transformed cells were grown overnight on plates containing chloramphenicol (25 µg/mL). These M13cp-cells were made chemically competent using a the protocol described in (Inoue et al., 1990), and used as bacterial packaging cell lines as to produce large quantities of pure ssDNA from the phagemids pGSM and pGSA without the need of a helper phage.

For this, M13cp-cells were transformed with the recombinant plasmids pGSM and pGSA using a heat shock transformation protocol and grown on LB agar-ampicillin-chloramphenicol plates. Colonies from each transformation were picked and grown overnight in LB-ampicillin-chloramphenicol media at 30°C at 250 r.p.m. The bacterial cells were separated form the broth by pelleting, and the ssDNA extraction from the supernatant was performing using PEG-Phenol-chloroform extraction and ethanol precipitation as described previously (Sambrook and Russell, 2001). Simultaneously, a silica column-based protocol described previously was also employed (Zhou, B. et al., 2009). Using this approach large amount of specific ssDNA was produced. The four plasmid/phagmid constructs described above, namely pGSM-t, pGSM-b, pGSA-t, and pGSA-b led to the production of circular ssDNAs containing C-, G-, A- and T-nucleotides at the target restriction site, respectively.

4.3.4 Heteroduplex synthesis

To synthesize the desire heteroduplex, 1 µg ssDNA prepared as described above was mixed with 350ng of plasmid linearized using *Sca*I (or *Nae*I) and containing non-complementary base at the target restriction site. Slow annealing was done after denaturing the mixture for 5 min at 94°C on a heat block. The annealed mixture was digested with plasmid-safe ATP-dependent DNase (Epicentre Biotechnologies, USA). This reaction leads to degradation of all linear as well as single-stranded leftover DNA in the reaction, leaving only the nicked heteroduplex plasmid. See Figure 4.3 for the schematic illustration of steps required. This plasmid was subsequently purified using the NucleoSpin Gel and PCR cleanup kit and was quality controlled on a 1% agarose gel (Figure 4.4). This procedure led to the generation of a G/T or an A/C mismatch.

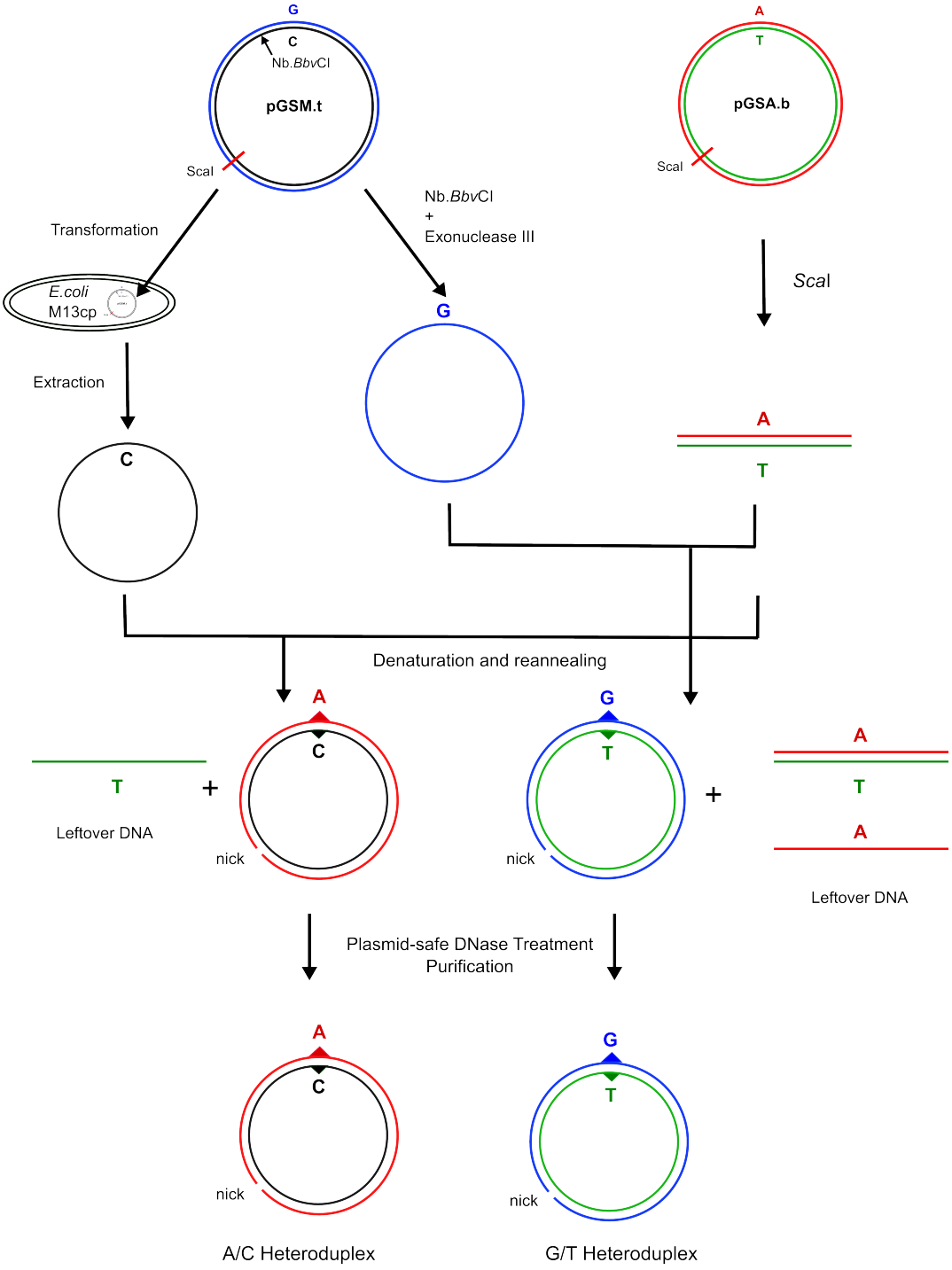

Figure 4.3 The heteroduplex substrate preparation protocol.

Flow chart shows the procedure for preparation of G/T and A/C heteroduplex substrates for MMR assay, in brief. Both methods of obtaining circular ssDNA are depicted (refer to the text for details). pGSM.t and pGSA.b plasmids were used for this particular procedure. Similarly the plasmids pGSM.b and pGSM.t (Figure 2) can also be used.

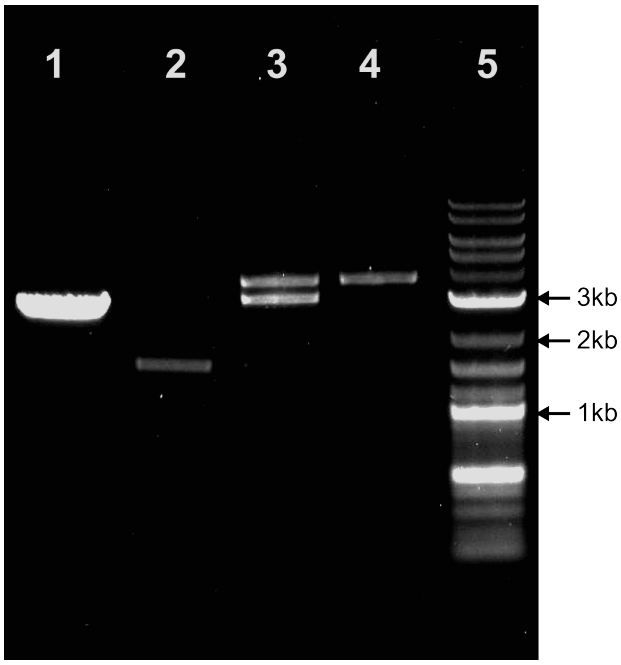

Figure 4.4 Electrophoretic analysis

1% agarose gel showing linear pGSA.b plasmid (lane 1); circular ssDNA (lane 2); heteroduplex plasmid after denaturation and re-annealing (lane 3) with the uppermost band is heteroduplex (with a nick), middle band is excess linear plasmid and lower faint band is circular ssDNA; purified G/T heteroduplex substrate after Plasmid-safe DNase treatment (lane 4); 2-Log DNA ladder (lane 5). (See supplement S1 for original image both G/T and A/C on one gel). Restriction digestion and sequencing was performed to confirm the presence of mismatched bases.

4.4 Conclusion

We devised simple, convenient, reproducible, and flexible parallel strategies to prepare heteroduplex DNA plasmids containing varied mismatch lesions. These strategies can be easily adopted in any molecular biology laboratory with basic facilities, making the *in vitro* MMR assay more accessible. The bacterial packaging cell lines can be used as a source of ssDNA in large quantities for many other applications without the need of additional helper phages.

4.5 Appendix

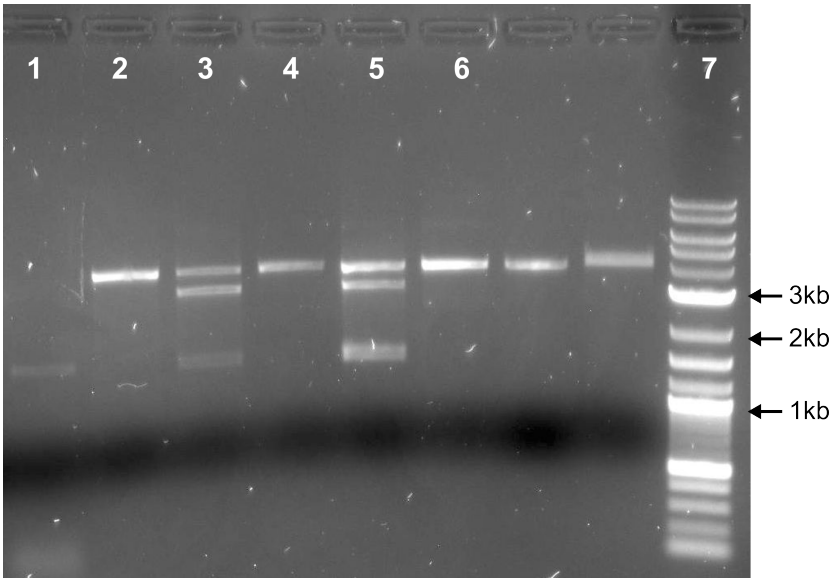

Figure 1: Gel image showing results of electrophoretic analysis of both G/T and A/C heteroduplexes.

Circular ssDNA (lane1), Heteroduplex (HD) as a positive control (lane 2), G/T HD (upper band) after re-annealing step (lane 3), purified G/T HD (lane 4), A/C HD (upper band) after reannealing (lane 5), purified A/C HD (lane 6), and 2-Log DNA ladder (lane 7).

CHAPTER 5

A Cautionary Tale of the Octocoral Mitochondrial DNA-encoded Mismatch Repair (mtMutS) Protein Expression in *E. coli*

This chapter will be submitted as a standalone publication.

Chapter 5

A Cautionary Tale of the Octocoral Mitochondrial DNA-encoded Mismatch Repair (mtMutS) Protein Expression in *E. coli*

5.1 Introduction

Mismatch repair (MMR) is a pivotal DNA repair mechanism dedicated to maintaining the genomic integrity of the nuclear DNA. MMR proteins primarily involved in recognizing and repairing the mismatched bases belong to the mutS homolog family (Su and Modrich, 1986). Moreover, mutS homologs are also capable of recognizing small DNA insertions/deletion loops (IDLs) along with unpaired bases (Parker and Marinus, 1992). The mismatch correction by these MMR proteins during DNA replication enhances the DNA replication fidelity by several folds thereby reducing the mutation load (Modrich and Lahue, 1996). Hence, MMR malfunction has also been linked to the development of various types of cancers (Modrich and Lahue, 1996; Hsieh and Yamane, 2008). Several isoforms of mutS homologs have been identified in most eukaryotes. The core mutS homolog (MSH) family of proteins, however, is evolutionarily highly conserved throughout taxonomic domains, forming a monophyletic group among eukaryotes (Culligan et al., 2000). MMR pathways and the role of mutS homologs have been extensively studied in varied organisms in last 50 years after its discovery (Fishel, 2015).

Mitochondria, the tiny cellular powerhouses, evolved from an ancient endosymbiosis of a bacteria-like ancestor, harbor their own compact genomes (Gray, 1993). The integrity of this small but crucial genetic material is fundamental for the cellular homeostasis as essential proteins involved in energy production are encoded in the mitochondrial genomes. The reactive oxygen species (ROS) generated as a result of electron leakage from the electron transport chain (ETC) during oxidative phosphorylation (OXPHOS) tends to damage the mitochondrial DNA (mtDNA), which is highly susceptible to this oxidative damage due to its proximity to ETC (Richter et al., 1988). The damage and mutation of mtDNA has been linked to several neurodegenerative diseases, ageing and

cancer (Wallace, 2005; Greaves et al., 2012). Although cell possesses a myriad of repair mechanisms for nuclear DNA (nDNA) repair, the activity and efficacy of mitochondria mtDNA repair appears limited (Boesch et al., 2011; Cline, 2012; Alexeyev et al., 2013); despite the presence of several repair pathways including base excision repair, direct reversal, and double-strand break repair. Studies indicate that the occurrence of mismatch repair (MMR) in animal mitochondria is likely (Mason et al., 2003; de Souza-Pinto et al., 2009), however the presence of MMR ability due to the **M**ut**S** protein **H**omolog (MSH)-like protein is not known.

Surprisingly, Octocoral mitochondrial genomes harbor an additional gene, a mutS bacterial homolog (Pont-Kingdon et al., 1995) not found in any other metazoan mitochondrial genome sequenced so far. This octocoral mitochondrial mismatch repair gene or *mtMutS* appears to be of bacterial or viral origin and likely to have been horizontally transferred to the mitogenome of octocorals (Bilewitch and Degnan, 2011). The *mtMutS* is known to be transcribed and bioinformatic analyses suggest a potential self-contained mismatch repair function due to presence of all four domains sufficient for this activity in the protein coding region of the gene (Bilewitch and Degnan, 2011). However, the exact role of *mtMutS* gene product remains undetermined despite that the gene has been speculated to be involved in the maintenance of observed low variation in mtDNA of octocorals (Shearer et al., 2002; Hellberg, 2006), and in mismatch as well as recombination repair (Bilewitch and Degnan, 2011; Brockman and McFadden, 2012). Therefore, the *mtMutS* gene product is an ideal candidate to further enhance our understanding of organellar MMR and to elucidate the structure, potential self-contained functionality as well as the origin of this unique mitochondrial protein.

Because the mtMutS is a bacterial homolog, here we strive to express mtMutS protein and its domains using in an *E.coli* bacterial expression system. We discuss several properties of the gene and the protein under investigation and provide precautionary measures and future directions for successful expression of mtMutS and similarly challenging proteins using *E.coli* expression systems.

5.2 Materials and methods

5.2.1 Strains and plasmids

The octocoral species, *Sinularia* cf. *cruciata* used in the present study was purchased and kept in a control, salt water, closed-circuit aquarium at Molecular Geo- & Paleobiology lab, LMU, Munich. The full-length *mtMutS* gene was initially cloned using pCR4-TOPO vector (Invitrogen) and *Escherichia coli* DH5α cells were transformed with the resulting plasmid. The expression vector used was pET15b, which after cloning was expressed in Origami™ B (DE3) cells (Novagen).

5.2.2 Isolation of Mitochondria

To detect the presence of protein product of *mtMutS* gene, mitochondrial fraction was extracted using the Mitochondria Isolation Kit for Tissue (Thermo-Fisher) following the supplier's instructions. Intact mitochondria were observed under the fluorescent microscope (Lyca) at 40X magnification. Mitochondrial pellet was boiled with SDS-PAGE sample buffer and applied to the gel. Mitochondrial proteins were analyzed on 10% SDS-PAGE. Cytosolic fraction was used for comparison.

5.2.3 Nucleic acid extraction and cDNA synthesis

Genomic DNA from *Sinularia* cf. *cruciata* was isolated using NucleoSpin Tissue kit (Macherey-Nagel) whereas total RNA extraction was performed using TRIzol reagent (Invitrogen), both following the manufacture's instructions. The final RNA pellet was dissolved in 100 µl DEPC treated water and the contaminating DNA was eliminated from RNA extracts by performing a DNase treatment at 37 °C for 30 min using The RQ1 RNase-free DNase (Promega). The RNA was purified after inactivating the DNase as per manufacture's protocol. The purity of RNA was determined using a Nanodrop ND-1000 spectrophotometer (Thermo Fisher Scientific). RNA samples with absorbance at OD260/280 and OD260/230 ratio ~ 2.0 were used for reverse transcription. RNA integrity was also verified by 1% agarose gel electrophoresis. These extracts were stored at -80 °C until use. In total, ~1 µg of total RNA was reverse transcribed in 20 µl reactions using the ProtoScript® First Strand cDNA Synthesis Kit (NEB, Germany) with an anchored oligo-(dT) primer according to the manufacture's instructions.

5.2.4 PCR amplification, cloning and construction of recombinant expression vectors

The full-length mtMutS gene was amplified from genomic DNA and cDNA using primers, 5'- AGACCG**CATATG**ATGAACCAGATACCTATGC -3' (*Nde*I, forward) and 5'- AGACCG**GGATCC**TTACTCAGTTCCACTGTC -3' (*Bam*HI, reverse). These primers include cloning sites for *Nde*I and *Bam*HI to facilitate cloning (bold nucleotides). PCR and RT-PCR were performed in a 50 µl reactions using Crimson LongAmp™ *Taq* DNA polymerase (New England Biolabs) following the supplier's protocol. A touchdown thermal profile consisting of 3 min denaturation at 95°C followed by 10 cycles of 94°C-20sec, 55°C-40sec, 72°C-3min, followed by 20 cycles at 94°C-20sec, 55°C-40sec, 72°C-3min, and an additional extension of 5 min was used for PCR amplification on a Thermocycler (Biometra). The PCR products were subsequently checked for amplification on 1% agarose gel and were initially cloned into pCR4-TOPO vector using the TOPO cloning kit (Invitrogen) following the manufacturer's instructions. Clones containing *mtMutS* gene were sequenced to verify the insert identity and those colonies containing the desired construct (i.e. pCR4-mtMutS) were propagated for plasmid preparation. Clones were were overnight in LB Medium and the plasmid were extracted using PeqGOLD Miniprep kit II (PeqLab). These plasmids and the expression vector pET15b vectors digested using *Nde*I-*Bam*HI restriction enzymes. The digestion products were visualized on 1% agarose gels and the bands of interest were cut and purified with the NucleoSpin Gel and PCR clean-up kit (Macherey-Nagel). Directional cloning was performed into *Nde*I-*Bam*HI sites of pET15b using T4 DNA ligase (Promega). The resulting pET15b-mtMutS recombinant plasmids were sequenced to confirm the presence of in-frame full-length *mtMutS* gene sequence and further used for protein expression (see below).

5.2.5 Domain isolation and cloning

The attempts at cloning the full mtMutS gene yielded at least three variants of it. On close inspection of DNA sequences it was established that these clones originated from the amplification product of artificially deleted cDNA (see (Cocquet et al., 2006) for more details). One of the clones containing in-frame complete mtMutS-Domain I (N-terminal), and homing endonuclease (HNH) domain (C-terminal) was cloned into pET15b for protein expression (pET15b-MD1-HE).

5.2.6 Protein Expression and solubilization

The Origami B (DE3) E. coli cells were transformed with either pET15b-mtMutS or pET15b-MD1H expression plasmids via heat shock. The resulting colonies were selected on LB agar plates supplemented with Ampicillin (50 µg/ml), Kanamycin (50 µg/ml) and Tetracycline (12.5 µg/ml). 10ml volume of LB medium containing the antibiotics mentioned above was inoculated with well-grown single colonies that were allowed to grow overnight at 37°C. 500ml LB medium containing appropriate antibiotic amounts was inoculated with this 10ml primary culture and allowed to grow at 37°C until the OD_{600} was 0.8. The expression of recombinant proteins was achieved by IPTG induction, followed by growth for 4 to 6 hours at different temperatures ranging from 15°C to 37°C. Different IPTG concentrations ranging from 0.1mM to 1mM were tested for induction of expression. Bacterial cells were harvested by centrifugation (10 min at 4800g, 4°C) and the cells pellets were stored at -80°C for further use.

Proteins were extracted by suspending the cells in resuspension buffer (50mM NaH_2PO_4, 300mM NaCl, pH 8.0). This buffer was complemented with 8M Urea depending on the nature of protein expressed. Lysis was achieved using sonication on ice followed by centrifugation at 10,000g for 30min at 4°C.

Affinity purification of the proteins was performed done using Protino Ni-IDA pre-packed columns (Macherey-Nagel, Germany) following the manufacturer's instructions for either soluble or insoluble protein purification, depending on the requirement. The proteins were eluted with the help of 250mM imidazole. Elution fractions were analyzed in 12% SDS-PAGEs.

5.2.7 *In silico* analysis of DNA/Protein sequences

DNA and protein sequence analysis was performed using Geneious 6.1 (Biomatters, New Zealand) (Kearse et al., 2012). Internal repeats in the *mtMutS* DNA sequence were detected using a web tool FAIR (Find All Internal Repeats) (http://bioserver1.physics.iisc.ernet.in/fair/). A web tool called Rare Codon Calculator (RaCC) was used for detecting the presence of rare codons in the *mtMutS* gene sequence (http://nihserver.mbi.ucla.edu/RACC/). Hydrophobicity analysis was done using the Kyte-Doolittle (KD) method (Kyte and Doolittle, 1982). Additionally, Pepcalc.com provided by Innovagen AB, (Lund, Sweden) was used for hydropathicity profiling.

5.3 Results and discussion

5.3.1 Mitochondria preparation and localization of mtMutS analogous protein band

The sequenced complete *mtMutS* gene in *S.* cf. *cruciata* is 2986bp long (993 amino acid, theoretical molecular weight = 112.99 kD). The sequences will be submitted to European Nucleotide Archive (ENA). The prepared mitochondrial fraction from *S.* cf. *cruciata* tissue, when examine by SDS-PAGE and Coomassie Brilliant Blue staining yielded one band approximately of the predicted similar molecular weight (Figure 5.1A). No protein band was observed at that position in the cytosolic fraction control. Although this is a good candidate for the mtMutS protein, due to absence of specific antibodies against this protein, the identity of the observed band remained undetermined.

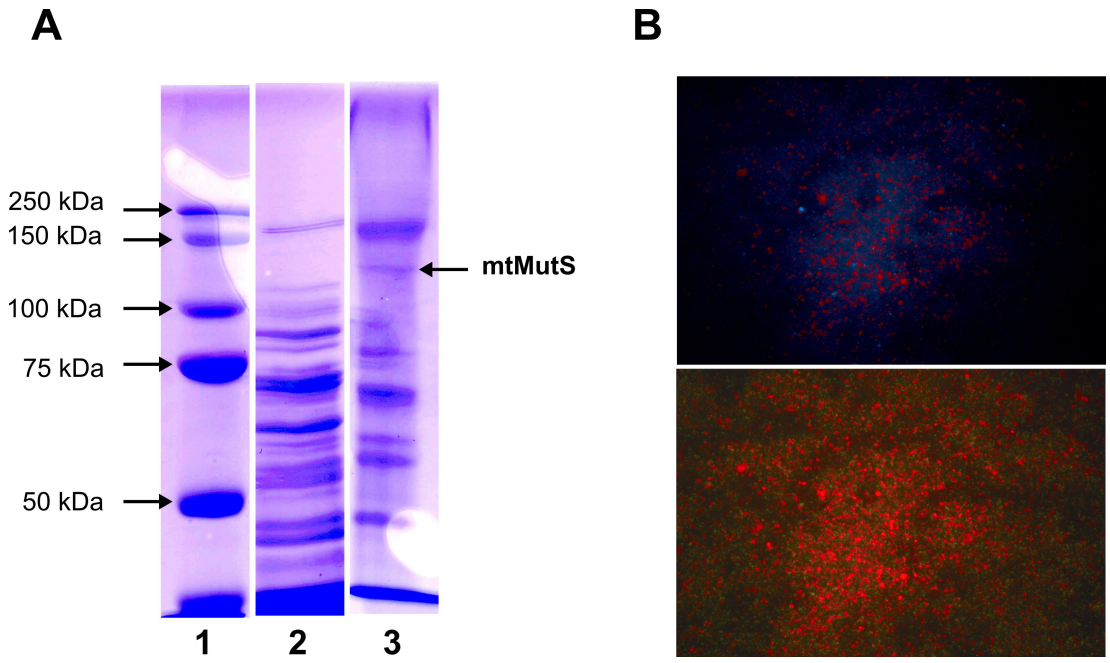

Figure 5.1 Mitochondria isolation and the mtMutS protein localization

(A) 10% SDS-PAGE showing the band at analogous position to octocoral mtMutS protein (112.99 kDa) in lane 3; lane1, Precious Plus Dual Color Protein Marker (Bio-rad, USA); lane 2, cytosolic fraction of *S.* cf. *cruciata.* **(B)** Fluorescent microscopic images showing isolated mitochondrial fraction. The red dots in both images represent chlorophyll from *Symbiodinium sp*. (broad autofluorescence), whereas the blue (in upper image) and the green (in lower image) exhibit the fluorescence from the octocoral mitochondrial NADH (excitation at 360 nm, emission at 470 nm longpass) and oxidized flavoproteins FAD^{++} (excitation at 440-490 nm, emission at 515 nm longpass), respectively.

Sinularia cf. *cruciata* is a zooxanthellate octocoral forming a mutualistic relationship with unicellular algal symbionts belonging to *Symbiodinium sp.,* which resides in the endoderm of the host. To examine the possibility of co-isolation of symbionts during mitochondrial isolation and to determine the purity of preparation, we observed the isolated mitochondrial fraction using fluorescence microscopy. The reduced form of NAD^+ (NADH) is a natural fluorophore present in the mitochondria, making it emit autofluorescence with maximal excitation and emission spectra in the region of 340 and 450 nm, respectively (Rodrigues et al., 2011). Similarly, oxidized flavoproteins, FAD^{++}, from isolated mitochondria emit autofluorescence at 520 nm with excitation spectra between 430-470 nm (Frostig et al., 2009). The chlorophyll pigment from *Symbiodinium,* on the other hand, also exhibit autofluorescence properties with a persistent broad fluorescence range making it readily detectable (Loram et al., 2007; Murchie and Lawson, 2013). The mitochondria isolation was partially successful, as the isolate was observed to contain contaminating symbionts (Figure 5.1B). Thus, despite our observation of a protein band of expected size of mtMutS in the mitochondrial fraction, the lack of specific antibodies and presence of symbionts in the extracts the identity of this band remains uncertain.

5.3.2 Construction of recombinant vectors for mtMutS protein production

The coding sequence of *S.* cf. *cruciata mtMutS* gene from genomic DNA and cDNA was successfully cloned into pET15b expression vector. This vector contains a stretch of six histidine (his_6) residues at the N-terminal region, which co-translate with the protein of interest acting as a tag and facilitating purification using metal affinity chromatography (Figure 5.2A). Additionally, an in-frame deleted cDNA fragement comprising the N-terminal mutS-Domain I, and the C-terminal HNH-domain was also successfully cloned. The octocoral mtMutS protein is predicted to be comprised of four domains, out of which Domain I is suggested to have resemblance with mismatch recognition domains, whereas the 3'end region of the mRNA translates into an HNH homing endonuclease (Bilewitch and Degnan, 2011). The artificially deleted cDNAs are formed through intramolecular template switching during reverse transcription, if the RNA template contains a direct repeat of ≥8 nucleotides and result in alternate transcripts, which are artifacts (Cocquet et al., 2006). The *mtMutS* gene is nearly 3kb in

length, contains several such repeats of up to 14bp in length detected using an online tool called FAIR (Senthilkumar et al., 2010). Cloning of *mtMutS* gene RT-PCR product revealed at least 3 alternative variants of *mtMutS* transcripts generated during cDNA synthesis as explained above. A 9bp direct repeat (5'-CTCAAGTTT-3') contributed to the formation of the deleted cDNA containing sequence of N-and C-terminal domains of mtMutS. Higher temperature of reverse transcription helped to avoid occurrence of deleted cDNAs, as suggested previously (Cocquet et al., 2006). The insert from the pCR4-TOPO plasmid was sub-cloned into pET15b resulting in pET15b-MD1-HE construct (Figure 5.2B).

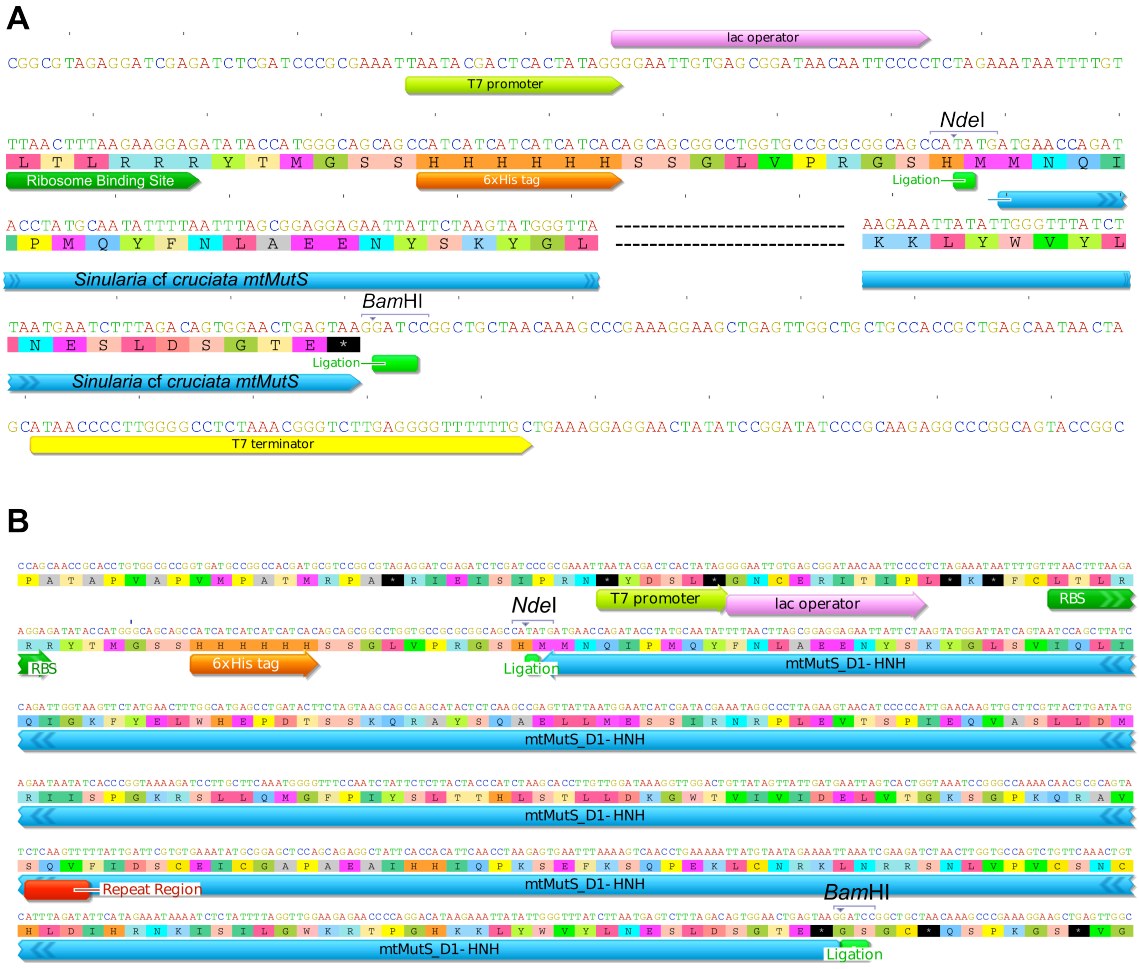

Figure 5.2 The construction of expression plasmids

The expression plasmids constructs bearing histidine-tagged, **(A)** full-length mtMutS protein, and **(B)** partial mtMutS protein containing N- and C-terminal domains. Insertion sites (*Nde*I, *Bam*HI), Ribosome binding site, 6X histidine tag, T7 promoter and terminator, and amino acid sequence are shown. Repeat region is indicated for the later. Region upstream of repeat is Domain 1 and downstream belongs to HNH domain.

5.3.3 Expression and purification

The *E.coli* Origami B (DE3) cells transformed with the full mtMutS protein construct i.e., pET15b-mtMutS failed to express any detectable amount of the 112.99 kDa protein. Several protocols were used to obtain an expressed protein including varying concentrations of IPTG and different induction temperatures. However, none of the attempts resulted in expression of this protein in *E. coli*. Several studies have exploited similar approaches to express bacterial mutS protein with success (Biswas and Hsieh, 1996; Takamatsu et al., 1996; Wu and Marinus, 1999; Stanislawska-Sachadyn et al., 2003). However, despite of being a bacterial homolog protein expression was not possible for the octocoral *mtMutS* gene. Several reasons may contribute to the failure of protein expression (discussed by (Rosano and Ceccarelli, 2014)). In this case, the large size of the protein of interest, stretches of hydrophobic amino acid residues, and codon usage may have led to expression failure (discussed below).

Nevertheless, protein expression of pET-MD1-HE containing two mutS domains (220 amino acids, 25.115 kDa excluding his_6-tag) was successful using the same approach. The expressed protein was found to be insoluble, forming inclusion bodies in *E.coli* cells. This insoluble protein was purified using a buffer containing strong denaturant such as Urea, and was successfully purified using metal affinity chromatography (Figure 5.3). *In vitro* refolding and solubilization was attempted under variety of conditions described by (Burgess, 2009), which included dialysis (Sorensen et al., 2003), and on-column refolding (Zhu et al., 2005). However, the protein was difficult to refold using these established methods, and highest possible concentration of soluble protein from inclusion bodies was obtained using a protocol described by Santos et al. (2012), which is based on stepwise dialysis in the presence of glycerol (Santos et al., 2012). Nevertheless, even using this method only a small fraction of protein (20%) could be solubilized.

Disparities in codon bias are thought to be one of the major contributing factor in failure to achieve heterologous protein expression in *E. coli* host (Gustafsson et al., 2004). The presence of rare codons may have negative influence on protein expression capacity in *E. coli* (Tøndervik et al., 2013). Comparison of rare codon usage between octocoral mtMutS studied here and extensively studied *E. coli* mutS gene (GenBank ID: AP009048) suggests that the *mtMutS* has as many as 70 rare codons including 28 Arg codons, whereas *E. coli* comprise only 11 including 3 Arg codons. On the other hand,

the smaller counterpart of *mtMutS* gene expressed successfully here in *E. coli* consists of 19 rare including 10 Arg codons (Appendix 5.1). These observations indicate that, even though the octocoral *mtMutS* gene is a bacterial derivative, codon usage differs greatly.

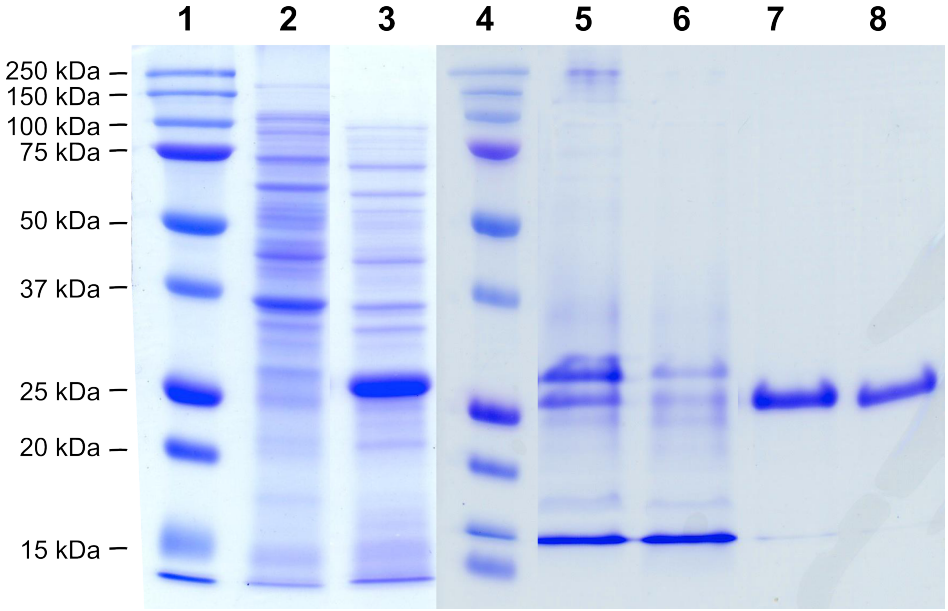

Figure 5.3 Protein expression and purification

The 12% SDS-PAGE gel showing overexpression and purification of fused N- and C-terminal domains of mtMutS protein. Lane1, Precious Plus Dual Color Protein Marker (Bio-rad, USA); lane 2, total lysate from control *E. coli* (pET15b); lane 3, lysate from expressed partial mtMutS (pET15b-MD1H), lane 4, Protein Marker as above; lane 5 and 6, Ni-IDA column was through; lane 7 and 8, purified his6-tagged partial mtMutS protein (Domain 1-HNH).

The evident difficulties in expression/solubilization of these proteins may correlate with the high hydrophobicity of the mtMutS protein. The hydropathy profile of the full mtMutS protein indicates, as expected due to its function likely in the matrix, absence of any possible transmembrane regions (Figure 5.4A). However, this protein possesses regions of high hydrophobicity. A comparison of hydrophobicity plots between the extensively studied *E.coli* mutS protein (Wu and Marinus, 1999; Lamers et al., 2000) and the octocoral mtMutS studied here indicates an apparent difference in amino acid composition and hydrophobicity profile. The mtMutS exhibited significantly higher local hydrophobicity compared to *E.coli* mutS protein (Figure 5.4B). Similarly, the domain fusion construct amino acid sequence also possessed residues with high hydrophobicity (Figure 5.4C). These differences may have cause the in failure of expression for the formar and the successful expression of the later.

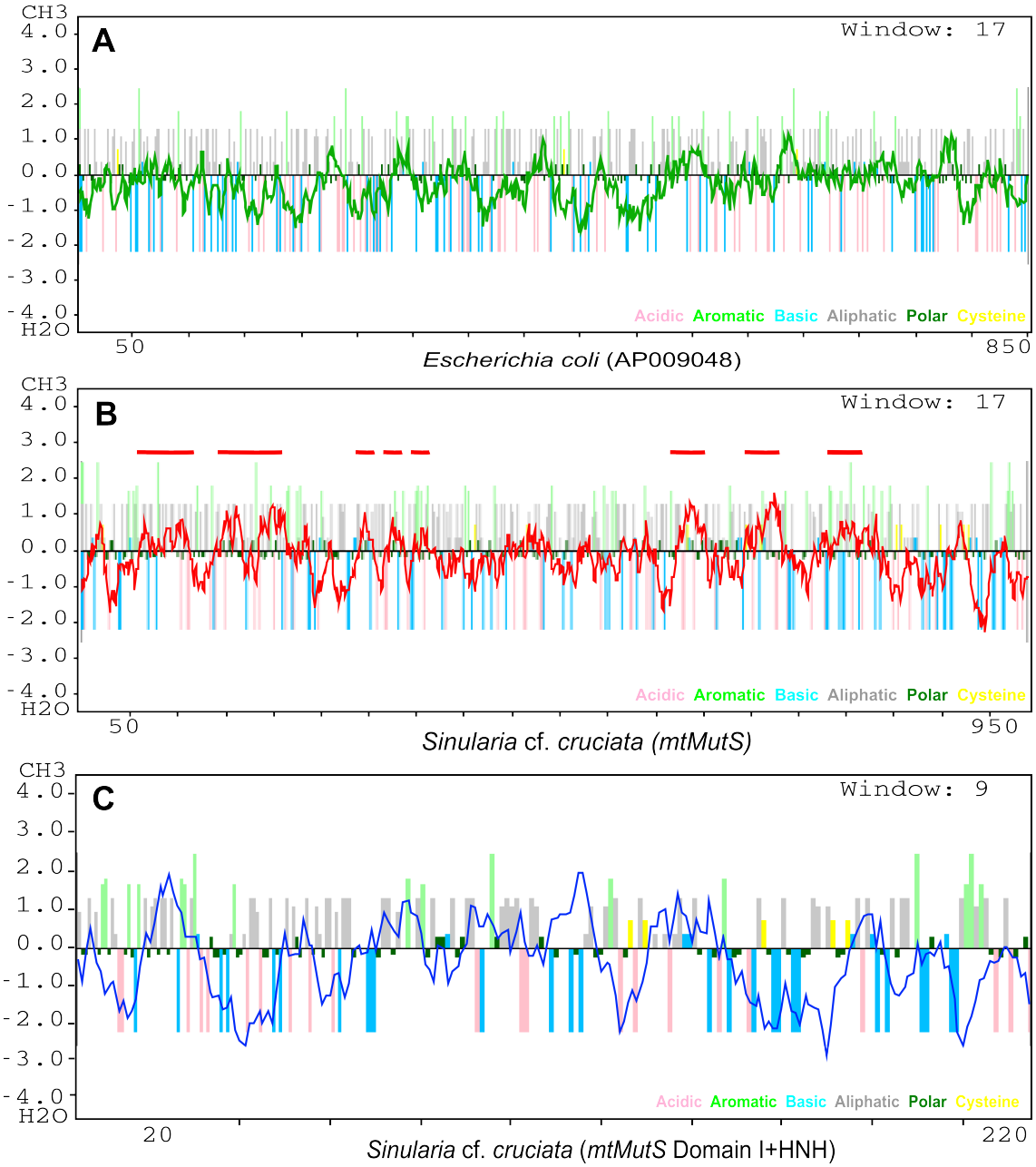

Figure 5.4 Comparison of hydropathicity

(A) Hydropathicity profile of *E. coli* mutS protein (green profile), **(B)** *S.* cf. *cruciata* mtMutS protein (red profile) where red bars above the plot indicate hydrophobic regions, and **(C)** partial expressed mtMutS protein (blue profile). Hydropathicity was calculated using sliding window of 17 residues for A and B and 9 residues for C. The x-axis denotes amino acid number and y-axis present hydrophobicity value. The bars in the background represent PepCalc (Innovagen) hydropathy analysis. Amino are color-coded based on their properties. The regions above zero indicate hydrophobic and below zero are hydrophilic stretches.

Typical animal mitochondria features very compact genomes, as most of their gene content is transferred to the nuclear genome (Boore, 1999). However, octocoral *mtMutS* is the largest gene in their mitochondrial genomes occupying as much as 16% of it. Their genomes are also known for high occurrence of reorganization through intramolecular recombination (Brockman and McFadden, 2012). Maintenance of a large gene such as *mtMutS,* which is also know to be fastest evolving gene in octocoral mitogenomes, points towards a strong selection pressure enabling its continuous presence, as speculated earlier (Bilewitch and Degnan, 2011). On the other hand, according to the "hydrophobicity hypothesis", the intracellular gene transfer from mitochondrial to nuclear genome was assisted by reduction in local hydrophobicity of encoded proteins suggesting only hydrophobic protein-coding genes remained in the metazoan mitochondrial genome (Daley et al., 2002). On the contrary, the observed high hydrophobicity of mtMutS protein indicates its possible transformation from a less hydrophobic (bacterial homologs, such as *E. coli* discussed above) to a more hydrophobic protein for retaining its putative function in the octocoral mitochondria. However, more studies are needed in order to understand the presence and the role of this unique gene and protein in octocoral mitochondria.

5.4 Conclusions

We show potential presence of the mtMutS protein in the mitochondrial fraction of *S.* cf. *cruciata* and discuss the difficulties associated with its expression using *E.coli* expression system. Additionally, we demonstrated the presence of artificially deleted cDNA for *mtMutS* gene due to the presence of direct repeat indicating a need for caution during cDNA synthesis. We were unable to determine the biological function of mtMutS protein and its isolated domains. However, the successful expression and purification of a recombinant protein comprising fused N-terminal and C-terminal domains will help to generate polyclonal antibodies against the full protein for its detection in mitochondria, as well as to further understand the biological activities of mismatch recognition and binding of the mtMutS-Domain I and homing endonuclease function in future.

5.5 Appendix

Appendix 5.5.1 Rare Codon Analysis (RaCC) of full-length *mtMutS* gene and mtMuS-Domain I-HNH fusion protein

Appendix 5.5.1 Rare Codon Analysis (RaCC) of full length *mtMutS* gene and mtMuS-Domain I-HNH fusion protein

A. Full length *mtMutS* gene

RaCC Results http://nihserver.mbi.ucla.edu/RACC/racc.cgi?dna_seq=AT...

RaCC results:

Red = rare Arg codons **AGG, AGA, CGA**
Green = rare Leu codon **CTA**
Blue = rare Ile codon **ATA**
Orange = rare Pro codon **CCC**

for the following input sequence:

```
atg aac cag ATA cct atg caa tat ttt aat tta gcg gag gag aat tat tct aag tat ggg
tta tca gta atc caa ctt atc cag att ggt aag ttc tat gaa ctt tgg cat gag CCC gat
act tct agt aag cac CGA gta tgc tct caa gcc gag tta tta gtt gag tca tcg aca CGA
agt AGG cct tta gag gta aca tcc CCC att gaa caa gtt gct tcg tta ctt gat atg AGA
ATA ATA tca CCC agt aaa AGA tct ttg ctt caa atg gga ttt cca atc tat tcc ctt act
acc cat tta acc act ttg ttg gat aaa ggt tgg act gtt gta gtt att gat gaa tta gtc
act ggt aaa tcc ggg cca aaa caa cgc gca gta tct caa gtt tat tct cct agt tgc aat
tca gaa gat tgt tcg gaa tta tcc tat gtg tta tca att tat ttt tct caa gac aac tta
CTA ggt att act tta ttt tca gcc atg aat ggg cat agt ATA atg ttt cct gtc tct tga
acg gac AGG gac aaa gta acc cgg tta tta gtc agt tat cgt att AGA gaa ATA gta att
tgg gtg gac tcg ggg gta ggt tta aat gtt tta ATA aat aag ATA tat aat tta tta att
ggt tgg aat tta ttc CCC tct gaa cct aat gct aaa att gaa gtt atg ggg gaa gta CTA
acc aat tta ccg tgt tat tta tct tat AGG tac gaa aat aat aat aag gag tgg ctt ttg
ctt cat att tat ATA ggc act aac gca gag tgg ttg aac aaa aat tat caa aaa tat acc
ctt agt aag ATA ttt caa agt act tgg aca gaa aat gtt gat cag gca aat tta att agt
ctt tta gga gta tta caa ttt att aaa gat CGA aac cct aat ctt att aag aat ctt caa
ctt cct gag tgt tat aat tct gtt gtc agt CCC tta aat tta ATA tta tgt aat CGA gca
gaa tat caa ttg gac tta tta cct aag AGG ggg aag ttg ggt ggt tta ctt aat ctg gtt
gat tat tgt tct act gca atg ggt aaa AGA ctt ttc aaa ttt AGA ctt ctt aac cct att
aca gat tat tct gaa tta aat ctt cgt tat aag gag att gct ATA ttt aaa caa tta ctt
gac AGG aaa ATA ttt gac aat ttc gag tta aaa cac att aaa gat tta tct tct tta cat
cgt caa tgg gca ATA tgt gcc tca agt gat act acc ttg tcc cct aaa aag tta agt caa
att tac cac tct tat ttg ttt gct aat cag tta ATA agt aaa ttg ATA aat aat aaa tga
att aac att caa tta cct cct tta atc gga CCC caa CTA gaa tcg tta att gaa gaa ATA
ggt caa gtt ttt caa gta aat aat ctt tta ggt gat ttc aaa gat gta tta cag cca act
gat aat CTA act aac tta ctt gcg caa caa caa act tta AGG gcc caa ctt aca gag tgg
gcc gaa caa att tca aat att gtg ttt caa gac aca att tct att aaa gcc gaa tat ttt
aat aaa gag ggt tat gct ttt tct att tta tct aaa aag tta act aag tta gaa cat tac
atg act aat gct tct ATA tct aat aat tca att att gta ttg ggt aaa AGA gga agc cac
cat ATA att act agt cct act att cat aaa gta tca atc gaa tta aat tta tta gaa gag
caa att aat act tac gtt aaa caa act tat aac cag gaa ctt aaa AGA tta tat ttt agt
tat tct gaa ctt ttt tcg CCC tta gta aat atg att tct aaa tta gat gtt gca tta agc
ggg gct att gcg gct att aaa ttc aat tat act aaa cct tgc tta aca CTA gcg aaa CCC
caa caa acc aaa ggt ttt ATA gaa gca att aac tta CGA cac cca tta gta gaa caa tta
aac act caa gaa gaa tgt gta gct cat aat att agt tta gag gat aag gga atg tta ATA
ttc tca gta aat ggt gca ggt aaa tct act CTA ctt AGA gca atc gga atc aac gta atc
tta gct caa gca gga atg tat gta gct gca gat tca ttt aaa tta AGG cct tat aat tat
tta att act cgt att tta ggg gga gac gat ctt cat aaa ggc caa ggt act ttt gag gtc
gaa atg AGA gat ctt tca act ATA tta aag tta ggt aat tat aac agt tta ATA tta ggt
gac gaa att tgt cat gga aca gaa gtt agt tca gga aca gcg ATA ttg gct gca aca att
gaa AGA tta aca act gca caa act agt ttt gtt ctt tct act cat tta cat CGA gtt tgt
tct tta att gat tcg cca gtt cgg tgc tat cat tta tct gtt att caa caa gaa gat tcg
ggc CTA att tat gaa cgt aaa ttg aaa cct ggc cca ggg CCC tct caa tat ggc att gaa
gtt atg ggt cac ATA att aat gat aaa aaa ttt tat aac agt gct ttg aaa tac cgt aaa
ctt att aac tgg gag CTA cca tcc CGA aat gag ttt agc cct tta aca gta ttc cgc cct
tct aaa tat aat gct caa gtt ttt att gat tcg tgt gaa ATA tgc gga gct cca gca gaa
gct att cac cac att caa cct aag agt gaa ttt aaa aat caa cct gag AGA tta tgt aat
aaa aaa tta aat CGA aaa tct aac ttg gtg cca gtt tgt tca agc tgc cat tta aat att
cac AGA aat aaa atc tct att tta ggt tgg aag AGA acc cca gga cat aag aaa tta tat
tgg gtt tat ctt aat gaa tct tta gac agt gga act gag taa
```

A. Full length *mtMutS* gene (continued)

The length is: 2982 nucleotides

Number of total single rare Arg codons: 28
occurring at codons:
46, 60, 62, 80, 87, 183, 196, 250, 311, 339, 350, 370, 375, 402, 514, 577, 616, 673, 713, 736, 763, 802, 818, 889, 937, 945, 962, 972

Number of tandem rare Arg codon double repeats: 0
Number of tandem rare Arg codon triple repeats: 0

Too lazy to beautify this new part right now...Results are in order for Arginine, Leucine, Isoleucine, and Proline, respectively (delimited by numbers 1.1, 2.1, 3.1, 4.1 for singles; 1.2, 2.2, 3.2, 4.2 for doubles; etc.).
Single rare codons at positions:
46 60 62 80 87 183 196 250 311 339 350 370 375 402 514 577 616 673 713 736 763 802 818 889 937 945 962 972 (agg)|(aga)|(cga)1.1 161 240 473 503 657 711 842 886 cta2.1 4 81 82 174 198 212 215 265 284 335 395 404 425 452 456 480 566 582 667 700 768 778 795 865 914 ata3.1 39 69 84 226 331 471 627 660 854 ccc4.1

Double rare codons at positions:
(agg)|(aga)|(cga)1.2 cta2.2 82 ata3.2 ccc4.2

Triple rare codons at positions:
(agg)|(aga)|(cga)1.3 cta2.3 ata3.3 ccc4.3

Cameron Mura
cmura@ucsd.edu

B. mtMuS-Domain I-HNH fusion protein

RaCC results:

Red = rare Arg codons **AGG, AGA, CGA**
Green = rare Leu codon **CTA**
Blue = rare Ile codon **ATA**
Orange = rare Pro codon **CCC**

for the following input sequence:

```
atg aac cag ATA cct atg caa tat ttt aac tta gcg gag gag aat tat tct aag tat gga
tta tca gta atc cag ctt atc cag att ggt aag ttc tat gaa ctt tgg cat gag cct gat
act tct agt aag cag CGA gca tac tct caa gcc gag tta tta atg gaa tca tcg ATA CGA
aat AGG CCC tta gaa gta aca tcc CCC att gaa caa gtt gct tcg tta ctt gat atg AGA
ATA ATA tca CCC ggt aaa AGA tcc ttg ctt caa atg ggg ttt cca atc tat tct ctt act
acc cat CTA agc acc ttg ttg gat aaa ggt tgg act gtt ATA gtt att gat gaa tta gtc
act ggt aaa tcc ggg cca aaa caa cgc gca gta tct caa gtt ttt att gat tcg tgt gaa
ATA tgc gga gct cca gca gag gct att cac cac att caa cct aag agt gaa ttt aaa agt
caa cct gaa aaa tta tgt aat AGA aaa tta aat CGA AGA tct aac ttg gtg cca gtc tgt
tca aac tgt cat tta gat att cat AGA aat aaa atc tct att tta ggt tgg aag AGA acc
cca gga cat aag aaa tta tat tgg gtt tat ctt aat gag tct tta gac agt gga act gag
taa
```

The length is: 663 nucleotides

Number of total single rare Arg codons: 10
occurring at codons:
46, 60, 62, 80, 87, 168, 172, 173, 189, 199

Number of tandem rare Arg codon double repeats: 1
occurring at codons:
173

Number of tandem rare Arg codon triple repeats: 0

Too lazy to beautify this new part right now...Results are in order for Arginine, Leucine, Isoleucine, and Proline, respectively (delimited by numbers 1.1, 2.1, 3.1, 4.1 for singles; 1.2, 2.2, 3.2, 4.2 for doubles; etc.).
Single rare codons at positions:
46 60 62 80 87 168 172 173 189 199 (agg)|(aga)|(cga)1.1 103 cta2.1 4 59 81 82 114 141 ata3.1 63 69 84 ccc4.1

Double rare codons at positions:
173 (agg)|(aga)|(cga)1.2 cta2.2 82 ata3.2 ccc4.2

Triple rare codons at positions:
(agg)|(aga)|(cga)1.3 cta2.3 ata3.3 ccc4.3

Cameron Mura
cmura@ucsd.edu

Concluding Remarks

Octocorals, by virtue of the novelties of their mitogenomes, provide unique opportunity to understand mitochondrial biology from the environmental as well as the evolutionary perspective. For this dissertation several aspects of octocoral mitochondrial biology were investigated, which included mtDNA repair, gene and protein expression, and transcription; providing first glimpse into the complexity of non-bilaterian mitochondria and their potential for enhancing our understanding of important molecular event occurring in mitochondria, oxidative stress response and their adaptive as well as evolutionary implications.

Quantitative RT-PCR (qPCR) is considered a gold standard for its sensitivity and accuracy in gene expression profiling with some quality control. The first systematic validation of suitable reference genes for ocean acidification- and warming-induced abiotic stress related qPCR-based studies on the octocoral *Sinularia* cf. *cruciata* is provided. The experimental condition-dependent validity of RGs was observed, Moreover, a stress-dependent differential response of the octocoral *HSP70* transcriptional levels was reported; highlight their specific strategies of potential resilience. We expect these results will aid gene expression studies and provide the basis for future investigations directed towards increasing our understanding of the genetic mechanisms involved in octocoral stress responses and their resilience to adverse future ocean conditions.

A mitochondria-centric outlook on oxidative stress response with an emphasis on the response of mitochondria during global climate change scenarios among corals was presented. MtDNA damage repair quantification and copy number dynamics revealed a rapid reversal of to oxidative stress induced mtDNA damage, recorded for the first time in non-bilaterians. We demonstrated the stress-specific gene expression strategies exhibited by octocorals and upregulation of *mtMutS* gene during acidification stress supporting its potential role in mtDNA repair.

A potentially complex nature of mitochondrial mRNA processing in early branching metazoan was explored for the first time. The “special" and diverse mitogenome of

octocorals revealed drastically different patterns of mtDNA transcription from bilaterians, likely due to the lack of tRNAs as punctuation marks. The presence of polycistronic mature mRNAs for the majority of genes agrees with this hypothesis. The occurrence of alternately polyadenylated transcripts for the *mtMutS* gene, the existence of 5' and 3' UTRs, and the presence of lnc*ATP6* transcripts are additional features highlighting the complexity of the post-transcriptional modifications used by early branching metazoans. The project contributes to better understand the mitobiology of early branching animals from functional perspective, which will certainly only increase our knowledge on the evolutionary innovation that shaped the evolution of these organisms.

Simple, convenient, reproducible, and flexible parallel strategies were developed to prepare heteroduplex DNA plasmids containing varied mismatch lesions. These strategies can be easily adopted in any molecular biology laboratory with basic facilities, making the *in vitro* MMR assay more accessible. The bacterial packaging cell lines can be used as a source of ssDNA in large quantities for many other applications without the need of additional helper phages

The potential presence of the mtMutS protein is shown in the mitochondrial fraction of *S.* cf. *cruciata* and the difficulties associated with its expression using *E.coli* expression system are discussed. Although, we were unable to determine the biological function of mtMutS protein and its isolated domains, the successful expression and purification of a recombinant protein comprising fused N-terminal and C-terminal domains will help to generate polyclonal antibodies against the full protein for its detection in mitochondria, as well as to further understand the biological activities of mismatch recognition and binding of the mtMutS-Domain I and homing endonuclease function in future.

The project covered diverse aspect of mitochondrial biology of octocorals, revealing its complexity, uniqueness and importance, providing a strong foundation for future studies in the direction of understanding early branching metazoan mitochondria from mechanistic, functional and evolutionary perspectives.

Bibliography

Aceret, T. L., Coll, J. C., Uchio, Y. and Sammarco, P. W. (1998). Antimicrobial activity of the diterpenes flexibilide and sinulariolide derived from Sinularia flexibilis Quoy and Gaimard 1833 (Coelenterata: Alcyonacea, Octocorallia). *Comparative Biochemistry and Physiology. Part C, Pharmacology, Toxicology & Endocrinology* **120**, 121-126.

Adams, K. L. and Palmer, J. D. (2003). Evolution of mitochondrial gene content: gene loss and transfer to the nucleus. *Mol Phylogenet Evol* **29**, 380-395.

Ahmed, A. F., Hsieh, Y.-T., Wen, Z.-H., Wu, Y.-C. and Sheu, J.-H. (2006). Polyoxygenated sterols from the Formosan soft coral Sinularia gibberosa. *Journal of Natural Products* **69**, 1275-1279.

Alexeyev, M., Shokolenko, I., Wilson, G. and LeDoux, S. (2013). The maintenance of mitochondrial DNA integrity--critical analysis and update. *Cold Spring Harb Perspect Biol* **5**, a012641.

Andersen, C. L., Jensen, J. L. and Ørntoft, T. F. (2004). Normalization of Real-Time Quantitative Reverse Transcription-PCR Data: A Model-Based Variance Estimation Approach to Identify Genes Suited for Normalization, Applied to Bladder and Colon Cancer Data Sets. *Cancer Research* **64**, 5245-5250.

Austin, R. C., Sood, S. K., Dorward, A. M., Singh, G., Shaughnessy, S. G., Pamidi, S., Outinen, P. A. and Weitz, J. I. (1998). Homocysteine-dependent alterations in mitochondrial gene expression, function and structure. Homocysteine and H2O2 act synergistically to enhance mitochondrial damage. *J Biol Chem* **273**, 30808-30817.

Bai, Y., Shakeley, R. M. and Attardi, G. (2000). Tight control of respiration by NADH dehydrogenase ND5 subunit gene expression in mouse mitochondria. *Mol Cell Biol* **20**, 805-815.

Baillon, S., Hamel, J.-F., Wareham, V. E. and Mercier, A. (2012). Deep cold-water corals as nurseries for fish larvae. *Frontiers in Ecology and the Environment* **10**, 351-356.

Bannwarth, S., Figueroa, A., Fragaki, K., Destroismaisons, L., Lacas-Gervais, S., Lespinasse, F., Vandenbos, F., Pradelli, L. A., Ricci, J. E., Rotig, A. et al. (2012). The human MSH5 (MutSHomolog 5) protein localizes to mitochondria and protects the mitochondrial genome from oxidative damage. *Mitochondrion* **12**, 654-665.

Barzilai, A. and Yamamoto, K. (2004). DNA damage responses to oxidative stress. *DNA Repair (Amst)* **3**, 1109-1115.

Bastidas, C., Benzie, J. A. H., Uthicke, S. and Fabricius, K. E. (2001). Genetic differentiation among populations of a broadcast spawning soft coral, Sinularia flexibilis, on the Great Barrier Reef. *Marine Biology* **138**, 517-525.

Bay, R. A. and Palumbi, S. R. (2015). Rapid acclimation ability mediated by transcriptome changes in reef-building corals. *Genome Biology and Evolution*.

Bayer, F. M. (1955). Contributions to the nomenclature, systematics, and morphology

of the Octocorallia. *Proceedings of the United States National Museum* **105**, 207-220.

Beagley, C. T., Okimoto, R. and Wolstenholme, D. R. (1998). The mitochondrial genome of the sea anemone Metridium senile (Cnidaria): introns, a paucity of tRNA genes, and a near-standard genetic code. *Genetics* **148**, 1091-1108.

Bellantuono, A. J., Hoegh-Guldberg, O. and Rodriguez-Lanetty, M. (2012). Resistance to thermal stress in corals without changes in symbiont composition. *Proceedings of the Royal Society of London B: Biological Sciences* **279**, 1100-1107.

Benayahu, Y. and Loya, Y. (1977). Space partitioning by stony corals soft corals and benthic algae on the coral reefs of the northern Gulf of Eilat (Red Sea). *Helgoländer wissenschaftliche Meeresuntersuchungen* **30**, 362-382.

Bengtson, S. (1981). Atractosella, a Silurian alcyonacean octocoral. *Journal of Paleontology*, 281-294.

Berg, O. G. and Kurland, C. G. (2000). Why Mitochondrial Genes are Most Often Found in Nuclei. *Molecular Biology and Evolution* **17**, 951-961.

Bernt, M., Bleidorn, C., Braband, A., Dambach, J., Donath, A., Fritzsch, G., Golombek, A., Hadrys, H., Juhling, F., Meusemann, K. et al. (2013). A comprehensive analysis of bilaterian mitochondrial genomes and phylogeny. *Mol Phylogenet Evol* **69**, 352-364.

Bilewitch, J. P. and Degnan, S. M. (2011). A unique horizontal gene transfer event has provided the octocoral mitochondrial genome with an active mismatch repair gene that has potential for an unusual self-contained function. *BMC evolutionary biology* **11**, 228.

Biswas, I. and Hsieh, P. (1996). Identification and characterization of a thermostable MutS homolog from Thermus aquaticus. *The Journal of Biological Chemistry* **271**, 5040-5048.

Blackstone, N. (2009). Mitochondria and the redox control of development in cnidarians. *Semin Cell Dev Biol* **20**, 330-336.

Blasiak, J., Glowacki, S., Kauppinen, A. and Kaarniranta, K. (2013). Mitochondrial and nuclear DNA damage and repair in age-related macular degeneration. *Int J Mol Sci* **14**, 2996-3010.

Blondel, A. and Thillet, J. (1991). A fast and convenient way to produce single stranded DNA from a phagemid. *Nucleic Acids Res* **19**, 181.

Boesch, P., Weber-Lotfi, F., Ibrahim, N., Tarasenko, V., Cosset, A., Paulus, F., Lightowlers, R. N. and Dietrich, A. (2011). DNA repair in organelles: Pathways, organization, regulation, relevance in disease and aging. *Biochimica et Biophysica Acta (BBA) - Molecular Cell Research* **1813**, 186-200.

Boore, J. L. (1999). Animal mitochondrial genomes. *Nucleic Acids Res* **27**, 1767-1780.

Brockman, S. A. and McFadden, C. S. (2012). The mitochondrial genome of Paraminabea aldersladei (Cnidaria: Anthozoa: Octocorallia) supports intramolecular recombination as the primary mechanism of gene rearrangement in octocoral mitochondrial genomes. *Genome biology and evolution* **4**, 994-1006.

Brown, B. E. (1997). Coral bleaching: causes and consequences. *Coral Reefs* **16**, S129-S138.

Brown, W. M., Prager, E. M., Wang, A. and Wilson, A. C. (1982). Mitochondrial

DNA sequences of primates: tempo and mode of evolution. *Journal of molecular evolution* **18**, 225-239.

Brugler, M. R. and France, S. C. (2008). The mitochondrial genome of a deep-sea bamboo coral (Cnidaria, Anthozoa, Octocorallia, Isididae): genome structure and putative origins of replication are not conserved among octocorals. *J Mol Evol* **67**, 125-136.

Burgess, R. R. (2009). Refolding solubilized inclusion body proteins. *Methods Enzymol* **463**, 259-282.

Bustin, S. A. (2002). Quantification of mRNA using real-time reverse transcription PCR (RT-PCR): trends and problems. *J Mol Endocrinol* **29**, 23-39.

Bustin, S. A., Benes, V., Garson, J. A., Hellemans, J., Huggett, J., Kubista, M., Mueller, R., Nolan, T., Pfaffl, M. W., Shipley, G. L. et al. (2009). The MIQE guidelines: minimum information for publication of quantitative real-time PCR experiments. *Clinical chemistry* **55**, 611-622.

Cadenas, E. (1989). Biochemistry of oxygen toxicity. *Annu Rev Biochem* **58**, 79-110.

Chan, N. C. and Connolly, S. R. (2013). Sensitivity of coral calcification to ocean acidification: a meta-analysis. *Glob Chang Biol* **19**, 282-290.

Chasteen, L., Ayriss, J., Pavlik, P. and Bradbury, A. R. (2006). Eliminating helper phage from phage display. *Nucleic Acids Res* **34**, e145.

Chen, I.-P., Tang, C.-Y., Chiou, C.-Y., Hsu, J.-H., Wei, N. V., Wallace, C. C., Muir, P., Wu, H. and Chen, C. A. (2009). Comparative analyses of coding and noncoding DNA regions indicate that Acropora (Anthozoa: Scleractina) possesses a similar evolutionary tempo of nuclear vs. mitochondrial genomes as in plants. *Marine biotechnology (New York, N.Y.)* **11**, 141-152.

Chen, W.-F., Yin, C.-T., Cheng, C.-H., Lu, M.-C., Fang, L.-S., Wang, W.-H., Wen, Z.-H., Chen, J.-J., Wu, Y.-C. and Sung, P.-J. (2015). Norcembranoidal Diterpenes from the Cultured-Type Octocoral Sinularia numerosa. *International Journal of Molecular Sciences* **16**, 3298-3306.

Clayton, W. (1985). Polyp density variability among colonies of the reef coral Pocillopora damicornis. *Bulletin of Marine Science*, 716-719.

Cline, S. D. (2012). Mitochondrial DNA damage and its consequences for mitochondrial gene expression. *Biochim Biophys Acta* **1819**, 979-991.

Cocquet, J., Chong, A., Zhang, G. and Veitia, R. A. (2006). Reverse transcriptase template switching and false alternative transcripts. *Genomics* **88**, 127-131.

Cornett, A. L. and Lutz, C. S. (2014). RHAPA: a new method to quantify alternative polyadenylation. *Methods Mol Biol* **1125**, 157-167.

Corrette-Bennett, S. E. and Lahue, R. S. (1999). Mismatch repair assay. *Methods Mol Biol* **113**, 121-132.

Coucheron, D. H., Nymark, M., Breines, R., Karlsen, B. O., Andreassen, M., Jørgensen, T. E., Moum, T. and Johansen, S. D. (2011). Characterization of mitochondrial mRNAs in codfish reveals unique features compared to mammals. *Current Genetics* **57**, 213-222.

Crawford, D. R., Abramova, N. E. and Davies, K. J. (1998). Oxidative stress causes

a general, calcium-dependent degradation of mitochondrial polynucleotides. *Free Radic Biol Med* **25**, 1106-1111.

Culligan, K. M., Meyer-Gauen, G., Lyons-Weiler, J. and Hays, J. B. (2000). Evolutionary origin, diversification and specialization of eukaryotic MutS homolog mismatch repair proteins. *Nucleic Acids Res* **28**, 463-471.

Daley, D. O., Clifton, R. and Whelan, J. (2002). Intracellular gene transfer: reduced hydrophobicity facilitates gene transfer for subunit 2 of cytochrome c oxidase. *Proc Natl Acad Sci U S A* **99**, 10510-10515.

Daly, M., Brugler, M. R., Cartwright, P., Collins, A. G., Dawson, M. N., Fautin, D. G., France, S. C., McFadden, C., Opresko, D. M. and Rodriguez, E. (2007). The phylum Cnidaria: a review of phylogenetic patterns and diversity 300 years after Linnaeus.

de Souza-Pinto, N. C., Mason, P. A., Hashiguchi, K., Weissman, L., Tian, J., Guay, D., Lebel, M., Stevnsner, T. V., Rasmussen, L. J. and Bohr, V. A. (2009). Novel DNA mismatch-repair activity involving YB-1 in human mitochondria. *DNA Repair (Amst)* **8**, 704-719.

De Spiegelaere, W., Dern-Wieloch, J., Weigel, R., Schumacher, V., Schorle, H., Nettersheim, D., Bergmann, M., Brehm, R., Kliesch, S., Vandekerckhove, L. et al. (2015). Reference gene validation for RT-qPCR, a note on different available software packages. *PLoS One* **10**, e0122515.

Deflandre-Rigaud, M. (1956). Les sclérites d'Alcyonaires fossiles: éléments d'une classification: Masson.

DeSalvo, M. K., Voolstra, C. R., Sunagawa, S., Schwarz, J. A., Stillman, J. H., Coffroth, M. A., Szmant, A. M. and Medina, M. (2008). Differential gene expression during thermal stress and bleaching in the Caribbean coral Montastraea faveolata. *Molecular Ecology* **17**, 3952-3971.

Dheda, K., Huggett, J. F., Bustin, S. A., Johnson, M. A., Rook, G. and Zumla, A. (2004). Validation of housekeeping genes for normalizing RNA expression in real-time PCR. *Biotechniques* **37**, 112-114, 116, 118-119.

Dheda, K., Huggett, J. F., Chang, J. S., Kim, L. U., Bustin, S. A., Johnson, M. A., Rook, G. A. and Zumla, A. (2005). The implications of using an inappropriate reference gene for real-time reverse transcription PCR data normalization. *Anal Biochem* **344**, 141-143.

Dixon, G. B., Davies, S. W., Aglyamova, G. A., Meyer, E., Bay, L. K. and Matz, M. V. (2015). CORAL REEFS. Genomic determinants of coral heat tolerance across latitudes. *Science* **348**, 1460-1462.

Doney, S. C., Fabry, V. J., Feely, R. A. and Kleypas, J. A. (2009). Ocean acidification: the other CO2 problem. *Annual Review of Marine Science* **1**, 169-192.

Downs, C. A., Mueller, E., Phillips, S., Fauth, J. E. and Woodley, C. M. (2000). A molecular biomarker system for assessing the health of coral (Montastraea faveolata) during heat stress. *Mar Biotechnol (NY)* **2**, 533-544.

Dowton, M. and Campbell, N. J. (2001). Intramitochondrial recombination - is it why some mitochondrial genes sleep around? *Trends Ecol Evol* **16**, 269-271.

Dunn, S. R., Pernice, M., Green, K., Hoegh-Guldberg, O. and Dove, S. G. (2012).

Thermal stress promotes host mitochondrial degradation in symbiotic cnidarians: are the batteries of the reef going to run out? *PLoS One* **7**, e39024.

Dyall, S. D., Brown, M. T. and Johnson, P. J. (2004). Ancient invasions: from endosymbionts to organelles. *Science* **304**, 253-257.

Dykens, J. A., Shick, J. M., Benoit, C., Buettner, G. R. and Winston, G. W. (1992). Oxygen radical production in the sea anemone Anthopleura elegantissima and its endosymbiotic algae. *Journal of Experimental Biology* **168**, 219-241.

Emblem, A., Okkenhaug, S., Weiss, E. S., Denver, D. R., Karlsen, B. O., Moum, T. and Johansen, S. D. (2014). Sea anemones possess dynamic mitogenome structures. *Mol Phylogenet Evol* **75**, 184-193.

Erpenbeck, D., Aryasari, R., Hooper, J. N. and Worheide, G. (2015). A mitochondrial intron in a verongid sponge. *J Mol Evol* **80**, 13-17.

Fabricius, K. E. (1995). Slow population turnover in the soft coral genera Sinularia and Sarcophyton on mid- and outer-shelf reefs of the Great Barrier Reef. *Marine Ecology Progress Series* **126**, 145-152.

Fabricius, K. K. and Alderslade, P. P. (2001). Soft corals and sea fans: a comprehensive guide to the tropical shallow water genera of the central-west Pacific, the Indian Ocean and the Red Sea: Australian Institute of Marine Science (AIMS).

Falkowski, P. G., Katz, M. E., Knoll, A. H., Quigg, A., Raven, J. A., Schofield, O. and Taylor, F. J. (2004). The evolution of modern eukaryotic phytoplankton. *Science* **305**, 354-360.

Ferguson, B. S., Nam, H., Hopkins, R. G. and Morrison, R. F. (2010). Impact of Reference Gene Selection for Target Gene Normalization on Experimental Outcome Using Real-Time qRT-PCR in Adipocytes. *PLoS ONE* **5**, e15208.

Fernández-Silva, P., Enriquez, J. A. and Montoya, J. (2003). Replication and transcription of mammalian mitochondrial DNA. *Experimental physiology* **88**, 41-56.

Figueroa, D. F. and Baco, A. R. (2014). Complete mitochondrial genomes elucidate phylogenetic relationships of the deep-sea octocoral families Coralliidae and Paragorgiidae. *Deep Sea Research Part II: Topical Studies in Oceanography* **99**, 83-91.

Figueroa, D. F. and Baco, A. R. (2015). Octocoral mitochondrial genomes provide insights into the phylogenetic history of gene order rearrangements, order reversals, and cnidarian phylogenetics. *Genome Biol Evol* **7**, 391-409.

Fink, L., Seeger, W., Ermert, L., Hanze, J., Stahl, U., Grimminger, F., Kummer, W. and Bohle, R. M. (1998). Real-time quantitative RT-PCR after laser-assisted cell picking. *Nat Med* **4**, 1329-1333.

Fishel, R. (2015). Mismatch Repair. *J Biol Chem*.

Flot, J. F. and Tillier, S. (2007). The mitochondrial genome of Pocillopora (Cnidaria: Scleractinia) contains two variable regions: the putative D-loop and a novel ORF of unknown function. *Gene* **401**, 80-87.

Freeman, W. M., Walker, S. J. and Vrana, K. E. (1999). Quantitative RT-PCR: pitfalls and potential. *BioTechniques* **26**, 112-122, 124-125.

Frostig, R. D., Husson, T. R. and Issa, N. P. (2009). Functional Imaging with Mitochondrial Flavoprotein Autofluorescence: Theory, Practice, and Applications.

Fukami, H., Chen, C. A., Chiou, C. Y. and Knowlton, N. (2007). Novel group I introns encoding a putative homing endonuclease in the mitochondrial cox1 gene of Scleractinian corals. *J Mol Evol* **64**, 591-600.

Gabay, Y., Benayahu, Y. and Fine, M. (2013). Does elevated pCO(2) affect reef octocorals? *Ecology and Evolution* **3**, 465-473.

Gabay, Y., Fine, M., Barkay, Z. and Benayahu, Y. (2014). Octocoral tissue provides protection from declining oceanic pH. *PLoS One* **9**, e91553.

Geer, L. Y., Domrachev, M., Lipman, D. J. and Bryant, S. H. (2002). CDART: protein homology by domain architecture. *Genome Res* **12**, 1619-1623.

Gibbin, E. M., Putnam, H. M., Davy, S. K. and Gates, R. D. (2014). Intracellular pH and its response to CO2-driven seawater acidification in symbiotic versus non-symbiotic coral cells. *J Exp Biol* **217**, 1963-1969.

Gibson, U. E., Heid, C. A. and Williams, P. M. (1996). A novel method for real time quantitative RT-PCR. *Genome Res* **6**, 995-1001.

Glinski, A. (1956). Plumalina conservata n. sp.(Gorgonaria) aus dem Mittel-Devon der Eifel. *Senckenbergiana Lethaea* **37**, 53-57.

Gogvadze, V., Orrenius, S. and Zhivotovsky, B. (2006). Multiple pathways of cytochrome c release from mitochondria in apoptosis. *Biochim Biophys Acta* **1757**, 639-647.

Goldstone, J. V. (2008). Environmental sensing and response genes in cnidaria: the chemical defensome in the sea anemone Nematostella vectensis. *Cell Biol Toxicol* **24**, 483-502.

Gray, M. W. (1993). Origin and evolution of organelle genomes. *Curr Opin Genet Dev* **3**, 884-890.

Greaves, L. C., Reeve, A. K., Taylor, R. W. and Turnbull, D. M. (2012). Mitochondrial DNA and disease. *J Pathol* **226**, 274-286.

Guénin, S., Mauriat, M., Pelloux, J., Van Wuytswinkel, O., Bellini, C. and Gutierrez, L. (2009). Normalization of qRT-PCR data: the necessity of adopting a systematic, experimental conditions-specific, validation of references. *Journal of experimental botany* **60**, 487-493.

Gustafsson, C., Govindarajan, S. and Minshull, J. (2004). Codon bias and heterologous protein expression. *Trends Biotechnol* **22**, 346-353.

Haen, K. M., Pett, W. and Lavrov, D. V. (2010). Parallel loss of nuclear-encoded mitochondrial aminoacyl-tRNA synthetases and mtDNA-encoded tRNAs in Cnidaria. *Mol Biol Evol* **27**, 2216-2219.

Haguenauer, A., Zuberer, F., Ledoux, J.-B. and Aurelle, D. (2013). Adaptive abilities of the Mediterranean red coral Corallium rubrum in a heterogeneous and changing environment: from population to functional genetics. *Journal of Experimental Marine Biology and Ecology* **449**, 349-357.

Halliwell, B. (2006). Reactive species and antioxidants. Redox biology is a fundamental theme of aerobic life. *Plant Physiol* **141**, 312-322.

Haugan, P. M. and Drange, H. (1996). Effects of CO 2 on the ocean environment. *Energy Conversion and Management* **37**, 1019-1022.

Hauton, C., Tyrrell, T. and Williams, J. (2009). The subtle effects of sea water acidification on the amphipod Gammarus locusta. *Biogeosciences* **6**, 1479-1489.

Heid, C. A., Stevens, J., Livak, K. J. and Williams, P. M. (1996). Real time quantitative PCR. *Genome Research* **6**, 986-994.

Hellberg, M. E. (2006). No variation and low synonymous substitution rates in coral mtDNA despite high nuclear variation. *BMC evolutionary biology* **6**, 24.

Henle, E. S., Luo, Y., Gassmann, W. and Linn, S. (1996). Oxidative damage to DNA constituents by iron-mediated fenton reactions. The deoxyguanosine family. *J Biol Chem* **271**, 21177-21186.

Hennige, S. J., Wicks, L. C., Kamenos, N. A., Bakker, D. C. E., Findlay, H. S., Dumousseaud, C. and Roberts, J. M. (2013). Short-term metabolic and growth responses of the cold-water coral Lophelia pertusa to ocean acidification. *Deep Sea Research Part II: Topical Studies in Oceanography*.

Higuchi, R., Fockler, C., Dollinger, G. and Watson, R. (1993). Kinetic PCR analysis: real-time monitoring of DNA amplification reactions. *Biotechnology (N Y)* **11**, 1026-1030.

Higuchi, T., Fujimura, H., Arakaki, T. and Oomori, T. (2009). The synergistic effects of hydrogen peroxide and elevated seawater temperature on the metabolic activity of the coral Galaxea fascicularis. *Marine Biology* **156**, 589-596.

Ho, E. C., Donaldson, M. E. and Saville, B. J. (2010). Detection of antisense RNA transcripts by strand-specific RT-PCR. *Methods Mol Biol* **630**, 125-138.

Hoegh-Guldberg, O., Mumby, P. J., Hooten, A. J., Steneck, R. S., Greenfield, P., Gomez, E., Harvell, C. D., Sale, P. F., Edwards, A. J., Caldeira, K. et al. (2007). Coral reefs under rapid climate change and ocean acidification. *Science* **318**, 1737-1742.

Hoover, C. A., Slattery, M. and Marsh, A. G. (2007). Gene expression profiling of two related soft corals, Sinularia polydactyla and S. maxima, and their putative hybrid at different life-history stages. *Comparative Biochemistry and Physiology Part D: Genomics and Proteomics* **2**, 135-143.

Hoover, C. A., Slattery, M., Targett, N. M. and Marsh, A. G. (2008). Transcriptome and metabolite responses to predation in a South pacific soft coral. *Biol Bull* **214**, 319-328.

Hsieh, P. and Yamane, K. (2008). DNA mismatch repair: molecular mechanism, cancer, and ageing. *Mech Ageing Dev* **129**, 391-407.

Huang, D., Meier, R., Todd, P. A. and Chou, L. M. (2008). Slow mitochondrial COI sequence evolution at the base of the metazoan tree and its implications for DNA barcoding. *Journal of molecular evolution* **66**, 167-174.

Hughes, T. P., Baird, A. H., Bellwood, D. R., Card, M., Connolly, S. R., Folke, C., Grosberg, R., Hoegh-Guldberg, O., Jackson, J. B. C., Kleypas, J. et al. (2003). Climate Change, Human Impacts, and the Resilience of Coral Reefs. *Science* **301**, 929-933.

Inoue, H., Nojima, H. and Okayama, H. (1990). High efficiency transformation of Escherichia coli with plasmids. *Gene* **96**, 23-28.

Jeng, M. S., Huang, H. D., Dai, C. F., Hsiao, Y. C. and Benayahu, Y. (2011). Sclerite calcification and reef-building in the fleshy octocoral genus Sinularia

(Octocorallia: Alcyonacea). *Coral Reefs* **30**, 925-933.

Jiricny, J. (2013). Postreplicative mismatch repair. *Cold Spring Harb Perspect Biol* **5**, a012633.

Kaniewska, P., Campbell, P. R., Kline, D. I., Rodriguez-Lanetty, M., Miller, D. J., Dove, S. and Hoegh-Guldberg, O. (2012). Major cellular and physiological impacts of ocean acidification on a reef building coral. *PLoS One* **7**, e34659.

Kayal, E., Roure, B., Philippe, H., Collins, A. G. and Lavrov, D. V. (2013). Cnidarian phylogenetic relationships as revealed by mitogenomics. *BMC Evol Biol* **13**, 5.

Kayal, E., Bentlage, B., Collins, A. G., Kayal, M., Pirro, S. and Lavrov, D. V. (2012). Evolution of linear mitochondrial genomes in medusozoan cnidarians. *Genome biology and evolution* **4**, 1-12.

Kazak, L., Reyes, A. and Holt, I. J. (2012). Minimizing the damage: repair pathways keep mitochondrial DNA intact. *Nat Rev Mol Cell Biol* **13**, 659-671.

Kearse, M., Moir, R., Wilson, A., Stones-Havas, S., Cheung, M., Sturrock, S., Buxton, S., Cooper, A., Markowitz, S., Duran, C. et al. (2012). Geneious Basic: an integrated and extendable desktop software platform for the organization and analysis of sequence data. *Bioinformatics* **28**, 1647-1649.

Keshavmurthy, S., Meng, P.-J., Wang, J.-T., Kuo, C.-Y., Yang, S.-Y., Hsu, C.-M., Gan, C.-H., Dai, C.-F. and Chen, C. A. (2014). Can resistant coral-Symbiodinium associations enable coral communities to survive climate change? A study of a site exposed to long-term hot water input. *PeerJ* **2**, e327.

Khalesi, M. K., Vera-Jimenez, N. I., Aanen, D. K., Beeftink, H. H. and Wijffels, R. H. (2008). Cell cultures from the symbiotic soft coral Sinularia flexibilis. *In Vitro Cell Dev Biol Anim* **44**, 330-338.

Kitahara, M. V., Cairns, S. D., Stolarski, J., Blair, D. and Miller, D. J. (2010). A comprehensive phylogenetic analysis of the Scleractinia (Cnidaria, Anthozoa) based on mitochondrial CO1 sequence data. *PLoS One* **5**, e11490.

Kleypas, J. A. and Langdon, C. (2013). Coral Reefs and Changing Seawater Carbonate Chemistry. In *Coral Reefs and Climate Change: Science and Management*, pp. 73-110: American Geophysical Union.

Kocurko, M. and Kocurko, D. (1992). Fossil Octocorallia of the Red Bluff Formation, lower Oligocene, Mississippi. *Journal of Paleontology*, 594-602.

Kozera, B. and Rapacz, M. (2013). Reference genes in real-time PCR. *J Appl Genet* **54**, 391-406.

Kubista M, S. R., Tichopad A, Bergkvist A, Lindh D, Forootan A. (2007). The Prime Technique: Real-time PCR Data Analysis. *GIT Lab J.* **11**, 33-35.

Kyte, J. and Doolittle, R. F. (1982). A simple method for displaying the hydropathic character of a protein. *J Mol Biol* **157**, 105-132.

Lakshmi, V. and Kumar, R. (2009). Metabolites from Sinularia species. *Natural Product Research* **23**, 801-850.

Lamers, M. H., Perrakis, A., Enzlin, J. H., Winterwerp, H. H., de Wind, N. and Sixma, T. K. (2000). The crystal structure of DNA mismatch repair protein MutS

binding to a G x T mismatch. *Nature* **407**, 711-717.

Larson, E. D., Nickens, D. and Drummond, J. T. (2002). Construction and characterization of mismatch-containing circular DNA molecules competent for assessment of nick-directed human mismatch repair in vitro. *Nucleic Acids Res* **30**, E14.

Lavrov, D. V. (2007). Key transitions in animal evolution: a mitochondrial DNA perspective. *Integrative and Comparative Biology* **47**, 734-743.

Lavrov, D. V., Pett, W., Voigt, O., Worheide, G., Forget, L., Lang, B. F. and Kayal, E. (2013). Mitochondrial DNA of Clathrina clathrus (Calcarea, Calcinea): six linear chromosomes, fragmented rRNAs, tRNA editing, and a novel genetic code. *Mol Biol Evol* **30**, 865-880.

Lee, H. C. and Wei, Y. H. (2005). Mitochondrial biogenesis and mitochondrial DNA maintenance of mammalian cells under oxidative stress. *Int J Biochem Cell Biol* **37**, 822-834.

Lesser, M. P. (2006). Oxidative stress in marine environments: biochemistry and physiological ecology. *Annu Rev Physiol* **68**, 253-278.

Lesser, M. P. (2011). Oxidative Stress in Tropical Marine Ecosystems. In *Oxidative Stress in Aquatic Ecosystems*, pp. 7-19: John Wiley & Sons, Ltd.

Lesser, M. P. (2013). Using energetic budgets to assess the effects of environmental stress on corals: are we measuring the right things? *Coral Reefs* **32**, 25-33.

Lesser, M. P. and Farrell, J. H. (2004). Exposure to solar radiation increases damage to both host tissues and algal symbionts of corals during thermal stress. *Coral reefs* **23**, 367-377.

Li, G., Zhang, Y., Deng, Z., van Ofwegen, L., Proksch, P. and Lin, W. (2005). Cytotoxic cembranoid diterpenes from a soft coral Sinularia gibberosa. *Journal of Natural Products* **68**, 649-652.

Li, G. M. (2008). Mechanisms and functions of DNA mismatch repair. *Cell Res* **18**, 85-98.

Lin, M. F., Kitahara, M. V., Luo, H., Tracey, D., Geller, J., Fukami, H., Miller, D. J. and Chen, C. A. (2014). Mitochondrial genome rearrangements in the scleractinia/corallimorpharia complex: implications for coral phylogeny. *Genome Biol Evol* **6**, 1086-1095.

Lipps, J. H. and Signor, P. W. (2013). Origin and early evolution of the Metazoa: Springer Science & Business Media.

Livak, K. J. and Schmittgen, T. D. (2001). Analysis of Relative Gene Expression Data Using Real-Time Quantitative PCR and the $2^{-\Delta\Delta CT}$ Method. *Methods* **25**, 402-408.

Lõhelaid, H., Teder, T. and Samel, N. (2014). Lipoxygenase-allene oxide synthase pathway in octocoral thermal stress response. In *Coral Reefs*, vol. 34, pp. 143-154: Springer Berlin Heidelberg.

Lõhelaid, H., Teder, T., Tõldsepp, K., Ekins, M. and Samel, N. (2014). Up-Regulated Expression of AOS-LOXa and Increased Eicosanoid Synthesis in Response to Coral Wounding. *PLoS ONE* **9**, e89215.

Loram, J. E., Boonham, N., O'Toole, P., Trapido-Rosenthal, H. G. and Douglas, A. E. (2007). Molecular quantification of symbiotic dinoflagellate algae of the genus

Symbiodinium. *Biol Bull* **212**, 259-268.

Lough, J. M. (2008). 10th Anniversary Review: a changing climate for coral reefs. *Journal of Environmental Monitoring* **10**, 21-29.

Loya, Y., Sakai, K., Yamazato, K., Nakano, Y., Sambali, H. and van Woesik, R. (2001). Coral bleaching: the winners and the losers. *Ecology Letters* **4**, 122-131.

Luirink, J. and Sinning, I. (2004). SRP-mediated protein targeting: structure and function revisited. *Biochim Biophys Acta* **1694**, 17-35.

Lutz, C. S. and Moreira, A. (2011). Alternative mRNA polyadenylation in eukaryotes: an effective regulator of gene expression. *Wiley Interdiscip Rev RNA* **2**, 22-31.

Lynch, M., Koskella, B. and Schaack, S. (2006). Mutation pressure and the evolution of organelle genomic architecture. *Science (New York, N.Y.)* **311**, 1727-1730.

Madeira, C., Madeira, D., Vinagre, C. and Diniz, M. (2015). Octocorals in a changing environment: Seasonal response of stress biomarkers in natural populations of Veretillum cynomorium. *Journal of Sea Research* **103**, 120-128.

Mallona, I., Weiss, J. and Egea-Cortines, M. (2011). pcrEfficiency: a Web tool for PCR amplification efficiency prediction. *BMC Bioinformatics* **12**, 404.

Mao, M., Austin, A. D., Johnson, N. F. and Dowton, M. (2014). Coexistence of minicircular and a highly rearranged mtDNA molecule suggests that recombination shapes mitochondrial genome organization. *Mol Biol Evol* **31**, 636-644.

Maor-Landaw, K., Karako-Lampert, S., Waldman Ben-Asher, H., Goffredo, S., Falini, G., Dubinsky, Z. and Levy, O. (2014). Gene expression profiles during short-term heat stress in the red sea coral Stylophora pistillata. *Glob Chang Biol* **20**, 3026-3035.

Marinus, M. G. (2012). DNA Mismatch Repair. *Ecosal Plus* **2012**.

Marubini, F., Ferrier-Pagès, C., Furla, P. and Allemand, D. (2008). Coral calcification responds to seawater acidification: a working hypothesis towards a physiological mechanism. *Coral Reefs* **27**, 491-499.

Mason, P. A., Matheson, E. C., Hall, A. G. and Lightowlers, R. N. (2003). Mismatch repair activity in mammalian mitochondria. *Nucleic acids research* **31**, 1052-1058.

McFadden, C. S., France, S. C., Sánchez, J. A. and Alderslade, P. (2006). A molecular phylogenetic analysis of the Octocorallia (Cnidaria: Anthozoa) based on mitochondrial protein-coding sequences. *Molecular phylogenetics and evolution* **41**, 513-527.

McFadden, C. S., Van Ofwegen, L. P., Beckman, E. J., Benayahu, Y. and Alderslade, P. (2009). Molecular systematics of the speciose Indo-Pacific soft coral genus, Sinularia (Anthozoa: Octocorallia). *Invertebrate Biology* **128**, 303-323.

McFadden, C. S., Benayahu, Y., Pante, E., Thoma, J. N., Nevarez, P. A. and France, S. C. (2011). Limitations of mitochondrial gene barcoding in Octocorallia. *Molecular ecology resources* **11**, 19-31.

Mercer, T. R., Neph, S., Dinger, M. E., Crawford, J., Smith, M. A., Shearwood, A. M., Haugen, E., Bracken, C. P., Rackham, O., Stamatoyannopoulos, J. A. et al. (2011). The human mitochondrial transcriptome. *Cell* **146**, 645-658.

Meyer, E., Aglyamova, G. V. and Matz, M. V. (2011). Profiling gene expression

responses of coral larvae (Acropora millepora) to elevated temperature and settlement inducers using a novel RNA-Seq procedure. *Molecular Ecology* **20**, 3599-3616.

Meyer, E., Davies, S., Wang, S., Willis, B. L., Abrego, D., Juenger, T. E. and Matz, M. V. (2009). Genetic variation in responses to a settlement cue and elevated temperature in the reef-building coral Acropora millepora. *Marine Ecology Progress Series* **392**, 81-92.

Meyer, J. N. and Bess, A. S. (2012). Involvement of autophagy and mitochondrial dynamics in determining the fate and effects of irreparable mitochondrial DNA damage. *Autophagy* **8**, 1822-1823.

Michel, U., Stringaris, A. K., Nau, R. and Rieckmann, P. (2000). Differential expression of sense and antisense transcripts of the mitochondrial DNA region coding for ATPase 6 in fetal and adult porcine brain: identification of novel unusually assembled mitochondrial RNAs. *Biochem Biophys Res Commun* **271**, 170-180.

Mignone, F., Gissi, C., Liuni, S. and Pesole, G. (2002). Untranslated regions of mRNAs. *Genome Biol* **3**, REVIEWS0004.

Moberg, F. and Folke, C. (1999). Ecological goods and services of coral reef ecosystems. *Ecological Economics* **29**, 215-233.

Modrich, P. and Lahue, R. (1996). Mismatch repair in replication fidelity, genetic recombination, and cancer biology. *Annu Rev Biochem* **65**, 101-133.

Mohanty, B. K. and Kushner, S. R. (2011). Bacterial/archaeal/organellar polyadenylation. *Wiley Interdiscip Rev RNA* **2**, 256-276.

Morel, Y. and Barouki, R. (1999). Repression of gene expression by oxidative stress. *Biochem J* **342 Pt 3**, 481-496.

Mounsey, K. E., Willis, C., Burgess, S. T., Holt, D. C., McCarthy, J. and Fischer, K. (2012). Quantitative PCR-based genome size estimation of the astigmatid mites Sarcoptes scabiei, Psoroptes ovis and Dermatophagoides pteronyssinus. *Parasites & Vectors* **5**, 3.

Moya, A., Huisman, L., Forêt, S., Gattuso, J. P., Hayward, D. C., Ball, E. E. and Miller, D. J. (2015). Rapid acclimation of juvenile corals to CO2-mediated acidification by upregulation of heat shock protein and Bcl-2 genes. *Molecular Ecology* **24**, 438-452.

Moya, A., Huisman, L., Ball, E. E., Hayward, D. C., Grasso, L. C., Chua, C. M., Woo, H. N., Gattuso, J. P., Foret, S. and Miller, D. J. (2012). Whole transcriptome analysis of the coral Acropora millepora reveals complex responses to CO(2)-driven acidification during the initiation of calcification. *Mol Ecol* **21**, 2440-2454.

Murchie, E. H. and Lawson, T. (2013). Chlorophyll fluorescence analysis: a guide to good practice and understanding some new applications. *J Exp Bot* **64**, 3983-3998.

Nagaike, T., Suzuki, T. and Ueda, T. (2008). Polyadenylation in mammalian mitochondria: insights from recent studies. *Biochim Biophys Acta* **1779**, 266-269.

Nakamura, M., Morita, M., Kurihara, H. and Mitarai, S. (2012). Expression of hsp70, hsp90 and hsf1 in the reef coral Acropora digitifera under prospective acidified conditions over the next several decades. *Biol Open* **1**, 75-81.

Nesa, B. and Hidaka, M. (2008). Thermal stress increases oxidative DNA damage in coral cell aggregates. In *Proceedings of the 11th International Coral Reef Symposium*,

vol. 1, pp. 149-151.

O'Donnell, M., Hammond, L. and Hofmann, G. (2009). Predicted impact of ocean acidification on a marine invertebrate: elevated CO2 alters response to thermal stress in sea urchin larvae. *Marine Biology* **156**, 439-446.

Obmolova, G., Ban, C., Hsieh, P. and Yang, W. (2000). Crystal structures of mismatch repair protein MutS and its complex with a substrate DNA. *Nature* **407**, 703-710.

Ojala, D., Montoya, J. and Attardi, G. (1981). tRNA punctuation model of RNA processing in human mitochondria. *Nature* **290**, 470-474.

Orr, J. C., Fabry, V. J., Aumont, O., Bopp, L., Doney, S. C., Feely, R. A., Gnanadesikan, A., Gruber, N., Ishida, A., Joos, F. et al. (2005). Anthropogenic ocean acidification over the twenty-first century and its impact on calcifying organisms. *Nature* **437**, 681-686.

Ott, M., Gogvadze, V., Orrenius, S. and Zhivotovsky, B. (2007). Mitochondria, oxidative stress and cell death. *Apoptosis* **12**, 913-922.

Pagarigan, L. and Takabayashi, M. (2008). Reference gene selection for qRT-PCR analysis of the Hawaiian coral Pocillopora meandrina subjected to evevated levels of temperature and nutrient. In *11th International Coral Reef Symposium*, pp. 169-173. Ft. Lauderale, Florida.

Park, E., Song, J. I. and Won, Y. J. (2011). The complete mitochondrial genome of Calicogorgia granulosa (Anthozoa: Octocorallia): potential gene novelty in unidentified ORFs formed by repeat expansion and segmental duplication. *Gene* **486**, 81-87.

Parker, B. O. and Marinus, M. G. (1992). Repair of DNA heteroduplexes containing small heterologous sequences in Escherichia coli. *Proc Natl Acad Sci U S A* **89**, 1730-1734.

Pfaffl, M. W., Horgan, G. W. and Dempfle, L. (2002). Relative expression software tool (REST) for group-wise comparison and statistical analysis of relative expression results in real-time PCR. *Nucleic Acids Res* **30**, e36.

Pfaffl, M. W., Tichopad, A., Prgomet, C. and Neuvians, T. P. (2004). Determination of stable housekeeping genes, differentially regulated target genes and sample integrity: BestKeeper – Excel-based tool using pair-wise correlations. *Biotechnology Letters* **26**, 509-515.

Plantivaux, A., Furla, P., Zoccola, D., Garello, G., Forcioli, D., Richier, S., Merle, P. L., Tambutte, E., Tambutte, S. and Allemand, D. (2004). Molecular characterization of two CuZn-superoxide dismutases in a sea anemone. *Free Radic Biol Med* **37**, 1170-1181.

Pont-Kingdon, G., Okada, N. A., Macfarlane, J. L., Beagley, C. T., Watkins-Sims, C. D., Cavalier-Smith, T., Clark-Walker, G. D. and Wolstenholme, D. R. (1998). Mitochondrial DNA of the coral Sarcophyton glaucum contains a gene for a homologue of bacterial MutS: a possible case of gene transfer from the nucleus to the mitochondrion. *Journal of molecular evolution* **46**, 419-431.

Pont-Kingdon, G. A., Okada, N. A., Macfarlane, J. L., Beagley, C. T., Wolstenholme, D. R., Cavalier-Smith, T. and Clark-Walker, G. D. (1995). A coral mitochondrial mutS gene. *Nature* **375**, 109-111.

Pörtner, H. (2008). Ecosystem effects of ocean acidification in times of ocean warming: a physiologist's view. *Marine Ecology Progress Series* **373**, 203-217.

Pratlong, M., Haguenauer, A., Chabrol, O., Klopp, C., Pontarotti, P. and Aurelle, D. (2015). The red coral (Corallium rubrum) transcriptome: a new resource for population genetics and local adaptation studies. *Molecular Ecology Resources*, n/a-n/a.

Rackham, O., Mercer, T. R. and Filipovska, A. (2012). The human mitochondrial transcriptome and the RNA-binding proteins that regulate its expression. *Wiley Interdiscip Rev RNA* **3**, 675-695.

Rackham, O., Shearwood, A. M., Mercer, T. R., Davies, S. M., Mattick, J. S. and Filipovska, A. (2011). Long noncoding RNAs are generated from the mitochondrial genome and regulated by nuclear-encoded proteins. *RNA* **17**, 2085-2093.

Radonić, A., Thulke, S., Mackay, I. M., Landt, O., Siegert, W. and Nitsche, A. (2004). Guideline to reference gene selection for quantitative real-time PCR. *Biochemical and Biophysical Research Communications* **313**, 856-862.

Ramakers, C., Ruijter, J. M., Deprez, R. H. L. and Moorman, A. F. M. (2003). Assumption-free analysis of quantitative real-time polymerase chain reaction (PCR) data. *Neuroscience Letters* **339**, 62-66.

Richier, S., Furla, P., Plantivaux, A., Merle, P.-L. and Allemand, D. (2005). Symbiosis-induced adaptation to oxidative stress. *Journal of Experimental Biology* **208**, 277-285.

Richier, S., Sabourault, C., Courtiade, J., Zucchini, N., Allemand, D. and Furla, P. (2006). Oxidative stress and apoptotic events during thermal stress in the symbiotic sea anemone, Anemonia viridis. *FEBS J* **273**, 4186-4198.

Richter, C., Park, J. W. and Ames, B. N. (1988). Normal oxidative damage to mitochondrial and nuclear DNA is extensive. *Proc Natl Acad Sci U S A* **85**, 6465-6467.

Rinn, J. L. and Chang, H. Y. (2012). Genome regulation by long noncoding RNAs. *Annu Rev Biochem* **81**, 145-166.

Robledo, D., Hernandez-Urcera, J., Cal, R. M., Pardo, B. G., Sanchez, L., Martinez, P. and Vinas, A. (2014). Analysis of qPCR reference gene stability determination methods and a practical approach for efficiency calculation on a turbot (Scophthalmus maximus) gonad dataset. *BMC Genomics* **15**, 648.

Rodrigues, R. M., Macko, P., Palosaari, T. and Whelan, M. P. (2011). Autofluorescence microscopy: a non-destructive tool to monitor mitochondrial toxicity. *Toxicol Lett* **206**, 281-288.

Rodriguez, A., Rodriguez, M., Cordoba, J. J. and Andrade, M. J. (2015). Design of primers and probes for quantitative real-time PCR methods. *Methods Mol Biol* **1275**, 31-56.

Rodriguez-Lanetty, M., Harii, S. and Hoegh-Guldberg, O. (2009). Early molecular responses of coral larvae to hyperthermal stress. *Mol Ecol* **18**, 5101-5114.

Rodriguez-Lanetty, M., Phillips, W. S., Dove, S., Hoegh-Guldberg, O. and Weis, V. M. (2008). Analytical approach for selecting normalizing genes from a cDNA microarray platform to be used in q-RT-PCR assays: a cnidarian case study. *Journal of biochemical and biophysical methods* **70**, 985-991.

Rosano, G. L. and Ceccarelli, E. A. (2014). Recombinant protein expression in

Escherichia coli: advances and challenges. *Front Microbiol* **5**, 172.

Rosic, N., Kaniewska, P., Chan, C.-K. K., Ling, E. Y. S., Edwards, D., Dove, S. and Hoegh-Guldberg, O. (2014). Early transcriptional changes in the reef-building coral Acropora aspera in response to thermal and nutrient stress. *BMC Genomics* **15**, 1052.

Rossmanith, W. (2012). Of P and Z: mitochondrial tRNA processing enzymes. *Biochim Biophys Acta* **1819**, 1017-1026.

Rot, C., Goldfarb, I., Ilan, M. and Huchon, D. (2006). Putative cross-kingdom horizontal gene transfer in sponge (Porifera) mitochondria. *BMC evolutionary biology* **6**, 71.

Rothfuss, O., Gasser, T. and Patenge, N. (2010). Analysis of differential DNA damage in the mitochondrial genome employing a semi-long run real-time PCR approach. *Nucleic acids research* **38**, e24.

Ruijter, J. M., Ramakers, C., Hoogaars, W. M. H., Karlen, Y., Bakker, O., van den Hoff, M. J. B. and Moorman, A. F. M. (2009). Amplification efficiency: linking baseline and bias in the analysis of quantitative PCR data. *Nucleic acids research* **37**, e45.

Sagara, Y., Dargusch, R., Chambers, D., Davis, J., Schubert, D. and Maher, P. (1998). Cellular mechanisms of resistance to chronic oxidative stress. *Free Radic Biol Med* **24**, 1375-1389.

Salinas-Giege, T., Giege, R. and Giege, P. (2015). tRNA biology in mitochondria. *Int J Mol Sci* **16**, 4518-4559.

Sambrook, J. and Russell, D. W. (2001). Molecular cloning : a laboratory manual, pp. 3.1-3.52. Cold Spring Harbor, N.Y. :: Cold Spring Harbor Laboratory Press.

Sammarco, P. W. and Strychar, K. B. (2013). Responses to High Seawater Temperatures in Zooxanthellate Octocorals. *PLoS ONE* **8**.

Santos, C. A., Beloti, L. L., Toledo, M. A. S., Crucello, A., Favaro, M. T. P., Mendes, J. S., Santiago, A. S., Azzoni, A. R. and Souza, A. P. (2012). A novel protein refolding protocol for the solubilization and purification of recombinant peptidoglycan-associated lipoprotein from Xylella fastidiosa overexpressed in Escherichia coli. *Protein Expression and Purification* **82**, 284-289.

Sawyer, D. E., Roman, S. D. and Aitken, R. J. (2001). Relative susceptibilities of mitochondrial and nuclear DNA to damage induced by hydrogen peroxide in two mouse germ cell lines. *Redox report: communications in free radical research* **6**, 182-184.

Schmittgen, T. D., Zakrajsek, B. A., Mills, A. G., Gorn, V., Singer, M. J. and Reed, M. W. (2000). Quantitative reverse transcription-polymerase chain reaction to study mRNA decay: comparison of endpoint and real-time methods. *Analytical Biochemistry* **285**, 194-204.

Schwarz, J. A., Mitchelmore, C. L., Jones, R., O'Dea, A. and Seymour, S. (2013). Exposure to copper induces oxidative and stress responses and DNA damage in the coral Montastraea franksi. *Comp Biochem Physiol C Toxicol Pharmacol* **157**, 272-279.

Schwarze, S. R., Weindruch, R. and Aiken, J. M. (1998). Oxidative stress and aging reduce COX I RNA and cytochrome oxidase activity in Drosophila. *Free Radic Biol Med* **25**, 740-747.

Scientists, G. C. o., Bracken-Grissom, H., Collins, A. G., Collins, T., Crandall, K.,

Distel, D., Dunn, C., Giribet, G., Haddock, S., Knowlton, N. et al. (2014). The Global Invertebrate Genomics Alliance (GIGA): developing community resources to study diverse invertebrate genomes. *J Hered* **105**, 1-18.

Seneca, F. O. and Palumbi, S. R. (2015). The role of transcriptome resilience in resistance of corals to bleaching. *Mol Ecol* **24**, 1467-1484.

Senthilkumar, R., Sabarinathan, R., Hameed, B. S., Banerjee, N., Chidambarathanu, N., Karthik, R. and Sekar, K. (2010). FAIR: A server for internal sequence repeats. *Bioinformation* **4**, 271-275.

Shearer, T. L., Van Oppen, M. J. H., Romano, S. L. and Wörheide, G. (2002). Slow mitochondrial DNA sequence evolution in the Anthozoa (Cnidaria). *Molecular ecology* **11**, 2475-2487.

Shigenaga, M. K., Hagen, T. M. and Ames, B. N. (1994). Oxidative damage and mitochondrial decay in aging. *Proceedings of the National Academy of Sciences of the United States of America* **91**, 10771-10778.

Shokolenko, I., Venediktova, N., Bochkareva, A., Wilson, G. L. and Alexeyev, M. F. (2009). Oxidative stress induces degradation of mitochondrial DNA. *Nucleic Acids Research* **37**, 2539-2548.

Silver, N., Best, S., Jiang, J. and Thein, S. L. (2006). Selection of housekeeping genes for gene expression studies in human reticulocytes using real-time PCR. *BMC Mol Biol* **7**, 33.

Slomovic, S. and Schuster, G. (2013). Circularized RT-PCR (cRT-PCR): analysis of the 5' ends, 3' ends, and poly(A) tails of RNA. *Methods Enzymol* **530**, 227-251.

Slomovic, S., Laufer, D., Geiger, D. and Schuster, G. (2005). Polyadenylation and degradation of human mitochondrial RNA: the prokaryotic past leaves its mark. *Mol Cell Biol* **25**, 6427-6435.

Solomon, S., Qin, D., Manning, M., Chen, Z., Marquis, M., Averyt, K. B., Tignor, M., Miller, H. L. and (eds.). (2007). IPCC, Climate Change: The Physical Science Basis. Contribution of Working Group I to the Fourth Assessment Report of the Intergovernmental Panel on Climate Change. Cambridge, United Kingdom

New York, NY, USA: Cambridge University Press.

Sorensen, H. P., Sperling-Petersen, H. U. and Mortensen, K. K. (2003). Dialysis strategies for protein refolding: preparative streptavidin production. *Protein Expr Purif* **31**, 149-154.

Soriano-Santiago, O. S., Liñán-Cabello, M. A., Delgadillo-Nuño, M. A., Ortega-Ortiz, C. and Cuevas-Venegas, S. (2013). Physiological responses to oxidative stress associated with pH variations in host tissue and zooxanthellae of hermatypic coral Pocillopora capitata. *Marine and Freshwater Behaviour and Physiology* **46**, 275-286.

Stanislawska-Sachadyn, A., Sachadyn, P., Jedrzejczak, R. and Kur, J. (2003). Construction and purification of his6-Thermus thermophilus MutS protein. *Protein Expr Purif* **28**, 69-77.

Stewart, J. B. and Beckenbach, A. T. (2009). Characterization of mature mitochondrial transcripts in Drosophila, and the implications for the tRNA punctuation model in arthropods. *Gene* **445**, 49-57.

Stocks, K. (2004). Seamount Invertebrates: Composition and vulnerability to fishing.

Fisheries Centre Research Reports, 17-24.

Strychar, K. B., Coates, M., Sammarco, P. W., Piva, T. J. and Scott, P. T. (2005). Loss of Symbiodinium from bleached soft corals Sarcophyton ehrenbergi, Sinularia sp. and Xenia sp. *Journal of Experimental Marine Biology and Ecology* **320**, 159-177.

Su, J.-H., Lo, C.-L., Lu, Y., Wen, Z.-H., Huang, C.-Y., Dai, C.-F. and Sheu, J.-H. (2008). Anti-Inflammatory Polyoxygenated Steroids from the Soft Coral *Sinularia* sp. *Bulletin of the Chemical Society of Japan* **81**, 1616-1620.

Su, S. S. and Modrich, P. (1986). Escherichia coli mutS-encoded protein binds to mismatched DNA base pairs. *Proc Natl Acad Sci U S A* **83**, 5057-5061.

Svanfeldt, K., Lundqvist, L., Rabinowitz, C., Sköld, H. N. and Rinkevich, B. (2014). Repair of UV-induced DNA damage in shallow water colonial marine species. *Journal of Experimental Marine Biology and Ecology* **452**, 40-46.

Szitenberg, A., Rot, C., Ilan, M. and Huchon, D. (2010). Diversity of sponge mitochondrial introns revealed by cox 1 sequences of Tetillidae. *BMC Evol Biol* **10**, 288.

Takamatsu, S., Kato, R. and Kuramitsu, S. (1996). Mismatch DNA recognition protein from an extremely thermophilic bacterium, Thermus thermophilus HB8. *Nucleic Acids Res* **24**, 640-647.

Tarrant, A. M., Reitzel, A. M., Kwok, C. K. and Jenny, M. J. (2014). Activation of the cnidarian oxidative stress response by ultraviolet radiation, polycyclic aromatic hydrocarbons and crude oil. *J Exp Biol* **217**, 1444-1453.

Tchernov, D., Kvitt, H., Haramaty, L., Bibby, T. S., Gorbunov, M. Y., Rosenfeld, H. and Falkowski, P. G. (2011). Apoptosis and the selective survival of host animals following thermal bleaching in zooxanthellate corals. *Proc Natl Acad Sci U S A* **108**, 9905-9909.

Teixeira, T., Diniz, M., Calado, R. and Rosa, R. (2013). Coral physiological adaptations to air exposure: Heat shock and oxidative stress responses in Veretillum cynomorium. *Journal of Experimental Marine Biology and Ecology* **439**, 35-41.

Temperley, R. J., Wydro, M., Lightowlers, R. N. and Chrzanowska-Lightowlers, Z. M. (2010). Human mitochondrial mRNAs--like members of all families, similar but different. *Biochim Biophys Acta* **1797**, 1081-1085.

Thomas, D. C., Umar, A. and Kunkel, T. A. (1995). Measurement of Heteroduplex Repair in Human Cell Extracts. *Methods* **7**, 187-197.

Thorrez, L., Van Deun, K., Tranchevent, L.-C., Van Lommel, L., Engelen, K., Marchal, K., Moreau, Y., Van Mechelen, I. and Schuit, F. (2008). Using Ribosomal Protein Genes as Reference: A Tale of Caution. *PLoS ONE* **3**, e1854.

Tøndervik, A., Balzer, S., Haugen, T., Sletta, H., Rode, M., Lindmo, K., Ellingsen, T. and Brautaset, T. (2013). High production of recombinant Norwegian salmonid alphavirus E1 and E2 proteins in Escherichia coli by fusion to secretion signal sequences and removal of hydrophobic domains. *Biotechnol Bioproc E* **18**, 742-750.

Tsai-Wu, J. J., Su, H. T., Fang, W. H. and Wu, C. H. (1999). Preparation of heteroduplex DNA containing a mismatch base pair with magnetic beads. *Anal Biochem* **275**, 127-129.

Turrens, J. F. (2003). Mitochondrial formation of reactive oxygen species. *J Physiol* **552**, 335-344.

Uda, K., Komeda, Y., Koyama, H., Koga, K., Fujita, T., Iwasaki, N. and Suzuki, T. (2011). Complete mitochondrial genomes of two Japanese precious corals, Paracorallium japonicum and Corallium konojoi (Cnidaria, Octocorallia, Coralliidae): notable differences in gene arrangement. *Gene* **476**, 27-37.

Untergasser, A., Cutcutache, I., Koressaar, T., Ye, J., Faircloth, B. C., Remm, M. and Rozen, S. G. (2012). Primer3--new capabilities and interfaces. *Nucleic Acids Res* **40**, e115.

van Oppen, M. J. and Gates, R. D. (2006). Conservation genetics and the resilience of reef-building corals. *Mol Ecol* **15**, 3863-3883.

van Oppen, M. J., McDonald, B. J., Willis, B. and Miller, D. J. (2001). The evolutionary history of the coral genus Acropora (Scleractinia, Cnidaria) based on a mitochondrial and a nuclear marker: reticulation, incomplete lineage sorting, or morphological convergence? *Molecular biology and evolution* **18**, 1315-1329.

van Oppen, M. J., Catmull, J., McDonald, B. J., Hislop, N. R., Hagerman, P. J. and Miller, D. J. (2002). The mitochondrial genome of Acropora tenuis (Cnidaria; Scleractinia) contains a large group I intron and a candidate control region. *J Mol Evol* **55**, 1-13.

van Waveren, C. and Moraes, C. T. (2008). Transcriptional co-expression and co-regulation of genes coding for components of the oxidative phosphorylation system. *BMC Genomics* **9**, 18.

Vandesompele, J., Preter, K. D., Pattyn, F., Poppe, B., Roy, N. V., Paepe, A. D. and Speleman, F. (2002). Accurate normalization of real-time quantitative RT-PCR data by geometric averaging of multiple internal control genes. *Genome Biology* **3**, research0034.

Vargas, S., Schuster, A., Sacher, K., Buttner, G., Schatzle, S., Lauchli, B., Hall, K., Hooper, J. N., Erpenbeck, D. and Worheide, G. (2012). Barcoding sponges: an overview based on comprehensive sampling. *PLoS One* **7**, e39345.

Vidal-Dupiol, J., Zoccola, D., Tambutte, E., Grunau, C., Cosseau, C., Smith, K. M., Freitag, M., Dheilly, N. M., Allemand, D. and Tambutte, S. (2013). Genes related to ion-transport and energy production are upregulated in response to CO2-driven pH decrease in corals: new insights from transcriptome analysis. *PLoS One* **8**, e58652.

Voigt, O., Erpenbeck, D. and Wörheide, G. (2008). A fragmented metazoan organellar genome: the two mitochondrial chromosomes of Hydra magnipapillata. *BMC genomics* **9**, 350.

Wallace, D. C. (2005). A mitochondrial paradigm of metabolic and degenerative diseases, aging, and cancer: a dawn for evolutionary medicine. *Annu Rev Genet* **39**, 359-407.

Wang, H. and Hays, J. B. (2000). Preparation of DNA substrates for in vitro mismatch repair. *Mol Biotechnol* **15**, 97-104.

Wang, W. N., Zhou, J., Wang, P., Tian, T. T., Zheng, Y., Liu, Y., Mai, W. J. and Wang, A. L. (2009). Oxidative stress, DNA damage and antioxidant enzyme gene expression in the Pacific white shrimp, Litopenaeus vannamei when exposed to acute pH stress. *Comp Biochem Physiol C Toxicol Pharmacol* **150**, 428-435.

Weis, V. M. (2008). Cellular mechanisms of Cnidarian bleaching: stress causes the collapse of symbiosis. *J Exp Biol* **211**, 3059-3066.

Williams, G. and Cairns, S. (2005). Systematic list of valid octocoral genera. *línea], disponible en:* http://www. *calacademy. org/research/izg/OCTOCLASS. htm*.

Wolstenholme, D. R. (1992). Genetic novelties in mitochondrial genomes of multicellular animals. *Curr Opin Genet Dev* **2**, 918-925.

Woo, S., Lee, A., Denis, V., Chen, C. A. and Yum, S. (2014). Transcript response of soft coral (Scleronephthya gracillimum) on exposure to polycyclic aromatic hydrocarbons. *Environ Sci Pollut Res Int* **21**, 901-910.

Wu, T. H. and Marinus, M. G. (1999). Deletion mutation analysis of the mutS gene in Escherichia coli. *J Biol Chem* **274**, 5948-5952.

Yakes, F. M. and Van Houten, B. (1997). Mitochondrial DNA damage is more extensive and persists longer than nuclear DNA damage in human cells following oxidative stress. *Proc Natl Acad Sci U S A* **94**, 514-519.

Yang, B., Liao, S., Lin, X., Wang, J., Liu, J., Zhou, X., Yang, X. and Liu, Y. (2013). New sinularianin sesquiterpenes from soft coral Sinularia sp. *Marine Drugs* **11**, 4741-4750.

Youle, R. J. and van der Bliek, A. M. (2012). Mitochondrial fission, fusion, and stress. *Science* **337**, 1062-1065.

Zhou, B., Huang, C., Yang, J., Lu, J., Dong, Q. and Sun, L.-Z. (2009). Preparation of heteroduplex enhanced green fluorescent protein plasmid for in vivo mismatch repair activity assay. *Analytical biochemistry* **388**, 167-169.

Zhou, B., Dong, Q., Ma, R., Chen, Y., Yang, J., Sun, L. Z. and Huang, C. (2009). Rapid isolation of highly pure single-stranded DNA from phagemids. *Anal Biochem* **389**, 177-179.

Zhu, X. Q., Li, S. X., He, H. J. and Yuan, Q. S. (2005). On-column refolding of an insoluble His6-tagged recombinant EC-SOD overexpressed in Escherichia coli. *Acta Biochim Biophys Sin (Shanghai)* **37**, 265-269.

Declaration

I hereby confirm that my thesis entitled **"Molecular Biology of Octocoral Mitochondria: mtDNA Repair, Expression, and Evolutionary Implications"**, is the result of my own original work. Furthermore, I certify that this work contains no material which has been accepted for the award of any other degree or diploma in my name, in any university and, to the best of my knowledge and belief, contains no material previously published or written by another person, except where due reference has been made in the text. In addition, I certify that no part of this work will, in the future, be used in a submission in my name, for any other degree or diploma in any university or other tertiary institution without the prior approval of the Ludwig-Maximilians-University Munich.

Place, Date Signature

Curriculum Vitae

Gaurav G. Shimpi

Department of Earth and Environmental-Science, Palaeontology & Geobiology
Ludwig-Maximilians-University, Munich
Richard-Wagner-Str. 10
80333 Munich, Germany.

Phone: +4915207180020
Email: nature.gaurav@gmail.com
Nationality: Indian
Date of Birth: 14.04.1984

EDUCATION

- Ludwig-Maximilians-University, Munich, Germany
  Ph.D., Geobiology, 2011-2015
  - Thesis: Oxidative stress response of octocorals: Gene expression, mtDNA damage, repair, and dynamics
  - Advisor: Prof. Dr. Gert Woerheide
- North Maharashtra University, Jalgaon, India
  M.Sc., Biochemistry, *First class with distinction* 2006-2008
  B.Sc., Zoology, *First class with distinction* 2003-2006
  Advanced Diploma in Biotechnology, *First class with distinction* 2003-2006

AWARDS AND HONORS

- DAAD (German Academic Exchange Service) Ph.D. scholarship 2011-2015
- Third rank in the University in M.Sc. Biochemistry 2006-2008
- Chief Minister Fund's Pujya Sane Guruji Scholarship during Master's for top rank 2006-2007
- Third rank in Advanced Diploma in Biotechnology at University 2006
- First rank in B.Sc. Zoology at graduate college (4th in Uni.) 2006

RESEARCH EXPERIENCE

- **Graduate Student**, Ludwig-Maximilians-University, Munich 2011-Present
  - Reference gene validation for accurate normalization of qPCR in octocorals
  - Oxidative stress response and gene expression in octocorals
  - Mitochondrial DNA damage, repair and dynamics in octocorals
  - Mapping mitochondrial mRNA transcripts of octocoral *Sinularia sp.*

- Mitochondrial mismatch repair (mtMutS) protein expression
- Impact of ocean acidification on calcification and growth rate of scleractinian coral *Euphyllia ancora* (co-supervised Master's project)

- **Junior Research Fellow**, Bombay Natural History Society, Mumbai 2010-2011
  - Molecular phylogeny of marine gastropods from Indian coastal regions using different molecular gene markers
- **Project Assistant**, National Centre for Cell Science, Pune 2008-2010
  - Development of DNA Barcode for amphibian fauna of the Western Ghats
  - Geomicrobiology of Lonar meteor impact crater, exploring the endolithic microbial diversity of basalts along geophysicochemical gradients
  - Molecular studies on commercial probiotic formulations identified possible presence of contaminant bacteria
- **Master's project**: 2007-2008
  - *In Vitro* phytochemical analysis and antimicrobial activity of selected Indian medicinal plants against multi-drug resistant bacteria.

ABSTRACTS AND PROCEEDINGS

- *Tethya wilhelma*: an emerging marine model for early-branching metazoans Gert Wörheide, Dirk Erpenbeck, **Gaurav Shimpi**, Oliver Voigt, Sergio Vargas, Jörg U. Hammel, Michael Nickel. Ninth World Sponge Conference 2013, Australia.

- Molecular characterization of microbial content to validate commercial probiotic formulations. **Shimpi G.G**., Kumar H., Gaikaiwari R. P., Wagh Shilpa, Shouche.Y.S., at 50th Annual Conference of Association of Microbiologists of India (AMI 2009), Pune, Dec 15-18, 2009.

- *Lactobacillus sp.* CD6: a potential folate producing probiotic strain isolated from Indian traditional fermented milk. Chaudhari B.L., Ahire J.J., Patil K.P., **Shimpi G.G.**, Shouche Y.S., Chincholkar S.B. at Fourth Inernational

Conference on “Fermented foods, health status & social well-being” Anand Agricultural University, Anand, Gujrat, India on Dec 11-12, 2009.

WORKSHOPS AND SYMPOSIA

- Evolutionary potential in marine populations. GEOMAR and AWI, List auf Sylt, Germany. Sept 17-21, 2012
- EES Summer School on protein evolution. WWU, Muenster, Chiemsee, Germany. Jul 22-27, 2012
- Deep metazoan phylogeny – new data, new challenges. LMU, Munich, Germany. Oct 11-14, 2011

PUBLICATIONS

Antony, C. P., Shimpi, G. G., Cockell, C. S., Patole, M. S. and Shouche, Y. S. (2013). Molecular Characterization of Prokaryotic Communities Associated with Lonar Crater Basalts. *Geomicrobiology Journal* **31**, 519-528.